

# **OPTIMIZATION OF CO<sub>2</sub>/N<sub>2</sub> FOAM PARAMETERS FOR EOR IN SANDSTONE RESERVOIRS**

**BY**

**AHMED ELSAYED AHMED IBRAHIM ABDELAAL**

**A Thesis Presented to the  
DEANSHIP OF GRADUATE STUDIES**

**KING FAHD UNIVERSITY OF PETROLEUM & MINERALS  
DHAHRAN, SAUDI ARABIA**

**In Partial Fulfillment of the  
Requirements for the Degree of**

**MASTER OF SCIENCE  
In  
PETROLEUM ENGINEERING**

**December 2019**



KING FAHD UNIVERSITY OF PETROLEUM & MINERALS  
DHAHRAN- 31261, SAUDI ARABIA  
**DEANSHIP OF GRADUATE STUDIES**

This thesis, written by **AHMED ELSAYED AHMED IBRAHIM ABDELAAL** under the direction of his thesis advisor and approved by his thesis committee, has been presented and accepted by the Dean of Graduate Studies, in partial fulfillment of the requirements for the degree of **MASTER OF SCIENCE IN PETROLEUM ENGINEERING**.



Dr. Dhafer A. Al Shehri  
Department Chairman



Dr. Salam A. Zummo  
Dean of Graduate Studies



22/12/19

Date



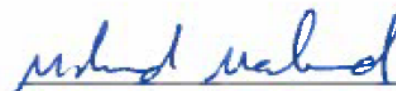
Dr. Rahul N. Gajbhiye  
(Advisor)



Dr. Dhafer A. Al Shehri  
(Co-Advisor)



Dr. Hasan Y. Al-Yousef  
(Member)



Dr. Mohamed Mahmoud  
(Member)



Dr. Shirish Patil  
(Member)

© Ahmed Elsayed Ahmed Ibrahim Abdelaal

2019

**To my great father, to my amazing mother, to my dear wife and to my son**

## **ACKNOWLEDGMENTS**

Praise and thanks to Allah, Almighty, from the beginning to the end. Allah gave me everything I have in my life, as I cannot count his blessings if I tried to count. Allah showered and still showers me with blessings.

I am extremely grateful to my father, Mr. Elsayed Abdelaal, and my mother, Hoda Elghazaly, for their love, prayers, sacrifice, caring they gave me throughout my life to educate and prepare me for the future. I am very thankful to my great wife, Basma Basem, and my son, Fares, for their love, understanding, prayers and everything. I would like to thank my father in law, Eng. Basem Rezk, and my mother in law, Hanan Abdelsalam, for their love, prayers and support. Thanks to my great brother, Dr. Omar, and my dear sister, Dalia.

I would like to thank my advisor, Dr. Rahul Gajbhiye, for his continuous support personally and academically. My thanks are extended to my co-advisor, Dr. Dhafer AL-Shehri, who supports all student in the department. I was tremendously fortunate to have committee members like Dr. Mohamed Mahmoud, Dr. Hasan Al-Yousef and Dr. Shirish Patil. They added a depth of knowledge to my thesis work by their valuable comments.

I would like to thank KFUPM and College of Petroleum Engineering and Geosciences for providing me with such great research facilities. KFUPM is a world-class university where you can find a professional environment to work in. I also would like to thank Deanship of Scientific Research that supported the project #IN171026 in which I worked.

I would like to thank Central Institute of Petroleum Research in KFUPM for providing me with the research facilities I needed for my research to be finished. I especially want to thank Mr. Xianmin Zhou and Mr. Redha for their continuous support and help. I also would like to thank lab coordinators in CPG especially Mr. Abdulsamd, Mr. Mobeen and Mr. Essa.

# TABLE OF CONTENTS

ACKNOWLEDGMENTS .....	VI
TABLE OF CONTENTS .....	VIII
LIST OF TABLES.....	XII
LIST OF FIGURES.....	XIII
LIST OF ABBREVIATIONS.....	XVI
ABSTRACT .....	XVII
ملخص الرسالة .....	XIX
CHAPTER 1 INTRODUCTION.....	1
CHAPTER 2 LITERATURE REVIEW .....	7
2.1 CO <sub>2</sub> Foam as a Potential Technique for EOR .....	7
2.2 CO <sub>2</sub> Foam Issues .....	9
2.3 Factors Affecting CO <sub>2</sub> Foam Stability .....	11
2.4 CO <sub>2</sub> Foam Properties and its Comparison with N <sub>2</sub> Foam.....	13
2.5 Solutions for CO <sub>2</sub> Foam Instability .....	16



2.5.1 Polymer .....	16
2.5.2 Nanoparticles .....	21
2.5.3 Injection Rate Control.....	21
2.5.4 Replacing part of CO <sub>2</sub> by N <sub>2</sub> .....	22
<b>CHAPTER 3 PROBLEM STATEMENT AND RESEARCH OBJECTIVE .....</b>	<b>24</b>
<b>CHAPTER 4 METHODS AND MATERIALS.....</b>	<b>26</b>
4.1 Materials .....	26
4.1.1 Salts .....	26
4.1.2 Core samples .....	26
4.1.3 Gases .....	26
4.1.4 Crude Oil .....	26
4.1.5 Surfactants .....	27
4.2 Devices .....	28
4.2.1 Core Flooding System .....	28
4.2.2 Laboratory Balances .....	30
4.2.3 External Pumps .....	30
4.3 Methods and Procedures .....	31

4.3.1 Brine Preparation .....	31
4.3.2 Core Drying and Firing .....	32
4.3.3 Core Saturation .....	32
4.3.4 Core Placement and Pre-start .....	33
4.3.5 Formation Brine Flooding and Oil Injection .....	33
4.3.6 Foam Flooding .....	34
<b>CHAPTER 5 RESULTS AND DISCUSSION .....</b>	<b>35</b>
5.1 Core Properties Measurements .....	35
5.2 Water flooding .....	37
5.3 Mixed CO <sub>2</sub> /N <sub>2</sub> Foam Flooding .....	38
5.4 Effect of flow rate .....	40
5.4.1 Experiment 1 .....	40
5.4.2 Experiment 2 .....	46
5.4.3 Experiment 3 .....	52
5.5 Effect of N <sub>2</sub> Percentage .....	58
5.5.1 Experiment 4 .....	58
5.5.2 Experiment 5 .....	64

<b>5.6 Effect of flow rate .....</b>	<b>70</b>
<b>5.6.1 Experiment 6 .....</b>	<b>70</b>
<b>5.6.2 Experiment 7 .....</b>	<b>76</b>
<b>5.7 Summary of Discussion and Comparison .....</b>	<b>82</b>
<b>5.7.1 Injection Rate .....</b>	<b>82</b>
<b>5.7.2 N<sub>2</sub> Percentage.....</b>	<b>83</b>
<b>5.7.3 Foam Quality .....</b>	<b>85</b>
<b>CHAPTER 6 CONCLUSION.....</b>	<b>87</b>
<b>REFERENCES.....</b>	<b>90</b>
<b>VITAE .....</b>	<b>96</b>

## LIST OF TABLES

Table 1 Summarizes the Results of Comparing CO <sub>2</sub> and N <sub>2</sub> Foams Performance.....	15
Table 2 Summarizes Polymers and Surfactants Usage for CO <sub>2</sub> Foam Stability.....	20
Table 3 Formula of Formation Brine and Seawater.....	32
Table 4 Summary of Cores Properties .....	36
Table 5 Different Variables Used in the Experiments .....	39
Table 6 Parameters Data Used for Experiments .....	39
Table 7 Summary of Experiment 1 Parameters .....	43
Table 8 Summary of Experiment 2 Parameters .....	49
Table 9 Summary of Experiment 3 Parameters .....	55
Table 10 Summary of Experiment 4 Parameters .....	61
Table 11 Summary of Experiment 5 Parameters .....	67
Table 12 Summary of Experiment 6 Parameters .....	73
Table 13 Summary of Experiment 7 Parameters .....	79

## LIST OF FIGURES

Figure 1 Oil Saturation Effect on CO <sub>2</sub> Foam Stability Flooding (Yin et al. 2009 ) .....	12
Figure 2 Novel Polymer Effect on Stability of CO <sub>2</sub> Foam Compared to (HPAM) .....	17
Figure 3 Novel Polymer Effect on CO <sub>2</sub> Foam Foamability Compared to (HPAM) .....	18
Figure 4 Schematic of Core Flooding System .....	28
Figure 5 Core Flooding System from the Backside .....	29
Figure 6 Core Flooding System from Front side .....	29
Figure 7 Brine Permeability Pressure Drop vs Pore Volume injected (Experiment 1) ....	40
Figure 8 Oil Injection Pressure Drop vs Pore Volume injected (Experiment 1) .....	41
Figure 9 RF for SW Flooding for Experiment 1 .....	42
Figure 10 SW Pressure Drop vs Pore Volume Injected (Experiment 1) .....	42
Figure 11 Pressure Drop vs Pore Volume injected for Foam Flooding (Experiment 1)	44
Figure 12 RF for Foam Flooding (Experiment 1) .....	44
Figure 13 RF for total Flooding (Experiment 1) .....	45
Figure 14 Brine Permeability Pressure Drop vs Pore Volume injected (Experiment 2) ..	46
Figure 15 Oil Injection Pressure Drop vs Pore Volume injected (Experiment 2) .....	47
Figure 16 SW Pressure Drop vs Pore Volume Injected (Experiment 2) .....	48
Figure 17 SW Recovery Factor vs Pore Volume Injected (Experiment 2) .....	48
Figure 18 Foam Flooding Recovery Factor vs Pore Volume Injected (Experiment 2) ....	50
Figure 19 SW Recovery Factor vs Pore Volume Injected (Experiment 2) .....	50
Figure 20 Foam Recovery Pressure Drop vs Pore Volume Injected (Experiment 2) .....	51
Figure 21 Brine Permeability Pressure Drop vs Pore Volume Injected (Experiment 3) ..	52

Figure 22 Oil Injection Pressure Drop vs Pore Volume Injected (Experiment 3) .....	53
Figure 23 SW Recovery Factor vs Pore Volume Injected (Experiment 3).....	54
Figure 24 SW Pressure Drop vs Pore Volume Injected (Experiment 3) .....	54
Figure 25 Foam Flooding Recovery Factor vs Pore Volume Injected (Experiment 3) ....	56
Figure 26 Recovery Factor vs Pore Volume Injected (Experiment 3).....	56
Figure 27 Foam Recovery Pressure Drop vs Pore Volume Injected (Experiment 3).....	57
Figure 28 Brine Permeability Pressure Drop vs Pore Volume Injected (Experiment 4) ..	58
Figure 29 Oil Injection Pressure Drop vs Pore Volume Injected (Experiment 4) .....	59
Figure 30 SW Recovery Factor vs Pore Volume Injected (Experiment 4).....	60
Figure 31 SW Pressure Drop vs Pore Volume Injected (Experiment 4) .....	60
Figure 32 Foam Flooding Recovery Factor vs Pore Volume Injected (Experiment 4) ....	62
Figure 33 Recovery Factor vs Pore Volume Injected (Experiment 4).....	62
Figure 34 Foam Recovery Pressure Drop vs Pore Volume Injected (Experiment 4).....	63
Figure 35 Brine Permeability Pressure Drop vs Pore Volume injected (Experiment 5) ..	64
Figure 36 Oil Injection Pressure Drop vs Pore Volume injected (Experiment 5) .....	65
Figure 37 SW Recovery Factor vs Pore Volume Injected (Experiment 5).....	66
Figure 38 SW Pressure Drop vs Pore Volume Injected (Experiment 5) .....	66
Figure 39 Foam Flooding Recovery Factor vs Pore Volume Injected (Experiment 5) ....	68
Figure 40 Recovery Factor vs Pore Volume Injected (Experiment 5).....	68
Figure 41 Foam Recovery Pressure Drop vs Pore Volume Injected (Experiment 5).....	69
Figure 42 Brine Permeability Pressure Drop vs Pore Volume Injected (Experiment 6) .	70
Figure 43 Oil Injection Pressure Drop vs Pore Volume injected (Experiment 6) .....	71

Figure 44 SW Recovery Factor vs Pore Volume Injected (Experiment 6).....	72
Figure 45 SW Pressure Drop vs Pore Volume Injected (Experiment 6) .....	72
Figure 46 Foam Flooding Recovery Factor vs Pore Volume Injected (Experiment 6) ....	74
Figure 47 Recovery Factor vs Pore Volume Injected (Experiment 6).....	74
Figure 48 Foam Recovery Pressure Drop vs Pore Volume Injected (Experiment 6).....	75
Figure 49 Brine Permeability Pressure Drop vs Pore Volume Injected (Experiment 7) ..	76
Figure 50 Oil Injection Pressure Drop vs Pore Volume Injected (Experiment 7) .....	77
Figure 51 SW Recovery Factor vs Pore Volume Injected (Experiment 7).....	78
Figure 52 SW Pressure Drop vs Pore Volume Injected (Experiment 7) .....	78
Figure 53 Foam Flooding Recovery Factor vs Pore Volume Injected (Experiment 7) ....	80
Figure 54 Recovery Factor vs Pore Volume Injected (Experiment 7).....	80
Figure 55 Foam Recovery Pressure Drop vs Pore Volume Injected (Experiment 7).....	81
Figure 56 Normalized Pressure Drop vs Normalized Pore Volume Injected.....	82
Figure 57 Normalized Recovery Factor vs Normalized Pore Volume Injected .....	83
Figure 58 Normalized Pressure Drop vs Normalized Pore Volume Injected .....	84
Figure 59 Normalized Recovery Factor vs Normalized Pore Volume Injected .....	84
Figure 60 Normalized Pressure Drop vs Normalized Pore Volume Injected .....	85
Figure 61 Normalized Recovery Factor vs Normalized Pore Volume Injected .....	86

## **LIST OF ABBREVIATIONS**

<b>EOR</b>	:	Enhanced Oil Recovery
<b>OOIP</b>	:	Oil Originally in Place
<b>GOR</b>	:	Gas Oil Ratio
<b>SAG</b>	:	Surfactant-Alternating-Gas
<b>WOR</b>	:	Water-Oil-Ratio
<b>AOS</b>	:	Alpha-Olefin-Sulfonate
<b>FS</b>	:	Fluor-Surfactant
<b>MMP</b>	:	Minimum Miscibility Pressure
<b>S<sub>wi</sub></b>	:	Initial Water Saturation
<b>HPHT</b>	:	High Pressure High Temperature
<b>S<sub>oi</sub></b>	:	Initial Oil Saturation
<b>OIIP</b>	:	Oil Initially in Place
<b>RF</b>	:	Recovery Factor
<b>MRF</b>	:	Mobility Reduction Factor
<b>WAG</b>	:	Water-Alternating-Gas



## **ABSTRACT**

Full Name : [Ahmed Elsayed Ahmed Ibrahim Abdelaal]

Thesis Title : [Optimization of CO<sub>2</sub>/N<sub>2</sub> Foam Parameters For EOR In Sandstone Reservoirs]

Major Field : [Petroleum Engineering]

Date of Degree : [December 2019]

N<sub>2</sub> and CO<sub>2</sub> are the most common gases utilized in foam EOR techniques. Foam with these two gases has been widely investigated and many studies compared between the foam generated by both of them. CO<sub>2</sub> exists at supercritical conditions at typical reservoir conditions. Its ability to create stable foam is reduced at these conditions. CO<sub>2</sub>-foam has a common problem to become weaker above its supercritical conditions of 1100 psi and 31° C. N<sub>2</sub> is found to form stronger foam at the same conditions when it is compared to CO<sub>2</sub>. As a result, the advantages of using CO<sub>2</sub> foam collapsed due to the weakness of CO<sub>2</sub> at supercritical conditions. The mobility of gas is not effectively decreased resulting in low sweep efficiency. Few researches have investigated usage of CO<sub>2</sub>/N<sub>2</sub> mixture foam in bulk medium. Limited work in the literature showed that addition of N<sub>2</sub> to CO<sub>2</sub> may produce more stable foam in oil free porous media. Many core flooding experiments using three injection pumps were conducted in this research to study the performance of mixed CO<sub>2</sub>/N<sub>2</sub> foam flooding in crude oil saturated sandstone cores. Alpha- Olefin Sulfonate (AOS) was used as a foaming agent to form the foam. Three parameters were investigated which are total injection rate, CO<sub>2</sub>/N<sub>2</sub> ratio, foam quality.

Three dependent variable were monitored during the experimental work, which are pressure drop that can give a good indication about foam stability, oil recovery and breakthrough time. Optimization of the previous parameters was performed to get maximum oil recovery factor and a good stable foam. Addition of  $N_2$  to  $CO_2$  introduces a solution to the issue of  $CO_2$  foam weakness in typical reservoir conditions. Increasing the percentage of  $N_2$  enhances the oil recovery and produces more stable foam up to 20 % by volume. Then the oil recovery will be affected adversely by increasing  $N_2$  above the range of 20 %. It is also concluded that increasing foam quality up to 80 % produces a foam with finer texture that gives more stability and recovery. Then, as the foam quality increases up to 90 %, the foam becomes coarser and resulting in instability issues and less recovery. This weakness may be attributed to dry foam formed with this foam quality range. It is also found that increasing the total injection rate affects foam stability and oil recovery. High injection rates produce higher shear rates that may lead to foam collapse. This research has proposed many useful outcomes. These outcomes may help to provide a solution for supercritical  $CO_2$  foam instability issues in sandstone reservoirs. It may help to understand more about foam behavior, as it is a developing research area.

## ملخص الرسالة

الاسم الكامل: أحمد السيد أحمد ابراهيم عبدالعال

عنوان الرسالة: تعظيم الاستفادة من عوامل خليط رغوة غاز ثاني أكسيد الكربون وغاز النيتروجين في تحسين استخلاص النفط من الخزانات الرملية

التخصص: هندسة البترول

تاريخ الدرجة العلمية: ديسمبر 2019

يعتبر غازي ثاني أكسيد الكربون والنيتروجين من أكثر الغازات المستخدمة في عملية تحسين استخلاص النفط. حيث ان الرغوة الناتجة من استخدام هذين الغازين تم دراستها بشكل موسع سابقا وتناولت دراسات كثيرة مقارنات بين كليهما. يتواجد غاز ثاني أكسيد الكربون في الحالة فوق الحرجة في ظروف الخزانات من الضغط ودرجة الحرارة. فقدرته على تكوين رغوة مستقرة وقوية تقل تحت هذه الظروف. فالرغوة الناتجة من استخدام غاز ثاني أكسيد الكربون تصبح اضعف في ظروف اعلى من 1100 باوند لكل انش و31 درجة سيليزية. على النقيض، يكون غاز النيتروجين رغوة مستقرة وقوية تحت نفس الظروف من الضغط ودرجة الحرارة عند مقارنته بغاز ثاني أكسيد الكربون. ونتيجة لذلك، فان مميزات استخدام رغوة غاز ثاني أكسيد الكربون تقل وتضعف بسبب ضعف غاز ثاني أكسيد الكربون في ظروف الغاز فوق الحرجة. فقد وجد ان حركية الغاز لا تقل بالشكل المطلوب وينتج عنها ضعف في ازالة النفط. لقد درست القليل من الدراسات خليط رغوة غازي ثاني أكسيد الكربون والنيتروجين معا من اجل تعظيم الاستفادة من مميزات هذه التقنية. وكذلك تناولت القليل من البحوث هذا الخليط في عينات من الصخور بدون وجود النفط. وبناء على ما تم في الدراسات السابقة، فقد تم اجراء عدد من التجارب باستخدام ثلاث مضخات في توقيت واحد لضخ غاز ثاني أكسيد الكربون و النيتروجين و محلول AOS في عينات من الحجر الرملي. حيث تم دراسة تأثير ثلاثة عوامل وهي معدل الضخ ونسبة النيتروجين و جودة الرغوة وأثرها على استقرار الرغوة ومدى الزيادة في تحسين استخراج النفط. فقد وجد ان اضافة غاز النيتروجين الى رغوة ثاني أكسيد الكربون قد قدمت حلا لضعف رغوة ثاني أكسيد الكربون بمفرده.

فقد وجد أيضا أن زيادة نسبة غاز النيتروجين قد حسنت نسبة استخلاص النفط وقد ولدت رغوة مستقرة حتى الوصول الى نسبة تقترب من 20 %. وبزيادة النسبة حتى وصلت الى 35 % قد ادت الى استقرار الرغوة ولكن أثرت بالسلب على انتاجية النفط. وقد استنتج أيضا أنه بزيادة جودة الرغوة من 70 % الى 80 % قد أدى الى تكوين رغوة مستقرة وزيادة في تحسين استخلاص النفط. ولكن عند زيادة جودة الرغوة لتصل الى 90 % تصبح الرغوة حجمها أكبر ويؤدي الى تكوين رغوة أضعف. هذا الضعف يمكن تفسيره بتكون رغوة جافة عند الوصول الى هذه النسبة. وقد وجد انه بزيادة المعدل الكلي للضخ يؤثر على كلا من تحسين استخلاص النفط واستقرار الرغوة. حيث يؤدي زيادة معد الضخ الى توليد قوى قص أكبر مما يؤدي الى عدم استقرار وضعف الرغوة المتكونة. وفي النهاية, فان هذا البحث قد قدم نتائج جيدة. فقد تساعد هذه النتائج في ايجاد حل لرغوة غاز ثاني اكسيد الكربون في الحالة الحرجة وعدم استقرارها في الصخور الرملية. وقد تساعد أيضا على فهم الكثير عن سلوك الرغوة لانها منطقة بحث مازالت تحت الدراسة والتطوير.

# CHAPTER 1 INTRODUCTION

After oilfield discovery, oil starts to move to the wellbore naturally due to the reservoir primary driving mechanisms. Natural energy of reservoirs such as change in rock volume, expansion of dissolved gases, aquifer influx, and gravity urges the hydrocarbons moving from the reservoir to the wellbore as pressure drops with production of different reservoir fluids (oil, water, or gas). The recovery of primary mechanisms ranges from 5 % to 20 % of the oil initially in place (OOIP) (Stalkup, 1984).

Then field operators apply the secondary recovery methods to overcome this low range of recovery. Secondary recovery techniques include water or gas injection into the reservoir for pressure maintenance or re-pressurizing it to serve as a gas and/or a water driving mechanism to effectively displace oil. These techniques provide sustainability of higher production rates and extending the productive reservoir life. Gas injection at top of oil reservoir or into the gas cap or water injection below the oil water contact (OWC) are the most common practices. Generally, the oil recovery before tertiary recovery stage ranges from 20 % to 40 % out of the oil initially in place (OIIP). However, Stalkup, 1984 reported that recoveries may be higher or lower in other cases. Tzimas et. Al, 2005 highlighted a higher recovery range from 35 % to 45 % of OIIP after secondary recovery stage in their investigation of oil reservoirs in North Sea.

A significant amount of oil remained in the reservoir after secondary recovery stage and becomes a target for next stage of recovery by application of EOR techniques. Oil that is left behind after secondary recovery because it was not exposed by the injected fluid, or can be due to the capillary pressure that exists between oil and water in the contacted portions that trap it.

Van Poollen, et.al 1981, classified EOR techniques into the following groups:

1. Thermal methods, which include steam flood (including hot water injection), steam stimulation (known as “huff and puff”), and in-situ combustion.
2. Chemical methods, which include polymer flooding, polymer/surfactant injection, and caustic flooding.
3. Miscible displacement techniques, which include injection of carbon dioxide gas, inert gas or hydrocarbon gas with high pressure.

Immiscible displacement method with carbon dioxide injection was not mentioned in the above classification, although it is an EOR mechanism.

To recover this residual oil, the oil and gas industry has invested billions of dollars to develop technologies of enhanced oil recovery (EOR). One of the most outstanding EOR methods developed was that one based on the usage of CO<sub>2</sub>. By 2010, the number of CO<sub>2</sub>-EOR projects around the world had reached 127, from which 112 projects were in the United States (P.Y. Zhang., 2004).

Under high pressure and temperature in the reservoir, CO<sub>2</sub> mixes with the oil to generate a low surface tension and a low viscosity fluid that can be displaced easily. Moreover, CO<sub>2</sub> has the ability of invading zones that were not invaded by water before resulting in reducing and releasing trapped oil (Holm, L.W., (1982). In 1952, Whorton, Brownscombe, and Dyes of the Atlantic Refining Company had the first patent for CO<sub>2</sub> EOR technology (Whorton L.P., Brownscombe E.R., and Dyes, A.B., 1952).

CO<sub>2</sub> injection as EOR method can be grouped into immiscible and miscible flooding depending on different phase behavior of crude oil and CO<sub>2</sub> at reservoir conditions (Holm, 1982; Hanssen et al., 1994). Miscible CO<sub>2</sub> displacement only takes place under specific conditions determined by four variables: reservoir pressure, reservoir temperature, oil chemical composition and injected gas composition (J.S. Solbakken et. al 2013). Carbon dioxide can be miscible with oil resulting in reduction in oil viscosity, causing oil swelling and lowering interfacial tension under specific conditions of pressure, temperature and oil composition. Moreover, CO<sub>2</sub> exists at huge amounts either in the natural resources or many industrial processes. Additionally, carbon dioxide injection underground has an environmental impact. Carbon capture, utilization, and storage (CCUS) is significant for reducing CO<sub>2</sub> emissions that attract researchers' attention nowadays (Li et al. 2016) (Zhang et al. 2011). Briefly, CO<sub>2</sub> injection for EOR is considered an efficient method to get more oil after water flooding or pressure depletion. Moreover, it is used to sequester large quantities of CO<sub>2</sub> at subsurface reservoirs (Malik et al. 2000).

Despite the previous advantages of using CO<sub>2</sub> in EOR, its success is limited by some challenges in many cases. The major problem of CO<sub>2</sub> injection technique is gas channeling that reduces its sweep efficiency significantly. Carbon dioxide is less viscous than the oil, so it has higher mobility than the oil in the porous media. CO<sub>2</sub> begins to move faster through viscous oil and high permeability zones.

This situation of unfavorable mobility results in viscous fingering which leads to gas breakthrough at earlier life of producing wells. The second problem is gravity override that arises from gravity segregation due to density difference between formation fluids and CO<sub>2</sub>. This issue could affect the oil recovery and sweep efficiency as well. Eventually, considerable oil quantities are left behind as the reservoir is partially swept by CO<sub>2</sub> resulting in poor volumetric sweep efficiency. Recovered oil reduction can be more severe in case the reservoir is heterogeneous.

Many studies have been performed trying to increase CO<sub>2</sub> sweeping efficiency and to reduce its mobility. Water alternating gas (WAG) injection technique and CO<sub>2</sub>-foam were introduced to find a solution to the previous problems. The WAG technique is a cyclic alternative injection of water and CO<sub>2</sub>, which can postpone the early gas breakthrough and improve the gas sweep efficiency when it compared with pure CO<sub>2</sub> injection. Injection of CO<sub>2</sub> foam was introduced in 1950s to solve the issues of poor sweep efficiency and early gas breakthrough happened during pure CO<sub>2</sub> injection flooding technique as reported by (Bond et al. 1958).



Foam is defined in a porous medium as gas dispersion into liquid (Gaughlitz et al. 2002). The continuous phase is liquid and the discontinuous phase is gas. Then, a thin film called lamella will be formed. The advantage of foam flooding initially results from the reduction of gas mobility (Schramm et. al 2009, Bian et al. 2012). At the same time, apparent viscosity of the gas will be enhanced when foam is added (Huh et. al 2008). Successful foam flooding depends mainly on the strong foam generation in a porous media, which previously investigated by (Nguyen et al. 2014) (Zhu et al. 2004).

Surfactant solution and CO<sub>2</sub> co-injection or the surfactant solution alternating CO<sub>2</sub> (SAG) injection are utilized for foam generation in the porous media to decrease gas mobility and to increase the sweep efficiency (Pang et. al 2010, Chen et al. 2014, Zhang et al. 2013). The sweep efficiency due to injected CO<sub>2</sub> large mobility can be improved by injection of CO<sub>2</sub> foam to generate a more desired mobility ratio to enhance sweeping efficiency and to increase oil recovery (Talebian et al. 2013).

CO<sub>2</sub> foam was introduced as a solution to overcome the challenges associated with CO<sub>2</sub> injection for EOR. Many experiments and pilot tests were performed to explore various mechanisms and to avoid challenges such as lack of stability, coalescence and restrictions of CO<sub>2</sub> foam. Carbon dioxide exists at a supercritical state under typical reservoir conditions with enhanced performance of mass transfer, which can produce environment of acidic or low pH. Under typical reservoir conditions, CO<sub>2</sub> generates weak and unstable foam as discussed in the literature. Additionally, at harsh environments, CO<sub>2</sub> foam is not recommended due to its instability and weakness at these conditions.

A stable and strong foam is significant in performing a successful CO<sub>2</sub> injection job as strong foam helps in displacement stabilization and sweep efficiency enhancement. Solving the problems and exploring the CO<sub>2</sub> foam mechanisms for EOR can lead to successful CO<sub>2</sub> foam field applications. Moreover, it can be used for oil recovery improvement for different oil reservoirs. The literature review highlights the most up to date studies of the mechanisms, applications, problems associated with CO<sub>2</sub>-foam technique and highlights the trials to solve these issues.

CO<sub>2</sub> and N<sub>2</sub> foams are the most widely used foams in EOR applications. In some applications, both of them are used for the same purpose, but they have different effects and properties in EOR. The main goal of this study is to test CO<sub>2</sub>/N<sub>2</sub> mixed foam performance in High Pressure/High Temperature oil saturated sandstone cores after secondary recovery by water flooding. This study will evaluate the effect of changing CO<sub>2</sub>/N<sub>2</sub> ratio, injection rate and Foam quality on the performance of CO<sub>2</sub>/N<sub>2</sub> mixed foam. With the increasing number of CO<sub>2</sub>-EOR projects worldwide in addition to the necessity of CO<sub>2</sub> sequestration, this study results may provide an effective solution to improve and optimize the parameters for CO<sub>2</sub>/N<sub>2</sub> foam Injection at sandstone reservoirs, which can produce more oil and keep as much as CO<sub>2</sub> underground.

## **CHAPTER 2 LITERATURE REVIEW**

### **2.1 CO<sub>2</sub> Foam as a Potential Technique for EOR**

The work conducted by (Patton et al. 1983) and (Mast 1972) proved that foam injection can be considered as an effective way for gas channeling mitigation, mobility ratio modification, sweeping efficiency enhancement, and oil recovery increasing in the gas flooding process. Foam has the capability of blocking high permeability zones and forcing the gas to enter the low permeability zones, consequently the crude oil recovery will be increased. Foams can block water and gas in porous media that is so-called water and gas shut off to improve sweep efficiency.

Aarra et al. 2011, showed that CO<sub>2</sub> foam is able to block water and gas at HPHT conditions in carbonate rocks. The gas blockage occurs at lower pressure gradient. The foam showed a reduction in blocking ability at high injection pressure, so production of gas started to increase. Some experiments showed the foam has ability to block water as well. CO<sub>2</sub> foam can improve oil recovery through different mechanisms including interfacial tension reduction because of the surfactant existence, enhancement of sweeping efficiency by increasing the viscosity of injected fluid, high permeability zone blockage, and forcing the injected fluid to invade the low permeability zones, decreasing the viscosity of oil and causing oil to swell by the CO<sub>2</sub> gas.

The performance of CO<sub>2</sub> foams in water blockage is affected by using either equilibrium or non-equilibrium conditions between the fluid in a porous medium and the injected fluid. Mass transfer takes place between the two fluids under non-equilibrium conditions.

Foam results in high water permeability in the cores when non-equilibrated fluids, that are not in equilibrium state, are used. This observation can be attributed to the transfer of mass between fluids and dissolving of CO<sub>2</sub> in the injected fluid. The mass transfer kinetics existing among the fluid phases has a great impact on foam stability. The N<sub>2</sub> foams stability is greater than CO<sub>2</sub> foams at typical reservoir conditions, so N<sub>2</sub> foam is performing better than CO<sub>2</sub> foam in water blockage. Therefore, foam instability is one of the most significant challenges of CO<sub>2</sub> foam application.

Foam injection in fractured reservoirs had been investigated by several authors. Mukherjee et al. 2014, Sanders et al. 2012, Li et al. 2009, Yu et al. 2008, had reported several pilots for foam conducted successfully in conventional reservoir rocks. On the other hand, limited number of foam pilots were performed in fractured reservoir rocks, and reported they were not successful (Enick et al. 2012, Smith 1988). These observations can be as a result of the lack of understanding regarding mechanisms of foam creation in fractured systems such as: snap-off, film division and leave-behind, or due to the operation challenges or shortage of suitable surfactants as reported by (Castanier et. al 1995).

However, some modern studies prove in-situ generation of foam in a single fractures as reported by (Buchgraber et al. 2012, Kovsky et al. 1995), leads to improved volumetric sweep efficiency and diversion of flow within a carbonate fractures network at the time of co-injection of gas and surfactant (Yan et al., 2006, Fernq et al., 2014). Foam injection in naturally fractured reservoirs is growing as a potential EOR method by introducing and using new surfactant types, (Cui et al. 2014, Farajzadeh et al. 2012, Elhag et al. 2014).

Fernq et al. 2015, studied the ability of pure CO<sub>2</sub> and CO<sub>2</sub> foam to be applied for EOR in fractured carbonate systems. It was concluded that CO<sub>2</sub> foam injection increased oil recovery when it compared to injection of pure CO<sub>2</sub> in fractured core samples. This can be due to better viscous displacement plus diffusion

## **2.2 CO<sub>2</sub> Foam Issues**

Injection of CO<sub>2</sub> foam for EOR applications mostly takes place at reservoirs condition at which CO<sub>2</sub> exists at supercritical condition. CO<sub>2</sub> at supercritical conditions produces weak and unstable foam. Supercritical CO<sub>2</sub> have properties midway between liquid and gas. Its critical temperature is 31.1°C and its critical pressure is 1071.8 psi. It acts like a supercritical fluid above its critical conditions to fill a container like a gas but with a density like a liquid. Generally, foam is not a stable fluid system. Especially, CO<sub>2</sub> foam becomes weaker and less stable at harsh conditions of pressure and temperature, which limited its applications. Compared to N<sub>2</sub>, CO<sub>2</sub> foam is less stable at HPHT conditions, which imposes a challenge to select the foam agents. The success of CO<sub>2</sub> flooding process depends on generating strong and stable foam to ensure the privileges of CO<sub>2</sub> EOR technique.

There are three processes by which the foam can be transported in porous medium, which are snap-off, leave behind, and lamella division. Kovscek et. al 1994, reported that gas diffusion and capillary coalescence decrease stability of foam. Aronson et al. 1994, also reported that diffusion of gas through the lamella and water drainage are the major reasons behind foam instability. CO<sub>2</sub> foams breakdown at reservoir conditions. In addition, salinity affects the foam flooding performance significantly. At high pressure in the reservoir, CO<sub>2</sub> becomes more lipophilic and more hydrophilic which causes CO<sub>2</sub> foam generation more difficult and becomes less stable, which considered a great challenge that limits its application.

CO<sub>2</sub> foams performance is influenced by the physicochemical properties of surfactants, such as dissolved electrolytes, pressure, and temperature. CO<sub>2</sub> foam stability is affected by the hydrophilic-lipophilic balance (HLB) value of surfactants. Zhang et al., 2013, reported that stability of CO<sub>2</sub> foam depends on the surfactant molecules arrangement on the interface between CO<sub>2</sub> and water. Foam must remain stable without failure when it meets oil to have a successful application (Almajid and Kovscek, 2016). Recently, experimental and theoretical research is performed to overcome the challenges of foam instability during EOR flooding applications (Sun et al., 2014). Additionally, a lot of laboratory work done to select and test the foam agents responsible for the stability of CO<sub>2</sub> foam (Khalil et. al 2006, Skoreyko et al., 2012, Sun et al. 2014 Fernø et al. 2015, Farzaneh et al. 2015).

Few field studies investigated the performance of different surfactants and different mixtures of them on CO<sub>2</sub> foam at HPHT conditions (Enick et al., 2012, Wang et al. 2017). Their results proved that CO<sub>2</sub> foams performance at high temperatures depends on surfactant type. CO<sub>2</sub> foam stability enhances with pressure but it is dependent on the HLB value of the surfactants used.

### **2.3 Factors Affecting CO<sub>2</sub> Foam Stability**

The success of foam application in EOR mainly depends on foam stability. Foams with high stability under typical reservoir conditions can efficiently reduce injected gas mobility, force the gas to enter low permeability zones and improve the volumetric sweep efficiency. Surfactant type, reservoir fluid types, placement method, injected gas properties, reservoir conditions and characteristics are affecting foam stability. Foam is unstable thermodynamically; consequently, it is hard to stable it under field applications.

Foam stability can be adversely affected by residual oil presence so; oil saturation should be as low as possible to minimize the effect on foam stability and strength. Stability of foams generated by using surfactants is greatly affected by temperature. Generally, surfactants have the affinity to degrade and losing their desired function, which is an important issue. In addition, surfactant adsorption takes place on reservoir rock in porous media, which results in huge chemicals consumption (Espinosa et.al 2010, J. Yu et al., 2012).

Yin et al. 2009, studied the effect of oil saturation on behavior of CO<sub>2</sub> foam. CO<sub>2</sub> foam flooding were performed on Berea sandstone cores saturated with oil. It was found that differential pressure increases as oil saturation decreases. Differential pressure increase reflects increase in foam stability. Fig.1 shows the effect of oil saturation on foam stability.

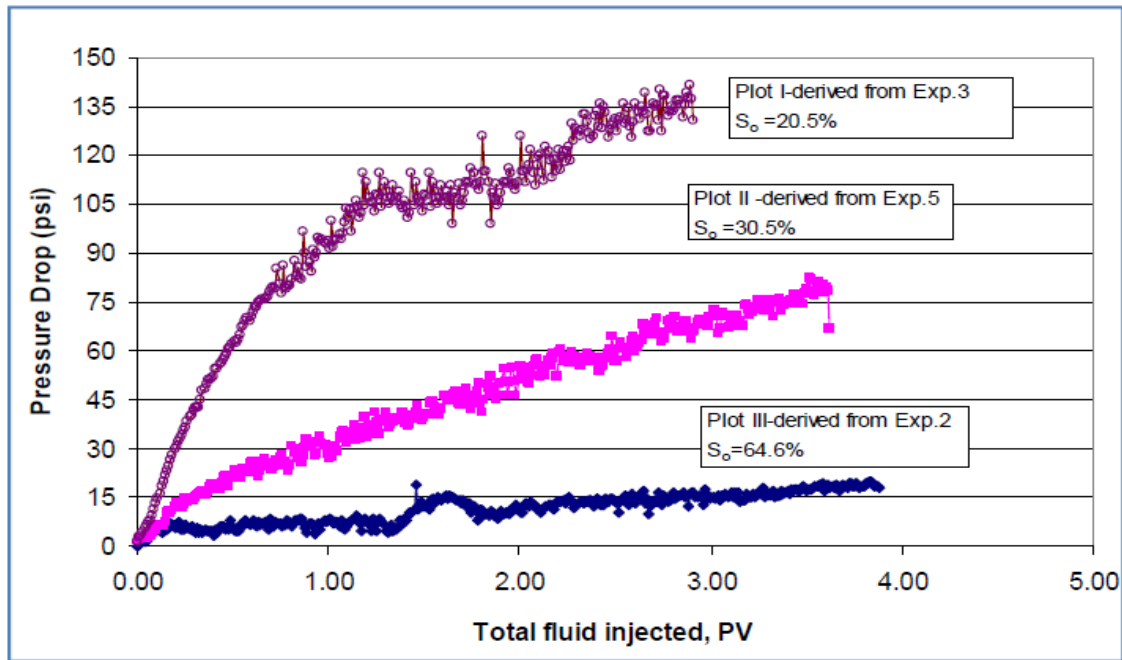


Figure 1 Oil Saturation Effect on CO<sub>2</sub> Foam Stability Flooding (Yin et al. 2009 )

Surfactant adsorption on rock surface results in decrease in surfactant concentration with distance so, foam will be no longer effectively stable and strong. Therefore, the surfactant selection is a key element in the success of gas injection assisted EOR. Successful surfactant must have the capability of generating strong and stable foam with least amount of adsorption on rock surface under typical reservoir conditions ( Farajzadeh et. al 2009).

Kapetas et al. 2015, studied temperature effect on foam stability and strength. They used AOS surfactant with temperature range from 20 to 80°C.



They observed destabilization of foam with increase in temperature. A severe reduction was recorded in apparent foam viscosity to reach 50 % of its original value when the temperature was 80 °C. Amro et al. 2015, studied pressure effect on the stability of bulk foam using N<sub>2</sub> and CO<sub>2</sub> foams in their experiments with pressure range up to 10 MPa.

They observed a decrease in CO<sub>2</sub> foam stability with increase in pressure and attributed this observation to enhancement of gas permeation between two adjacent gas bubbles. Moreover, CO<sub>2</sub> shows extraction on surfactant resulting in decreasing surfactant concentration in the leading film phase, which leads to foam film destabilization and reducing visco-elasticity at the end. On the other hand, pressure element does not affect the stability of N<sub>2</sub> foam.

## **2.4 CO<sub>2</sub> Foam Properties and its Comparison with N<sub>2</sub> Foam**

The most common foams used in EOR applications are CO<sub>2</sub> and N<sub>2</sub>. They have different properties and different effects on EOR although; both of them are used for the same purposes. Comparison between N<sub>2</sub> and CO<sub>2</sub> is established due to the lower pH and lower interfacial tension with CO<sub>2</sub> foam, increased viscosity and density for supercritical CO<sub>2</sub>, CO<sub>2</sub> solubility effects, and CO<sub>2</sub> foams higher mobility (Farajzadeh et al. 2009, Adkins et al., 2010). Zhou 2011 reported that the aqueous solution saturated with CO<sub>2</sub> at 0.1 MPa and 25 °C has a pH value of 3.7 or below. CO<sub>2</sub> foams are not recommended in harsh environment because their stability decreases compared to N<sub>2</sub> foams.

Li et al. 1993, performed a study to compare between CO<sub>2</sub> and N<sub>2</sub> water-based foams. They discovered that the effect of gas type on foam viscosity is minimal.

CO<sub>2</sub> exhibits remarkable physical properties change alongside increasing conditions of pressure and temperature. Chang et. al 1999, investigated the impact of flow rate and foam quality on properties of CO<sub>2</sub> foam at conditions of 38 ° C and 145 bar. This study concluded that as the flow rate increases, the foam mobility increases.

Khalil et. al 2006, studied the pressure effect in crushed carbonate rocks on properties of foam at 50 ° C and observed that as the pressure goes up, the CO<sub>2</sub>-foam mobility increases.

Du et al. 2008, established a comparison between CO<sub>2</sub> and N<sub>2</sub> foams by performing core flooding experiments. This work was analyzed by using CT-scan. It was observed that N<sub>2</sub> foam propagation is piston- like displacement unlike CO<sub>2</sub>. CO<sub>2</sub> foam showed weakness as system pressure increased, but N<sub>2</sub> foam showed no change.

Farajzadeh et al. 2009, established a comparison between N<sub>2</sub> and CO<sub>2</sub> foams at wide range of temperature and pressure. They observed that N<sub>2</sub> foam was stronger than CO<sub>2</sub> foam and CO<sub>2</sub> foam turned to be weaker as pressure and temperature increase, but the N<sub>2</sub> foam strength remained the same. Also, it was observed that N<sub>2</sub> foam had better frontal displacement. Farajzadeh et al. 2010 concluded that foams created by CO<sub>2</sub> are weaker than foams created by N<sub>2</sub>, although little pressure drop was reported across the cores.

Aarra et al. 2014, established a comparison between the properties of CO<sub>2</sub> and N<sub>2</sub> foams in porous media under a wide pressure range from 30 bar to 280 bar. CO<sub>2</sub> or N<sub>2</sub> and AOS surfactant co-injection with foam quality of 80 % and 40 mL/h injection rate is used to generate foam. The study shows that CO<sub>2</sub> foam at 30 bar was strong and supercritical CO<sub>2</sub> foam was weaker. N<sub>2</sub> foams were more stable and stronger than CO<sub>2</sub> ones.

It is concluded that mass transfer is key element for CO<sub>2</sub> foam stability. It was concluded that N<sub>2</sub> can create much stronger and more stable foams than CO<sub>2</sub>.

**Table 1 Summarizes the Results of Comparing CO<sub>2</sub> and N<sub>2</sub> Foams Performance.**

Reference	Key Points
<b>Li et al. (1993)</b>	<ol style="list-style-type: none"> <li>1. The effect of gas type on foam viscosity is minimal</li> <li>2. CO<sub>2</sub>-foam properties are highly affected by pressure and temperature</li> </ol>
<b>Chang and Grigg (1999)</b>	As flow rate increases, the CO <sub>2</sub> -foam mobility increases
<b>Khalil and Asghari (2006)</b>	As the pressure increases, the CO <sub>2</sub> foam mobility increases
<b>Du et al. (2008)</b>	<ol style="list-style-type: none"> <li>1. Propagation of N<sub>2</sub> foam was found to be piston like displacement unlike CO<sub>2</sub></li> <li>2. CO<sub>2</sub> foam showed weakness as system pressure increased, but N<sub>2</sub> foam showed no change</li> </ol>
<b>Aarra et al. (2014)</b>	<ol style="list-style-type: none"> <li>1. CO<sub>2</sub> foam at 30 bar was strong</li> <li>2. supercritical CO<sub>2</sub> foam was weaker</li> <li>3. N<sub>2</sub> foams were more stable and stronger than CO<sub>2</sub> ones</li> <li>4. Mass transfer is key element for CO<sub>2</sub> foam stability</li> <li>5. N<sub>2</sub> can create much stronger and more stable foams than CO<sub>2</sub></li> </ol>

## **2.5 Solutions for CO<sub>2</sub> Foam Instability**

It is important for foam to stay stable when it meets oil. The main challenge that faces CO<sub>2</sub> foam is easy ruptures when it meets oil (Almajid et. al 2016). Mannhardt et al. 1998 reported that some trials were done to cause foam lamellae stabilized and to delay foam decay. Destruction of lamellae and coalescence of foam impede foam creation under typical reservoir conditions. Generally, it is known that collapse of foam takes place under reservoir conditions and this greatly affects the performance of foam flooding as reported by Xu et al. 2016. Some attempts were performed trying to solve foam instability challenge such as using polymers, nanoparticles, injection rate control and replacing part of CO<sub>2</sub> with N<sub>2</sub>.

### **2.5.1 Polymer**

Polymer addition is one of the solutions that attract many researchers to work on it. Dong et al., 2016 added Hydrolyzed Poly-Acrylamide (HPAM) to the foam solution. This process is called Polymer Enhanced Foam (PEF). This enhances strength of lamellae surface, decelerates the gas diffusion and weakens the drainage of liquid membrane. As a result, stability of foam and flooding efficiency greatly increased.

Many attempts have studied the impact of many parameters like polymer types, molecular weights, concentration, salinity, concentration of surfactant on performance of PEF (Dong et al., 2016, Hernando et al. 2016, Lande 2016, Sydansk, 1994a, Azdarpour et al. 2013, Perttamo 2013; Shen et al. 2006). Sydansk 1994b reported that the performance of PEF in the case of high viscous crude oil is better than that of less viscous crude oil. Sydansk 1994, also reported that PEF can help in the injectivity due to its shear-thinning characteristics.

Generally, the characteristics of foam have been significantly enhanced with polymer addition; even it is added at small concentration.

A polymer called AVS used by Xu et al. 2016, trying to increase the stability and foamability of CO<sub>2</sub> foam at salinity of 50,000 ppm and 10,000 ppm at high temperature of 65 C. The proposed foam agent enhances the stability of foam in a good way. CO<sub>2</sub> foam apparent viscosity increased by around 36% in high permeability cores compared to the viscosity in low permeability cores. Fig. 2 and Fig. 3 show AVS results as a good polymer for foams stability.

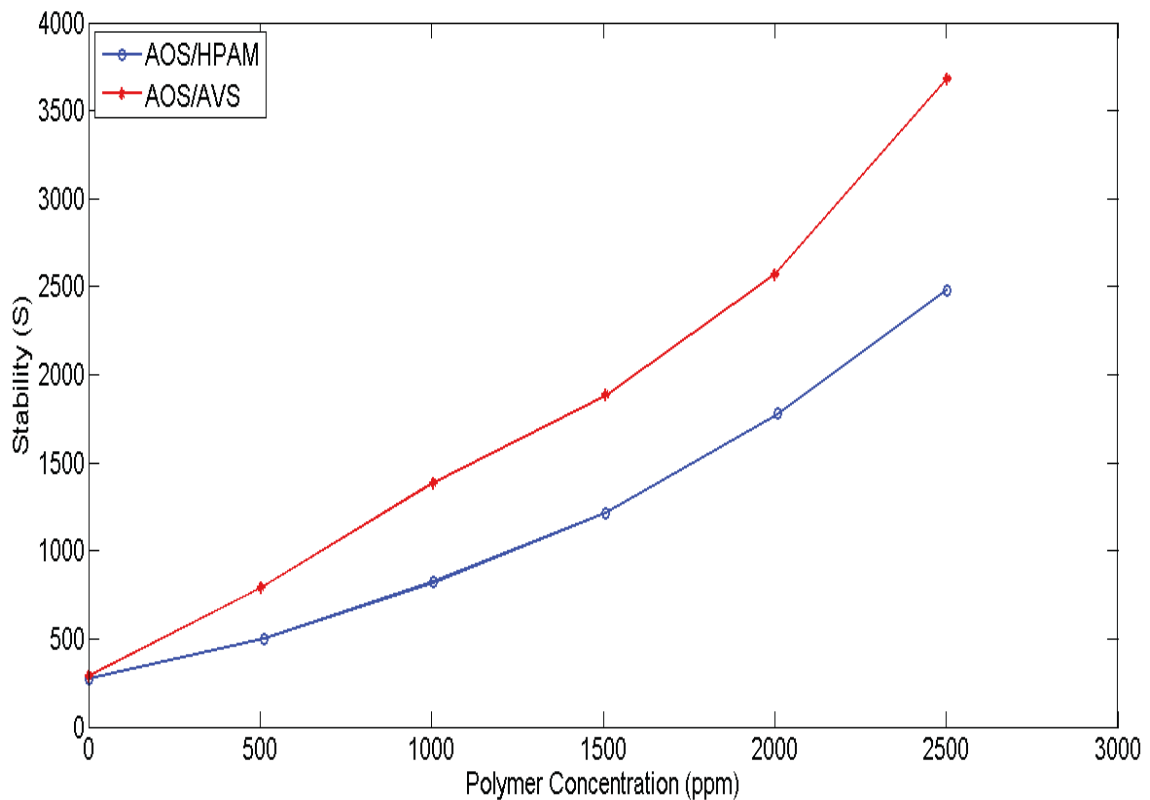


**Figure 2 Novel Polymer Effect on Stability of CO<sub>2</sub> Foam Compared to (HPAM), (CaCl<sub>2</sub> 100 ppm, 25oC +NaCl 10,000 ppm) Produced by (Xu et. Al 2016)**

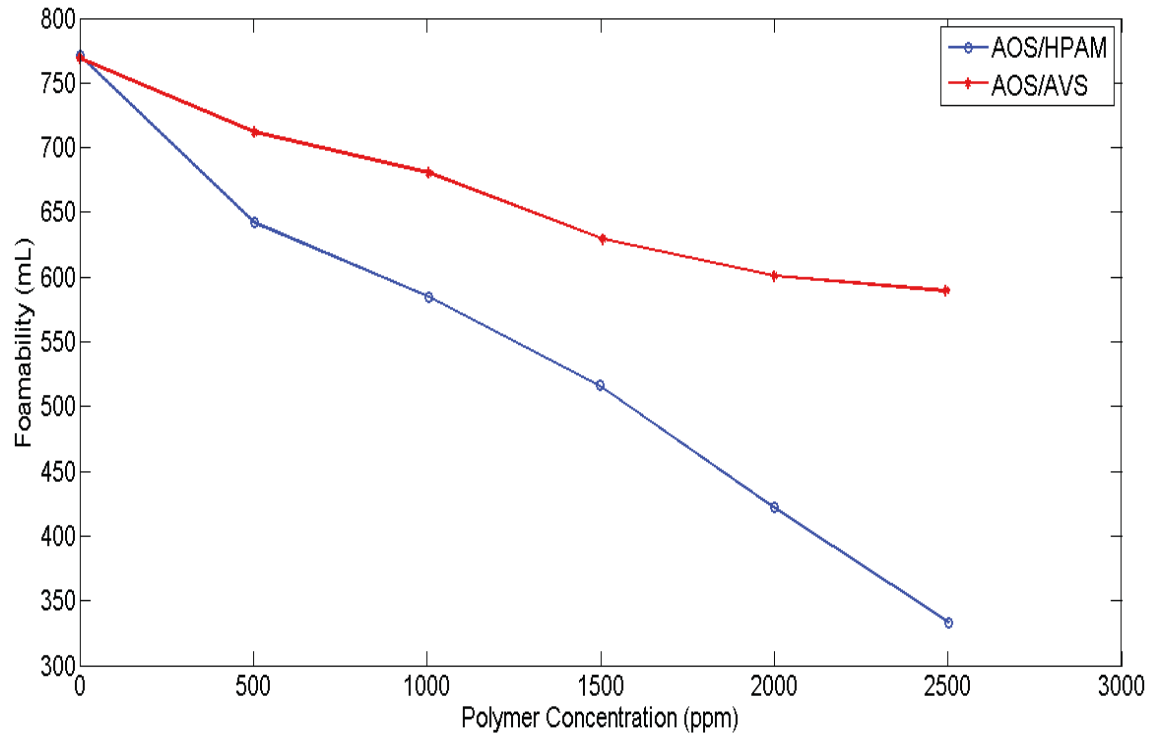


**Figure 3 Novel Polymer Effect on CO<sub>2</sub> Foam Foamability Compared to (HPAM), (CaCl<sub>2</sub> 100 ppm, 25°C +NaCl 10,000 ppm) produced by (Xu et. Al 2016)**

Pu et al. 2017, used various anionic and nonionic polymer acrylamide (PAM) polymers under HPHT conditions in reservoirs. They investigated the performance of CO<sub>2</sub> and N<sub>2</sub> gases in the presence of oil. The best CO<sub>2</sub> foam performance exists above CO<sub>2</sub> supercritical conditions. Additionally, recovery of oil was greatly increased through using the previous polymers in formations with heterogeneity.

Ahmed et al. 2017, used an associative polymer named Superpusher B 192. Then, its performance was compared with the conventional HPAM performance for improving foam viscosity and stability. By addition of the suggested polymer, foam stability and the apparent viscosity were found to be higher. Therefore, it has a potential to enhance the performance of foam in enhanced oil recovery applications.

HPAM molecules breakdown thermally under high temperature conditions. HPAM also got thickening due to it is sensitive to salt. HPAM is not preferred to be used in high salinity reservoirs where its molecules will be in colloidal form. As a result, HPAM causes foam to be thickened and that greatly affected under harsh reservoir conditions. To solve this problem, functional groups can be added to the conventional HPAM to cause this polymer capable of resisting high temperature or/and high salinity environment. 2-acrylamido-2-methylpropane sulphonic acid (AMPS), N-vinylpyrrolidones (NVP), and Polyvinylpyrrolidones (PVP), are the most widely used functional groups.

Li et al. 2017, investigated addition of an organic amine named octadecyl dipropylene triamine for generation of CO<sub>2</sub> foam. The results showed that this organic amine is good for generation of CO<sub>2</sub> foam and enhanced features at a high salinity and temperature range. The performance of CO<sub>2</sub> foam is significantly enhanced regarding foam apparent viscosity and stability. Table 2 shows a summary for studies of using polymers and surfactants to enhance CO<sub>2</sub> foam stability.

**Table 2 Summarizes Polymers and Surfactants Usage for CO<sub>2</sub> Foam Stability Reported by (Amin Daryasafar et.al 2018)**

<b>References</b>	<b>Key Results</b>
<b>(Xu et al. 2016)</b>	<ol style="list-style-type: none"> <li>1. Introduced a foam formula (AOS/AVS/N70K-T)</li> <li>2. Foam stability and foamability of CO<sub>2</sub> foam can be enhanced by using this foaming formula</li> </ol>
<b>(Wang et al. 2017)</b>	<ol style="list-style-type: none"> <li>1. Surfactant type is significant for CO<sub>2</sub> foams at higher temperature.</li> <li>2. Stability of CO<sub>2</sub> foams depends on surfactant HLB value.</li> </ol>
<b>(Pu et al. 2017)</b>	<ol style="list-style-type: none"> <li>1. Investigated various nonionic and anionic PAM polymers</li> <li>2. Compared both N<sub>2</sub> and CO<sub>2</sub> foams</li> <li>3. Polymers mixture can improve oil recovery</li> </ol>
<b>(Li et al. 2017)</b>	<ol style="list-style-type: none"> <li>1. Investigated an organic amine, octadecyl dipropylene triamine on CO<sub>2</sub> foam.</li> <li>2. Viscosity and stability enhanced at high temperatures and salinities</li> </ol>
<b>(Ahmed et al. 2017)</b>	<ol style="list-style-type: none"> <li>1. Utilized new polymer (Superpusher B 192) and HPAM</li> <li>2. Foam viscosity and stability were enhanced by new polymer usage</li> </ol>



Dong et al. 2016, reported that field application of polymer added to CO<sub>2</sub> foam gives good results for reservoirs with heterogeneity. A pilot test of Polymer Enhanced Foam (PEF) was conducted in Gudao oil field in 2003.

### **2.5.2 Nanoparticles**

Nanoparticles can be used to generate lamellae with the desired viscoelastic property so that foam can exhibit small deformations without lamellae rupture as reported by (Sun et al., 2014). Utilization of nanoparticles could cause stability for foam structure through two mechanisms. The first is nanoparticles adsorption into the interface between gas and liquid that can decrease the gravity drainage of liquid film. The second mechanism is nanoparticles stratification in bulk solution that could prevent the foam from collapsing by forming a 3D network structure. On the other hand, there are some obstacles of using nanoparticles in EOR such as aggregation of particles as they have large specific surface area as reported by (Ranjit et.al 2013). Moreover, preparation of a suitable nanomaterial is costly and nanomaterials could have undesirable effect on health of living things and environment.

### **2.5.3 Injection Rate Control**

Gas and surfactant solution injection rate can be controlled to decelerate lamellae thinning. Generally, foam behavior can be either shear thinning or shear thickening. Viscosity of foam and gas can be affected by flow rate, and surfactant solution flow rates affects foam quality.

Llave et al. 1990, investigated the factors resisting foam flowing as a function of foam quality and injection rate. They reported that a shear thinning behavior exists between injection rate and foam mobility. As the shear rate decreases, the foam viscosity increases. It was also reported that increase in foam quality could also improve foam apparent viscosity. Osei-Bonsu et al. 2016, reported that in case of foam quality exceeding 90%, dry foam will be formed and thus, the capillary pressure will increase surpassing the thickness of lamellae resulting in lamellae rupture.

#### **2.5.4 Replacing part of CO<sub>2</sub> by N<sub>2</sub>**

The disadvantage of CO<sub>2</sub> foam is that it becomes weaker as pressure increases. It is shown in the literature that N<sub>2</sub> can be stable at harsh conditions. Adding small quantity of N<sub>2</sub> to CO<sub>2</sub> could possibly solve or enhance this challenge. N<sub>2</sub> exists in a subcritical state under most of the reservoir conditions. Harris 1987, studied the rheological properties of mixed gas foams to be used fracturing fluids. He concluded that replacing part of CO<sub>2</sub> with N<sub>2</sub> could increase viscosity at low shear rates.

Few researches investigated usage of CO<sub>2</sub>/N<sub>2</sub> mixture foam in bulk medium. A study of foam texture and stability of mixed foam using both CO<sub>2</sub> and N<sub>2</sub> was introduced in porous media, but it was free of oil. Siddiqui et.al 2017, in that study conducted oil-free steady-state foam flooding experiments to study the CO<sub>2</sub>/N<sub>2</sub> foam performance at supercritical conditions of CO<sub>2</sub> in sandstone cores. Eventually, a formula for foam injection (N<sub>2</sub> fraction added, injection rate and foam quality) was obtained that leads to generation of a stable foam at these conditions.

Another study conducted by (Hassan et. al 2017) in which some core flooding experiments performed to compare the recovery factor and foam strength by foamed CO<sub>2</sub> to foamed mixed CO<sub>2</sub>/N<sub>2</sub>. Two types of surfactant were used which are alpha-olefin-sulfonate (AOS) and fluoro-surfactant (FS-51). N-decane was used as a model oil in all these experiments at temperature of 50°C. Brine flooding is performed prior to every gas or foam flooding to simulate the actual steps behavior in the oil and gas industry. This work highlighted a better foamed gas performance when it compared to gas injection without foam. Oil recovery using foam was greater than by gas injection based on his experimental work and conditions. Moreover, fluoro-surfactant approved its capability to produce foam in high salinity environments.

## **CHAPTER 3 PROBLEM STATEMENT AND RESEARCH OBJECTIVE**

CO<sub>2</sub> miscible flooding is considered the first method to recover light to medium oils and comes at the second place out of all EOR techniques due to many advantages. Despite the previous advantages of using CO<sub>2</sub> in EOR, its success is limited by some challenges in many cases. The major problem of CO<sub>2</sub> injection technique is gas channeling that significantly reduces its sweep efficiency. CO<sub>2</sub> is less viscous than the oil, so it has higher mobility than the oil in the porous media. CO<sub>2</sub> begins to move faster through viscous oil and high permeability zones. This situation of unfavorable mobility results in viscous fingering which leads to early gas breakthrough towards producing wells. The second problem is gravity override that arises from gravity segregation due to density difference between formation fluids and CO<sub>2</sub> can also affect the oil recovery and sweeping efficiency. Eventually, considerable oil quantities are left behind as the reservoir is partially swept by CO<sub>2</sub> resulting in poor volumetric sweep efficiency. Recovered oil reduction can be more severe if the reservoir is heterogeneous. Foam CO<sub>2</sub> was introduced as a technique to overcome this challenge to reduce the mobility of CO<sub>2</sub> and try to achieve a piston-like oil displacement. Finally, gas breakthrough could be delayed and the sweep efficiency could be improved.

Injection of CO<sub>2</sub> foam for EOR applications always takes place in deep sandstone reservoirs at which CO<sub>2</sub> exists at supercritical condition. CO<sub>2</sub> at supercritical conditions produces weak and unstable foam. Supercritical CO<sub>2</sub> has properties midway between liquid and gas. Its critical temperature is 31.1°C and its critical pressure is 1071.8 psi. It acts like a supercritical fluid above its critical conditions to fill a container like a gas but with a density like a liquid. Generally, foam is not a stable fluid system. Especially, CO<sub>2</sub> foam becomes weaker and less stable at harsh conditions of pressure and temperature, which reduces its usage. Compared to N<sub>2</sub>, CO<sub>2</sub> foam is less stable at typical reservoir conditions, which considered a challenge to select the foam agents. The success of CO<sub>2</sub> flooding process depends on generating strong and stable foam to ensure the privileges of CO<sub>2</sub> EOR technique.

Few researches in the literature investigated the mixed CO<sub>2</sub>/N<sub>2</sub> foam in EOR. Starting from the previous outcomes, the current study will investigate the CO<sub>2</sub>/N<sub>2</sub> mixed foam performance in oil saturated sandstone cores after secondary recovery by water flooding. It will investigate the effect of changing CO<sub>2</sub>/N<sub>2</sub> ratio, injection rate and foam quality on the performance of CO<sub>2</sub>/N<sub>2</sub> mixed foam. With the increasing number of EOR CO<sub>2</sub> projects worldwide in addition to the necessity of CO<sub>2</sub> sequestration, this study results may provide an effective solution to improve and optimize the parameters for CO<sub>2</sub>/N<sub>2</sub> foam Injection in sandstone reservoirs, which can produce more oil and keeping as much as CO<sub>2</sub> underground.

## **CHAPTER 4 Methods and Materials**

### **4.1 Materials**

#### **4.1.1 Salts**

Mineral salts were used to prepare synthetic brine solutions for formation brine and seawater brine. For that purpose, a group of mineral salts were used as following:

1. Sodium chloride ( $\text{NaCl}$ )
2. Calcium chloride ( $\text{CaCl}_2$ )
3. Magnesium chloride ( $\text{MgCl}_2$ )
4. Sodium sulfate ( $\text{Na}_2\text{SO}_4$ )
5. Sodium bicarbonate ( $\text{NaHCO}_3$ )

#### **4.1.2 Core samples**

Berea sandstone cores were utilized to run core flooding tests. All core samples are 10 inch length and 1.5 inch diameter.

#### **4.1.3 Gases**

Carbon dioxide ( $\text{CO}_2$ ) and nitrogen ( $\text{N}_2$ ) gases were supplied from Saudi Industrial Gas Company.  $\text{CO}_2$  was used as an injection fluid and  $\text{N}_2$  was used as injection fluid as well as to operate the valves in the core flooding system.

#### **4.1.4 Crude Oil**

An intermediate crude oil was used in this study to saturate the sandstone core samples by oil injection after formation brine saturation.

#### **4.1.5 Surfactants**

Alpha-Olefin Sulfonate (AOS) is a type of anionic surfactant processed by  $\alpha$ -olefin gas-phase sulfonation and continuous neutralization. It is good in making rich and fine foam.

## 4.2 Devices

### 4.2.1 Core Flooding System

The core flooding setup consists mainly of four parts: the fluid-delivery unit, the core unit, the production unit, and the data-acquisition and control unit. An illustration of this setup is shown in Fig. 4, Fig. 5 and Fig. 6.

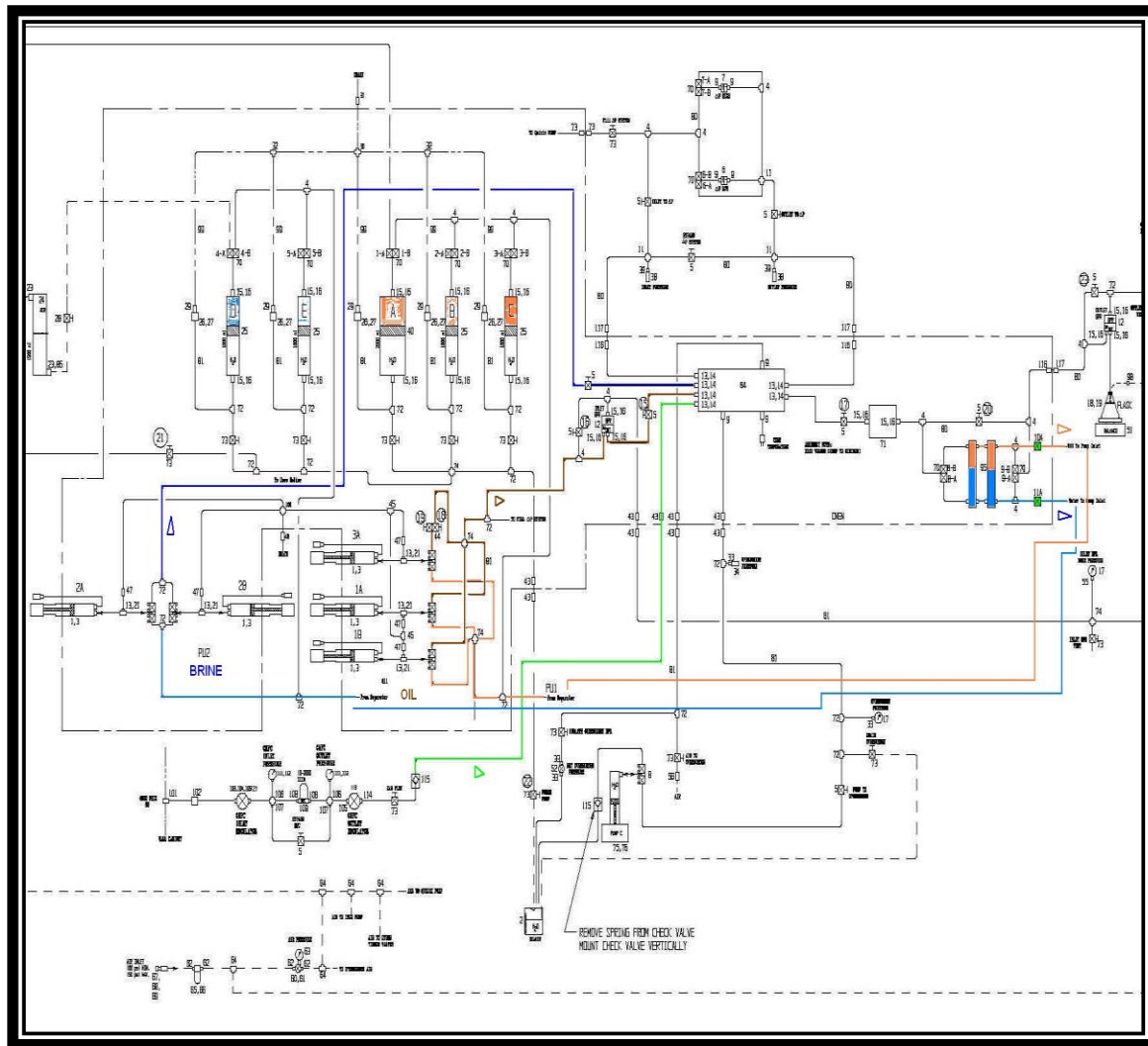


Figure 4 Schematic of Core Flooding System





**Figure 5 Core Flooding System from the Backside**



**Figure 6 Core Flooding System from Front side**

### **4.2.2 Laboratory Balances**

Two types of balances were used in this work. A digital analytical balance (Sartorius Cubis® Precision Balance MSE5203S-000-DE) was used to measure the weight of salts in making the brine solutions. The weighing capacity of this balance is 5200 g and its readability is 0.001 g. The other balance, a precision balance (Denver Instrument TR-4102 Toploading Balance), was used to measure both the dry and wet weights of the core. The weighing capacity of this balance is 4100 g and its readability is 0.01 g.

### **4.2.3 External Pumps**

Eldex Model BBB High Pressure Liquid Metering Pump. It has a flowrate range of 1-100 cc/min and high pressure capabilities up to 5000 psi. In addition, Eldex Model AA High Pressure Liquid Metering Pump with a flowrate range of 0.2-10 cc/min and high pressure capabilities up to 5000 psi. These two pumps were used in several tasks:

1. Core saturation initially with the synthetic formation brine
2. Cleaning the flow lines with toluene and distilled water.
3. Filling the core flooding system accumulators with injection liquids (seawater brine and surfactant solution).

Welch DirecTorr Model 8834 Vacuum Pump: it was used for many purposes;

1. Empty nitrogen and carbon dioxide accumulators from air molecules before filling.
2. Relief the high overburden pressure present around the core holder to release the core.
3. In the process of brine filtration.

ISCO 100DX Dual Syringe Pump: its flow rate ranges between 0.01 ml/min - 50 ml/min and pressure capability up to 10,000 psi. This pump was used to inject crude oil, nitrogen and surfactant solution, at different stages throughout the core flooding.

## **4.3 Methods and Procedures**

### **4.3.1 Brine Preparation**

Each of the above-mentioned salts were added, in a specific amount, to distilled/deionized water. The amounts of salts added to prepare both the formation brine and seawater brine are shown in table 3. Each salt was mixed with water separately to ensure it was dissolved completely and to avoid precipitation if salts were mixed together; a chemical reaction could take place. Then each salt solution was added to a bigger flask and water was added to obtain the required final volume. The final solution was stirred for a minimum of two hours and then filtered using a filter paper. The resulting salinity of the formation brine and seawater are 253.88 and 67.708 TDS (total dissolved salts), respectively.

**Table 3 Formula of Formation Brine and Seawater**

<b>Salts</b>	<b>Formation Brine (g/liter)</b>	<b>Seawater (g/liter)</b>
<b>Sodium chloride (NaCl)</b>	157.18	41.17
<b>Calcium chloride (CaCl<sub>2</sub>.2H<sub>2</sub>O)</b>	85.62	2.39
<b>Magnesium chloride (MgCl<sub>2</sub> .6H<sub>2</sub>O)</b>	10.60	17.64
<b>Sodium sulfate (Na<sub>2</sub>SO<sub>4</sub>)</b>	0.37	6.34
<b>Sodium bicarbonate (NaHCO<sub>3</sub>)</b>	0.11	0.17
<b>Total Dissolved Salts (TDS)</b>	253.88	67.71

#### **4.3.2 Core Drying and Firing**

The core was placed in an oven to be heated. This step is necessary to remove any moisture that might be trapped inside. After the heating, the dry weight of the core sample was measured. In later stage, when the core became saturated with brine, its wet weight was measured and used, along with the core dry weight, to estimate its porosity and pore volume.

#### **4.3.3 Core Saturation**

The core sample was placed in a high pressure cell to saturate the core initially with the formation brine. The core was first vacuumed for any trapped air, using the vacuum pump, for nearly 7 hours. Then, formation brine was pumped into the cell until the core became completely immersed. The pump kept injecting the brine until the pressure reached nearly 2000 psi. Then, the pump stopped and the cell was closed and left overnight to let the formation brine penetrate the pores.

Accordingly, the cell pressure would drop slightly. After the saturation, the wet weight of the core was measured to calculate its porosity and pore volume.

#### **4.3.4 Core Placement and Pre-start**

The core was placed inside the core holder. Before inserting the core holder inside the core flooding system, a leakage test was performed. An overburden pressure of about 800 psi was applied to check if there was any leak from the rubber sleeve. If leak was detected, the core would be removed from the core holder to replace the rubber sleeve. If not, after 4-6 hours, the core holder would be placed inside the system and the flow lines would be connected.

#### **4.3.5 Formation Brine Flooding and Oil Injection**

Several pore volumes of formation brine were injected into the core to fully saturate the core and build the pressure up to desired conditions. Injecting the brine was done with three flow rates, 0.5, 1 and 2 cc/min. At each flow rate, the brine injection continued until the pressure drop across the core was stabilized. Then, the drainage process was started by injecting 1-2 PV of crude oil at a rate of 0.5 cc/min, to displace the formation brine and establish the irreducible water saturation. Injection continued until no more brine was produced. The amount of produced brine in the separator would represent the amount of oil trapped into the core. In this process, the initial oil saturation ( $S_{oi}$ ), oil initially in place (OIIP), and the initial water saturation ( $S_{wi}$ ) are calculated as follows: OIIP = Volume of produced brine (cc)

$$S_{wi} = \frac{\text{Pore volume (cc)} - \text{Volume of produced brine (cc)}}{\text{Pore volume (cc)}}$$

$$S_{o_i} = \frac{\text{Volume of produced brine (cc)}}{\text{Pore volume (cc)}} = 1 - S_{w_i}$$

#### 4.3.6 Foam Flooding

After water flooding stage, three injection pumps were used simultaneously to inject supercritical CO<sub>2</sub>, N<sub>2</sub> gas and AOS Surfactant solution with different flow rates at 88 °C. Prior to opening the valves, the pump was used to raise the pressure inside every individual accumulator to the desired pore pressure, which was 1800 psi. This was performed in that way to prevent internal flow from an accumulator to another and to ensure the flow starts immediately without waiting for gas compression if its pressure is below 1800 psi. Once the valves were opened and the injection from different accumulators connected, the flow was steady and the pressure readings from different pumps reflected this case. Two electronic pressure gauges were used directly after the gases accumulators to know the pressure drop across the accumulators. This guaranteed that the pressure drop across the accumulators was almost constant during the experiments. Consequently, the flow rate injected by pumps can represent the gas flow rate entering the core as no more pressure from the pumps used to compress the gas once the experiments started. Co-injection technique was used for foam flooding as the three fluids mixed just before the core. CO<sub>2</sub>-foam was injected after water flooding stage. Co-injection technique was performed to generate foam.

## **CHAPTER 5 Results and Discussion**

This chapter introduces and discusses the outcomes of seven core flooding experiments conducted in this study. Each experiment was performed through the following steps:

1. Formation brine injection to measure the absolute permeability of the cores.
2. Crude oil injection to saturate the cores with crude oil and to establish  $Sw_i$ .
3. Aging in reservoir conditions.
4. Oil flushing.
5. Water flooding as a secondary recovery method.
6. Mixed  $CO_2/N_2$  foam flooding as a tertiary recovery method.

The pressure drop across the core sample takes place because of flow resistance. Its value depends on injection rate, fluid type being injected and core permeability. The values of pressure drop were recorded in each stage of injection and are introduced by charts in this chapter. Moreover, the recovered oil was collected using collection tubes and recovery factor was calculated during each flooding step. The performance of oil recovery is discussed and analyzed for each experiment.

### **5.1 Core Properties Measurements**

The core samples were dried in the oven for 24 hours to ensure that there is no moisture inside the cores. Then, they were placed in a cell connected to a vacuum pump for 4 hours. After that, they were saturated with formation brine using a saturation pressurized cell. The pore volume and porosity were calculated based on the brine density and difference in weight before and after saturation. The core was placed into the core holder and the overburden pressure was applied by using an Isco pump.

Many pore volumes were injected into the core at different flow rates until stabilized pressure drop took place for every individual rate. The absolute permeability was calculated by using stabilized pressure drop and the corresponding flow rate through Darcy law. Afterwards, the crude oil was injected at different flow rates to displace the formation brine until no more water comes out the core to calculate the irreducible water saturation. The main core properties for every experiment are shown in the table 4:

**Table 4 Summary of Cores Properties**

<b>Experiment Number</b>	<b>1</b>	<b>2</b>	<b>3</b>	<b>4</b>	<b>5</b>	<b>6</b>	<b>7</b>
<b>Dry Weight (gram)</b>	609	617	615.5	605	615.5	618.5	608.319
<b>Saturated Weight (gram)</b>	676.48	683.13	681.99	674.51	681.79	683.7	674.01
<b>Weight Difference (gram)</b>	67.48	66.13	66.49	69.51	66.29	65.2	65.691
<b>Diameter (cm)</b>	3.81	3.81	3.81	3.81	3.81	3.81	3.81
<b>Length (cm)</b>	25.4	25.4	25.4	25.4	25.4	25.4	25.50
<b>Area (cm<sup>2</sup>)</b>	11.40	11.40	11.40	11.40	11.40	11.40	11.40
<b>Pore Volume (cm<sup>3</sup>)</b>	58.49	57.31	57.63	60.24	57.45	56.51	56.93
<b>Bulk Volume (cm<sup>3</sup>)</b>	289.58	289.58	289.58	289.58	289.58	289.58	290.71
<b>Vol of Water Recovered (cm<sup>3</sup>)</b>	40	38	36	40	38	36	36
<b>Porosity (%)</b>	20.19	19.79	19.90	20.80	19.84	19.51	19.58
<b>Permeability (md)</b>	97.78	71.83	65	79.58	88.18	77.67	96.82
<b>Swi (%)</b>	31.61	33.70	37.53	33.60	33.86	36.29	36.77
<b>Soi (%)</b>	68.38	66.29	62.46	66.39	66.13	63.70	63.22



## 5.2 Water flooding

Water flooding was conducted as secondary recovery method prior to mixed CO<sub>2</sub>/N<sub>2</sub> foam flooding. This stage was performed with back pressure of 1800 psi and injection rate of 0.5 cc/min. Many pore volumes of seawater were injected until no more oil was recovered. Pressure drop across the core samples was monitored and recorded until stabilized pressure drop was achieved at the end of every experiment. The recovered crude oil was collected and expressed as a fraction of the oil initially in place (OIIP). Additionally, the breakthrough time was observed in the production side and from the pressure drop chart.

The trend by which the pressure drop changed was almost the same for all experiments. Initially, the pressure drop increased as seawater was pushing the crude oil ahead to the production side and this trend continued until breakthrough time. Then the trend started to decline and showing fluctuations ups and downs until the pressure drop stabilized around an average value and no more oil produced. At this stage, the remaining crude oil became immobile despite of extra water injection. This pressure drop variation across the core during water flooding is known for sandstone cores as reported by (S. Shaddel et.al, 2014)

Once the water flooding started, the core sample was saturated with crude oil and connate water. The initial water saturation in all experiments ranged from 0.31-0.37. Initially, crude oil started to appear in the collection tubes shortly after producing the water dead volume. Then, the oil production continued steadily with a considerable amount before the breakthrough took place. After breakthrough, oil and water were produced until the end of water flooding when no more oil was produced.

The recovery factor achieved by water flooding ranged between 45 % and 60 %. The remaining oil became immobile and more water injection was not able to recover more oil.

### **5.3 Mixed CO<sub>2</sub>/N<sub>2</sub> Foam Flooding**

After water flooding stage, three injection pumps were used simultaneously to inject supercritical CO<sub>2</sub>, N<sub>2</sub> gas and AOS Surfactant solution with different flow rates. Prior to opening the valves, the pump was used to raise the pressure inside every individual accumulator to the desired pore pressure, which was 1800 psi. This was performed in that way to prevent internal flow from an accumulator to another and to ensure the flow starts immediately without waiting for gas compression if its pressure is below 1800 psi. Once the valves were opened and the injection from different accumulators connected, the flow was steady and the pressure readings from different pumps reflected this case. Two electronic pressure gauges were used directly after the gases accumulators to know the pressure drop across the accumulators. This guaranteed that the pressure drop across the accumulators was almost constant during the experiments. Consequently, the flow rate injected by pumps can represent the gas flow rate entering the core as no more pressure from the pumps used to compress the gas once the experiments started. Co-injection technique was used for foam flooding as the three fluids mixed just before the core. Table 5 shows the independent, controlled and dependent variables that have been changed during the experiments. Table 6 shows the parameters data used in all experiments.

**Table 5 Different Variables Used in the Experiments**

<b>Controlled Variables</b>	<b>Independent Variables</b>	<b>Dependent Variables</b>
<ul style="list-style-type: none"> <li>• Pressure</li> <li>• Temperature</li> <li>• Reservoir rock type</li> <li>• Crude oil type</li> <li>• Surfactant type</li> <li>• Sea water formulation</li> <li>• Formation brine formulation</li> </ul>	<ul style="list-style-type: none"> <li>• Total injection rate</li> <li>• N<sub>2</sub> percentage</li> <li>• Foam quality</li> </ul>	<ul style="list-style-type: none"> <li>• Recovery factor</li> <li>• Pressure drop</li> <li>• Breakthrough time</li> </ul>

**Table 6 Parameters Data Used for Experiments**

<b>Experiment No</b>	<b>q total</b>	<b>N<sub>2</sub> Ratio</b>	<b>Foam Quality (Fg)</b>	<b>CO<sub>2</sub></b>	<b>q surfactant</b>	<b>q Gas</b>	<b>q N<sub>2</sub></b>	<b>q CO<sub>2</sub></b>
	<b>cc/min</b>	<b>Fraction</b>	<b>Fraction</b>	<b>Fraction</b>	<b>cc/min</b>	<b>cc/min</b>	<b>cc/min</b>	<b>cc/min</b>
1	0.75	0.2	0.8	0.8	0.15	0.6	0.12	0.48
(2)Base case	0.5	0.2	0.8	0.8	0.1	0.4	0.08	0.32
3	1	0.2	0.8	0.8	0.2	0.8	0.16	0.64
4	0.5	0.35	0.8	0.65	0.1	0.4	0.14	0.26
Base case	0.5	0.2	0.8	0.8	0.1	0.4	0.08	0.32
5	0.5	.10	0.8	0.9	0.1	0.4	0.04	0.36
6	0.5	0.2	0.7	0.8	0.15	0.35	0.07	0.28
Base case	0.5	0.2	0.8	0.8	0.1	0.4	0.08	0.32
7	0.5	0.2	0.9	0.8	0.05	0.45	0.09	0.36

## 5.4 Effect of flow rate

The first parameter to be investigated was the total injection rate to get the optimized rate for both foam stability and oil recovery. Three injection rates were used during the foam flooding stage.

### 5.4.1 Experiment 1

Three injection rates were used to estimate the absolute permeability for the core, which were 0.5, 1 and 1.25 cc/min. The core permeability is about 97 md. The pressure drop across the core sample is shown in Fig. 7.

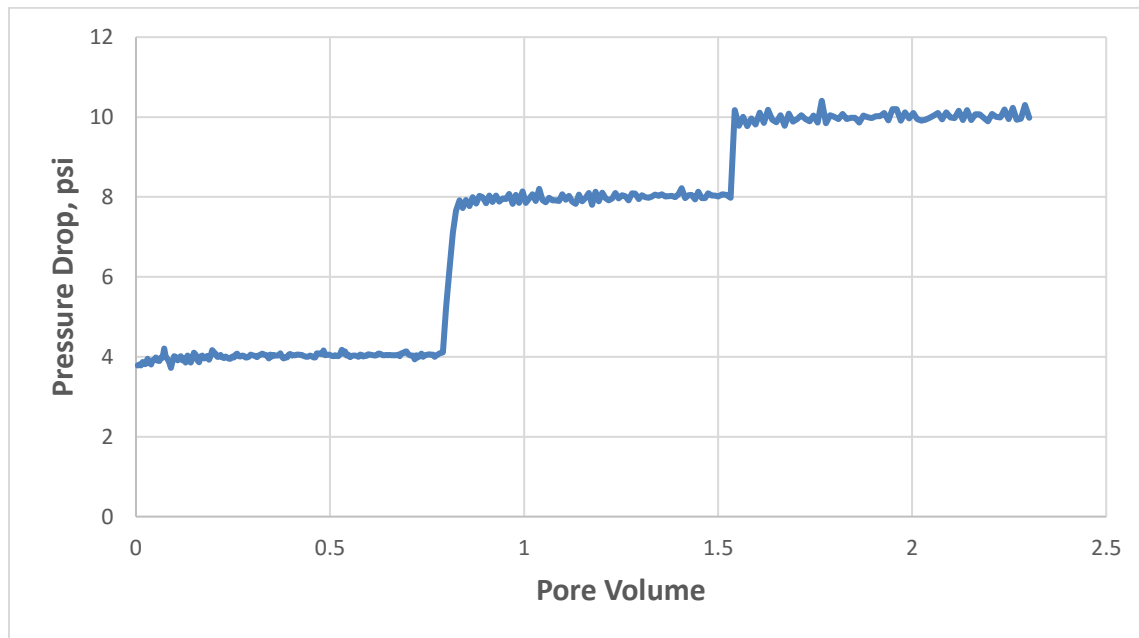
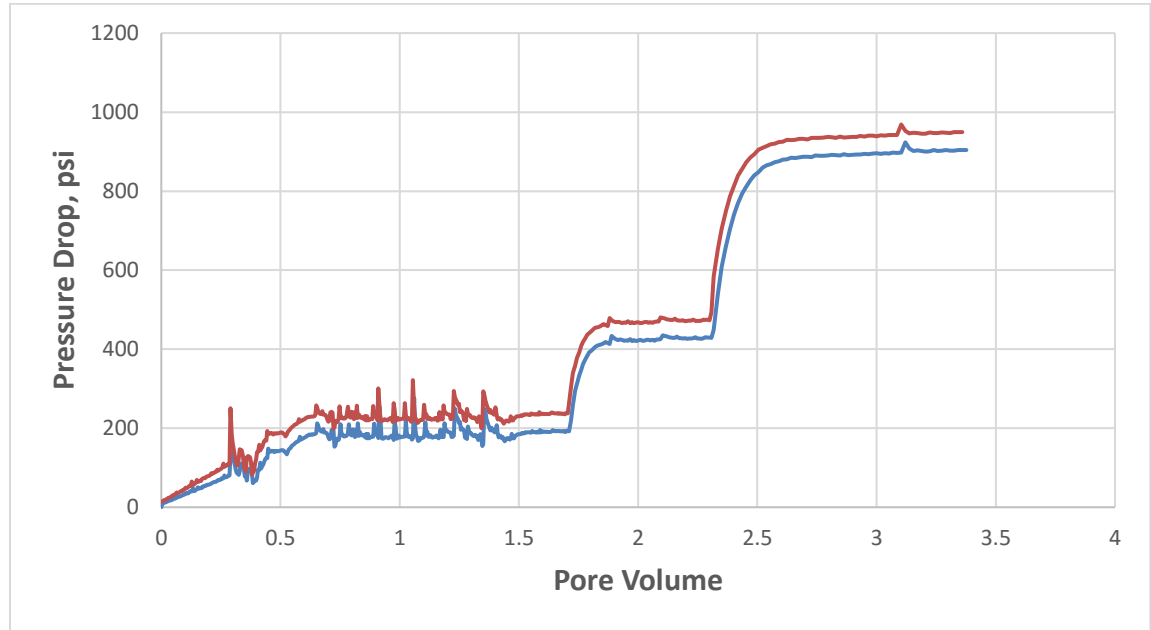


Figure 7 Brine Permeability Pressure Drop vs Pore Volume injected (Experiment 1)

Then, oil injection was performed to saturate the core and to establish initial water saturation, which was about 31.61 %. Different flow rates were used which were 0.5, 1 and 2 cc/min. Fig. 8 shows the pressure drop across the core sample during crude oil injection.



**Figure 8 Oil Injection Pressure Drop vs Pore Volume injected (Experiment 1)**

The core sample was aged for three months. Afterwards, oil flushing with the same crude oil used for saturation was performed by injecting around two pore volumes. Seawater flooding was performed until no more oil was coming out of the core. The breakthrough took place after injecting 0.27 pore volume. The recovery factor and the pressure drop during water flooding stage are shown in Fig. 9 and Fig. 10.

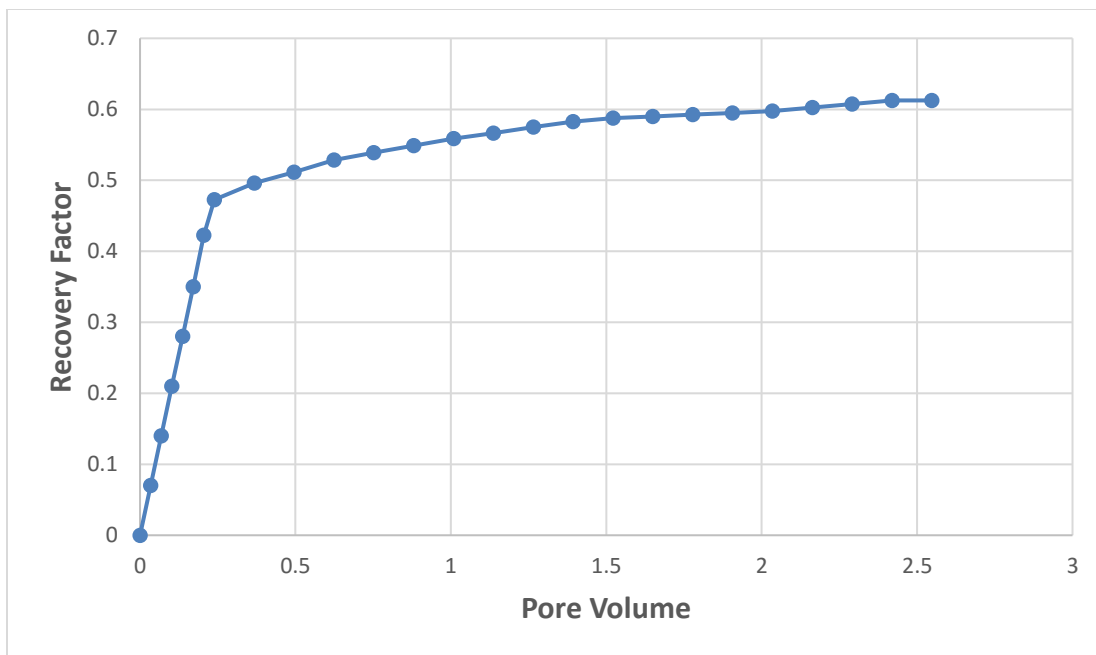


**Figure 9 RF for SW Flooding for Experiment 1**

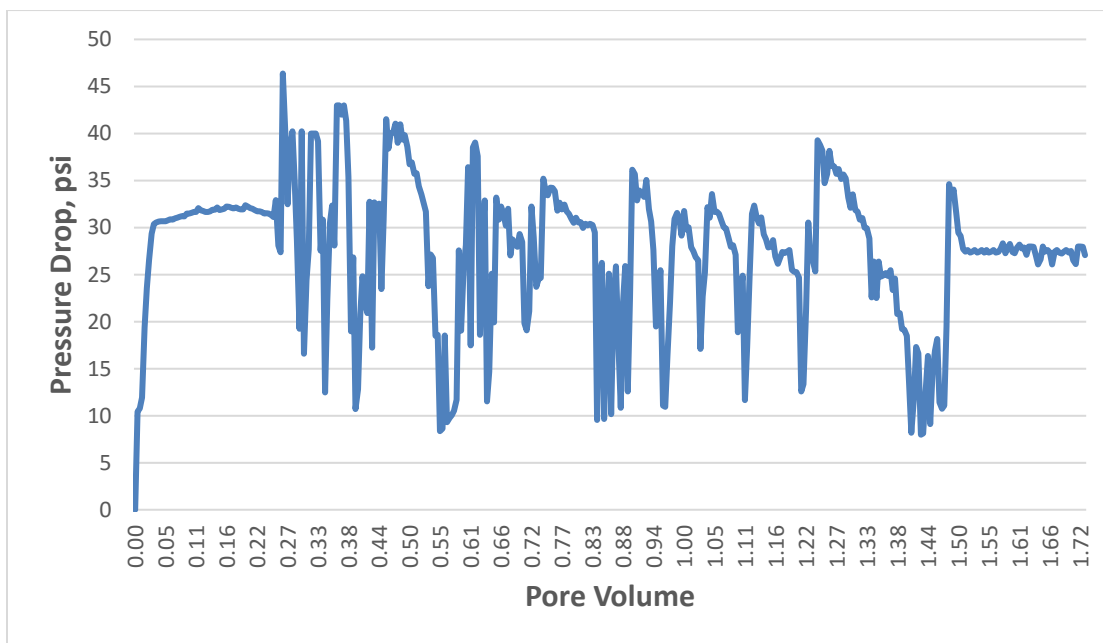


**Figure 10 SW Pressure Drop vs Pore Volume Injected (Experiment 1)**

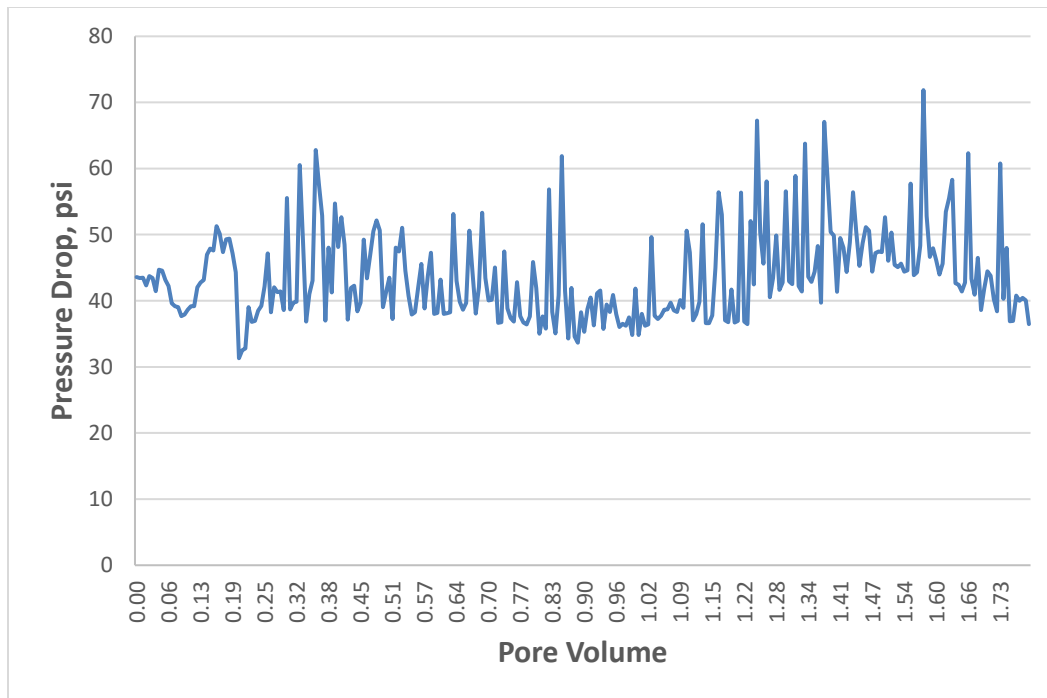
Mixed CO<sub>2</sub>/N<sub>2</sub> Foam flooding was performed following the water flooding stage to recover immobile crude oil that was impossible to be recovered by seawater. Table 7 shows the parameters used in this experiment.

**Table 7 Summary of Experiment 1 Parameters**

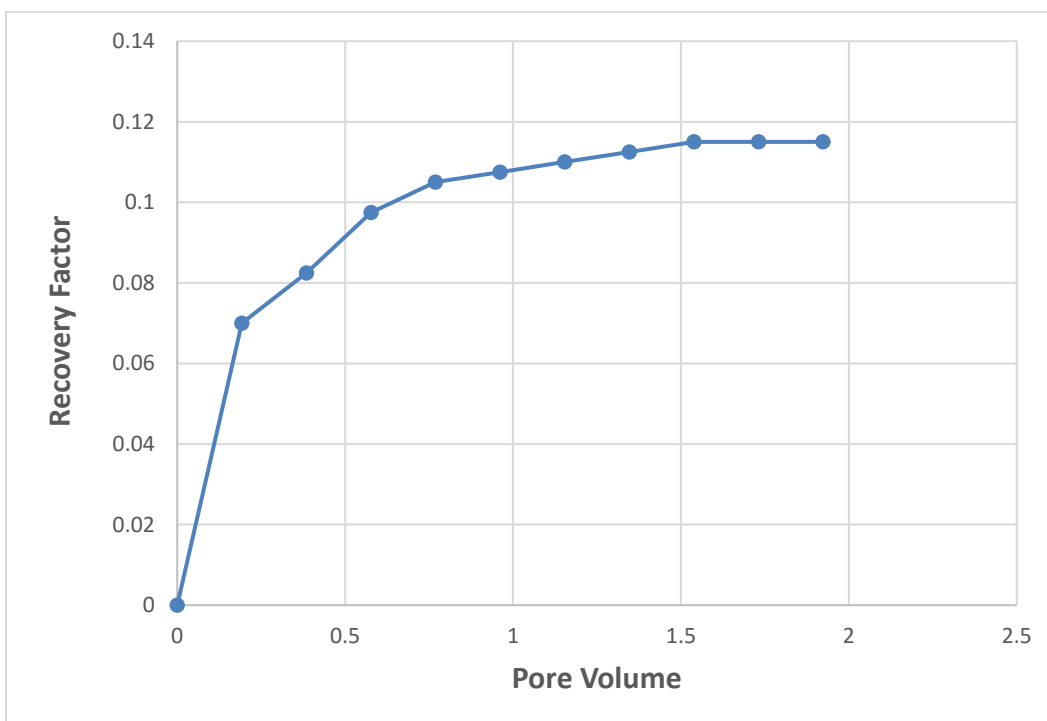
<b>Experiment No</b>	<b>q total</b>	<b>N<sub>2</sub> Ratio</b>	<b>Foam Quality</b>	<b>CO<sub>2</sub></b>	<b>q surfactant</b>	<b>q Gas</b>	<b>q N<sub>2</sub></b>	<b>q CO<sub>2</sub></b>
	<b>cc/min</b>	<b>Fraction</b>	<b>Fraction</b>	<b>Fraction</b>	<b>cc/min</b>	<b>cc/min</b>	<b>cc/min</b>	<b>cc/min</b>
1	0.75	0.2	0.8	0.8	0.15	0.6	0.12	0.48

Fig. 11 shows the pressure drop performance in this stage. Like water flooding, pressure drop increased up to gas breakthrough. Then, the pressure drop decreased and fluctuated up and down and its fluctuation decreased for the continuous injection. When this pressure drop chart was compared to the one developed by (Hasan et.al 2016), it shows greater stability around average value.

The pressure drop increases prior to gas breakthrough because of the high compressibility of gas. After breakthrough, gas flows through an open path with increasing gas saturation, so gas relative permeability increased and pressure drop decreased. The gas breakthrough occurred close to 0.36 PV injected, which is good relatively compared to other tertiary recovery techniques. Fig. 12 shows the recovery performance in this stage.



**Figure 11 Pressure Drop vs Pore Volume injected for Foam Flooding (Experiment 1)**



**Figure 12 RF for Foam Flooding (Experiment 1)**



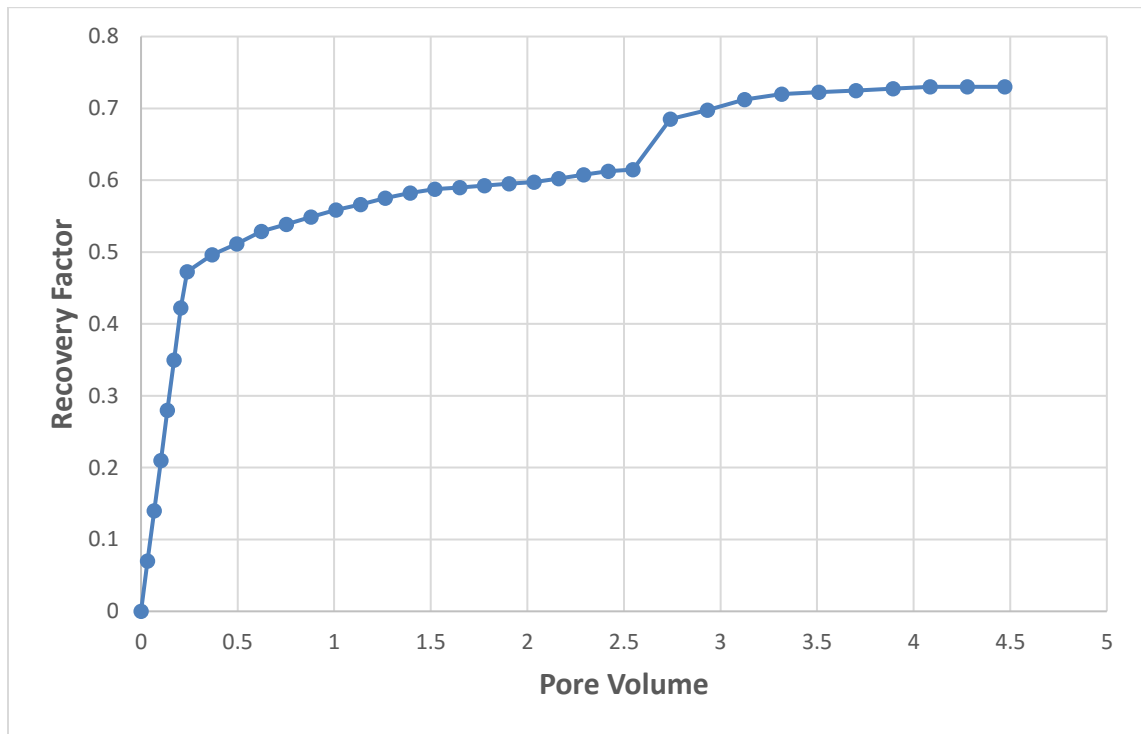


**Figure 13 RF for total Flooding (Experiment 1)**

### 5.4.2 Experiment 2

Two injection rates were used to estimate the absolute permeability for the core, which were 0.5 and 1 cc/min. The core permeability is about 72 md. The pressure drop across the core sample is shown in Fig. 14.

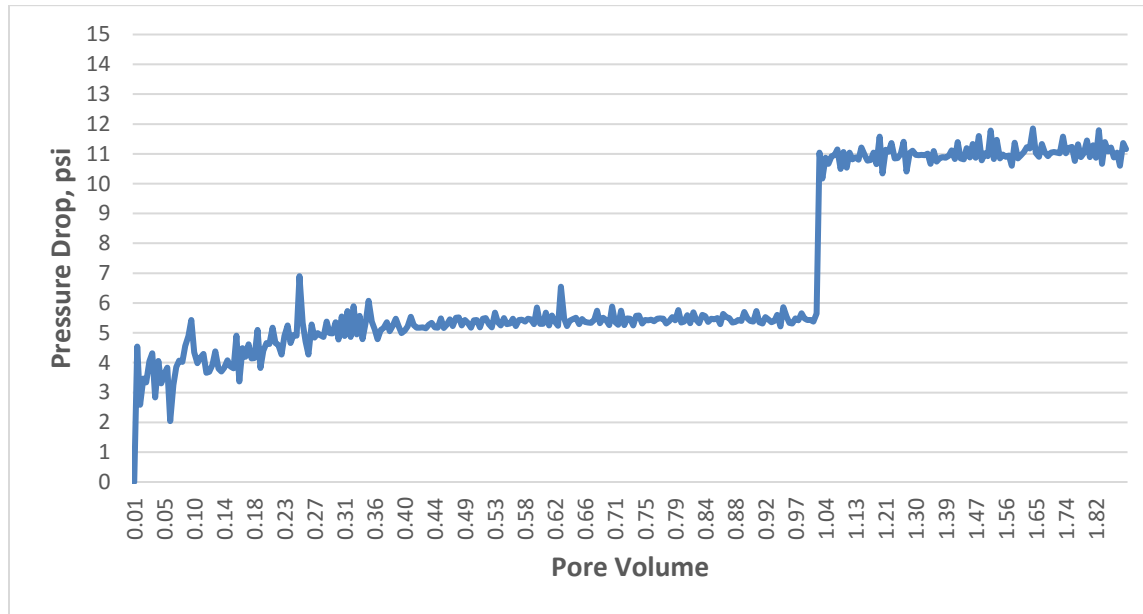


**Figure 14 Brine Permeability Pressure Drop vs Pore Volume injected (Experiment 2)**

Then, oil injection was performed to saturate the core and to establish initial water saturation, which was about 33.7 %. Two flow rates were used which were 0.5 and 1 cc/min. Fig. 15 shows the pressure drop across the core sample during crude oil injection.

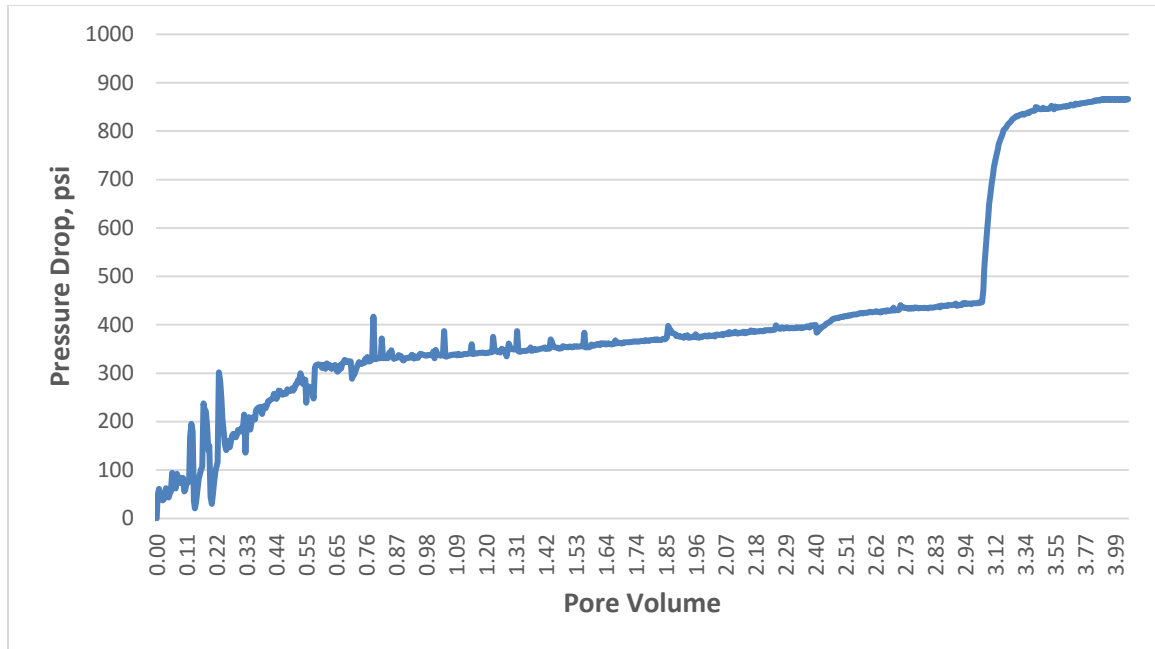


**Figure 15 Oil Injection Pressure Drop vs Pore Volume injected (Experiment 2)**

The core sample was aged for three months. Afterwards, oil flushing with the same crude oil used for saturation was performed by injecting around two pore volumes. Seawater flooding was performed until no more oil came out of the core. The breakthrough took place after injecting 0.38 pore volume. The recovery factor and the pressure drop during water flooding stage are shown in Fig. 16 and Fig. 17.

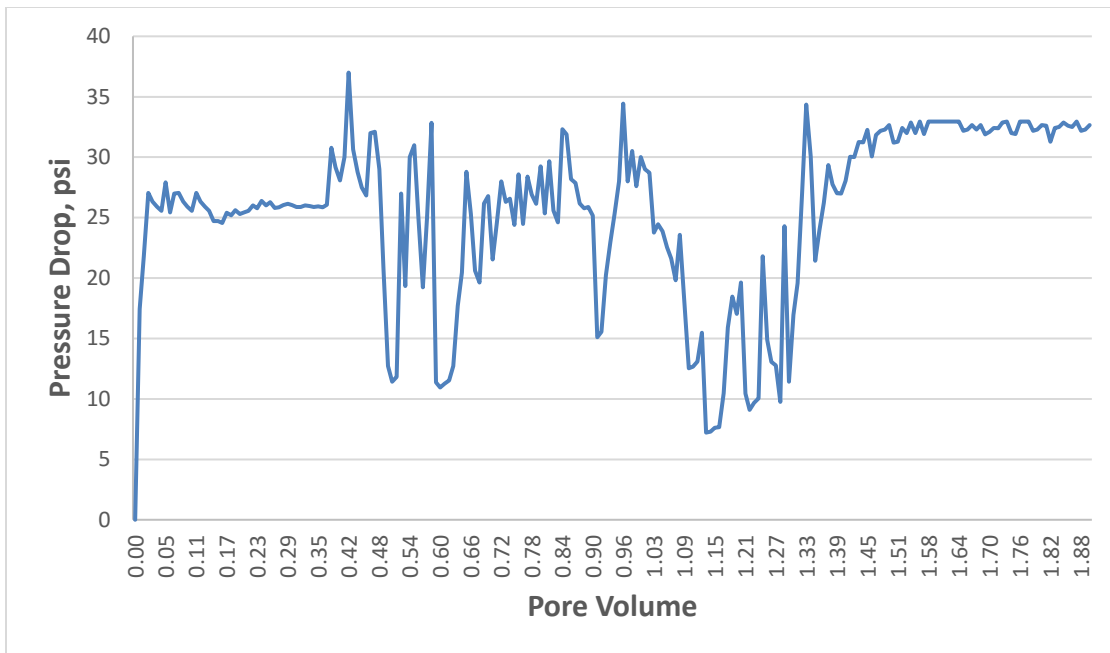


**Figure 16 SW Pressure Drop vs Pore Volume Injected (Experiment 2)**

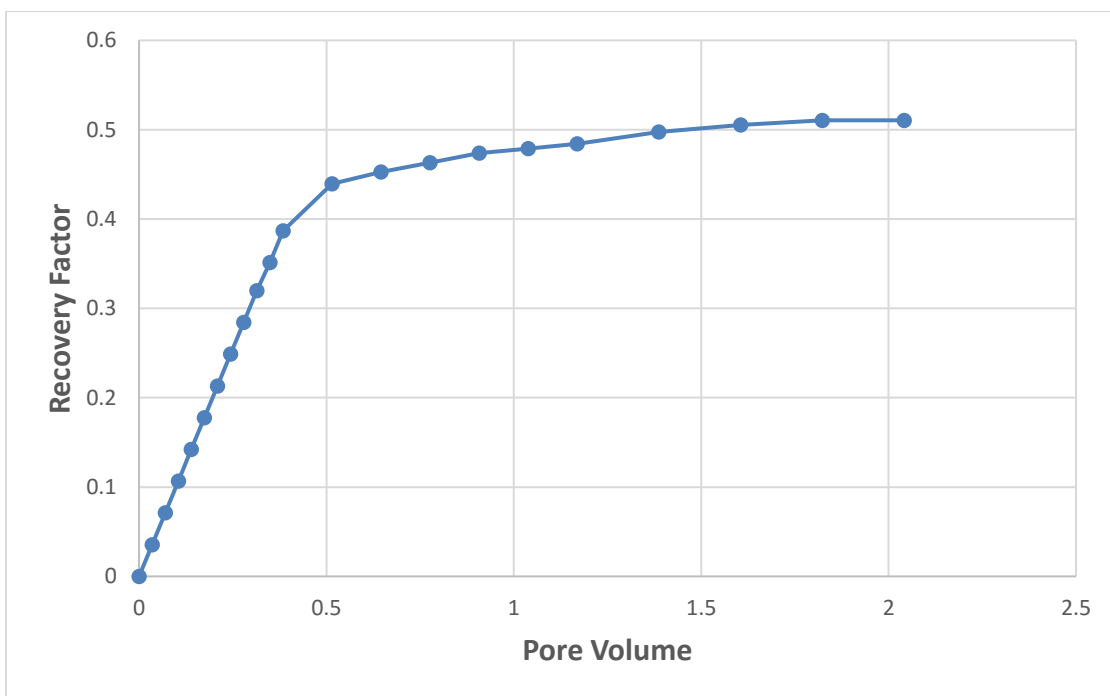


**Figure 17 SW Recovery Factor vs Pore Volume Injected (Experiment 2)**

In this experiment, N<sub>2</sub> was injected with supercritical CO<sub>2</sub> with a percentage of 20% by volume. The foam quality used was 80%. Like experiment 1 where the foam mixture composed of CO<sub>2</sub>, N<sub>2</sub> and AOS, the ratio of CO<sub>2</sub> and N<sub>2</sub> used in this test was 80:20 by volume. The injection rates for CO<sub>2</sub>, N<sub>2</sub>, and AOS were 0.32, 0.08 and 0.1 cc/min respectively, making the 0.5 cc/min total foam injection rate. Total flow rate was the only parameter changed from 0.75 cc/min in the first experiment to 0.5 cc/min in this one. Table 8 summarizes the parameters used in this experiment.

**Table 8 Summary of Experiment 2 Parameters**

<b>Experiment No</b>	<b>q total</b>	<b>N<sub>2</sub> Ratio</b>	<b>Foam Quality</b>	<b>CO<sub>2</sub></b>	<b>q surfactant</b>	<b>q Gas</b>	<b>q N<sub>2</sub></b>	<b>q CO<sub>2</sub></b>
	<b>cc/min</b>	<b>Fraction</b>	<b>Fraction</b>	<b>Fraction</b>	<b>cc/min</b>	<b>cc/min</b>	<b>cc/min</b>	<b>cc/min</b>
2	0.5	0.2	0.8	0.8	0.1	0.4	0.08	0.32

The mixed foam achieved oil recovery of 38.42 %. This is higher than the recovery achieved by foam flooding in the first experiment, which was only 11.5 %. The ultimate recovery for water flooding followed by foam injection reached 90.7 % while it was 73 % in the first experiment. The gas breakthrough took place after injecting around 0.31 PV calculated from the appearance of the first droplet of oil. This is relatively in the same range with breakthrough time for the first experiment, which happened after injection of 0.35 PV. Fig. 18 and Fig. 19 show the recovery performance in experiment 2.

Regarding the stability of the foam, the pressure drop chart shows a very good stability of differential pressure compared to the first experiment, which showed many fluctuations up and down. Fig. 20 shows the pressure drop performance in experiment 2.

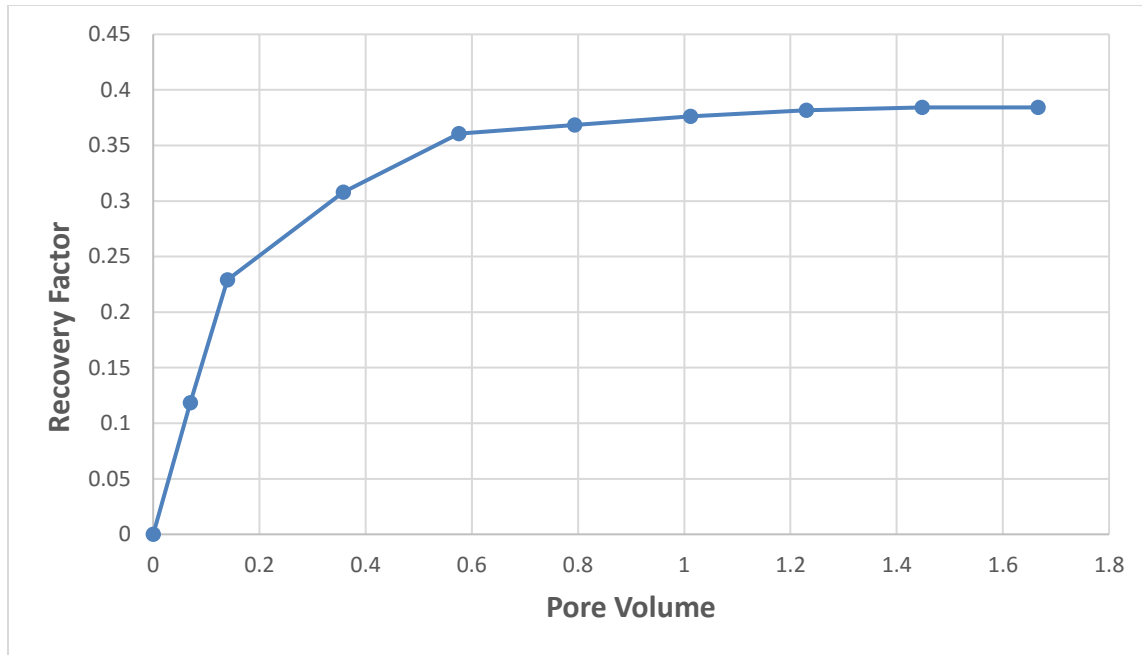


**Figure 18 Foam Flooding Recovery Factor vs Pore Volume Injected (Experiment 2)**

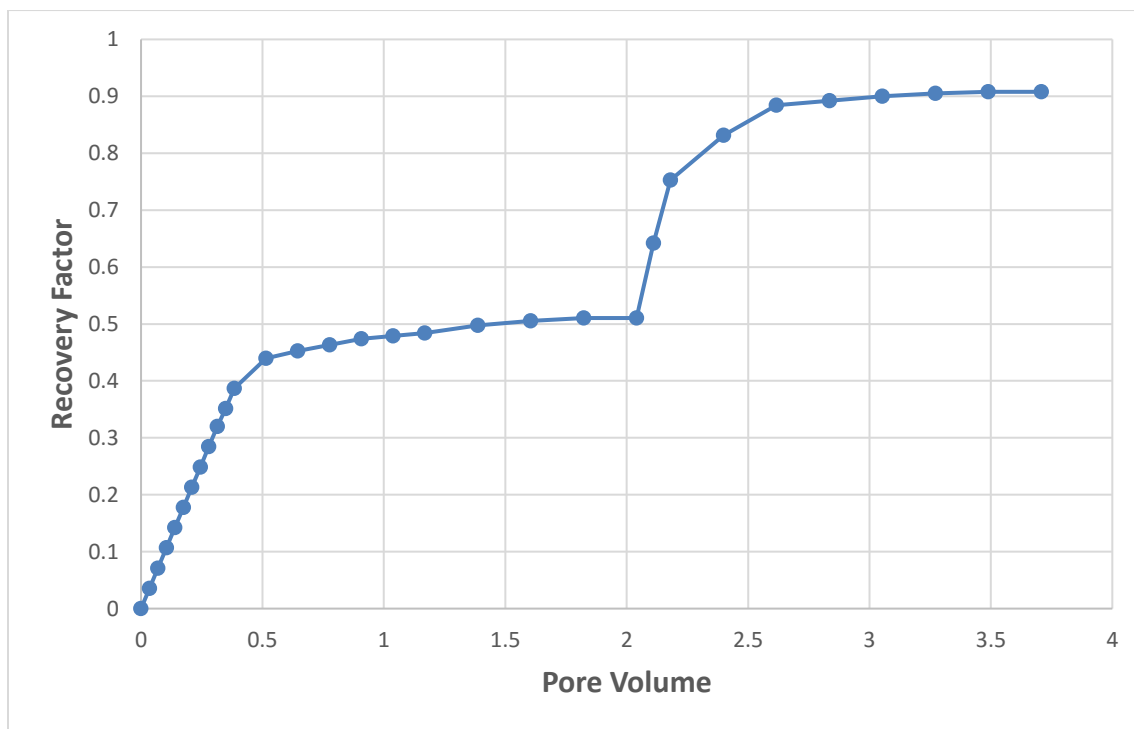


**Figure 19 SW Recovery Factor vs Pore Volume Injected (Experiment 2)**

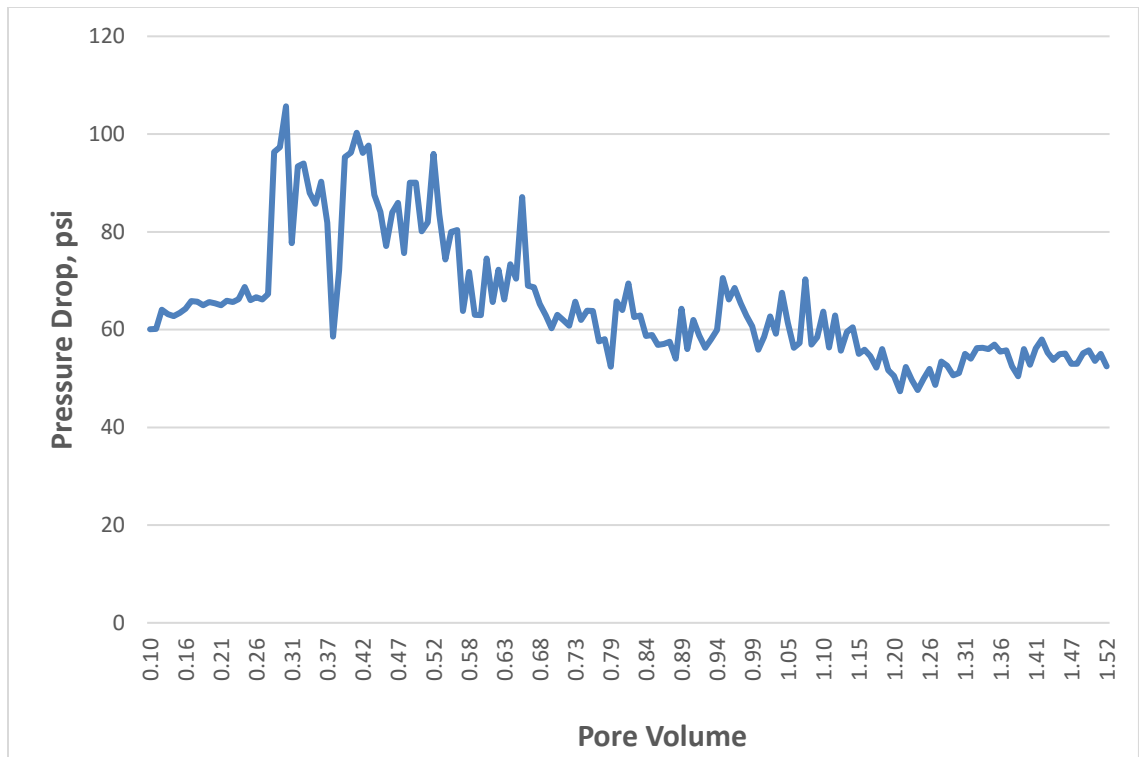


**Figure 20 Foam Recovery Pressure Drop vs Pore Volume Injected (Experiment 2)**

### 5.4.3 Experiment 3

Two injection rates were used to estimate the absolute permeability for the core, which were 0.5 and 1 cc/min. The core permeability is about 65 md. The pressure drop across the core sample is shown in Fig. 21.

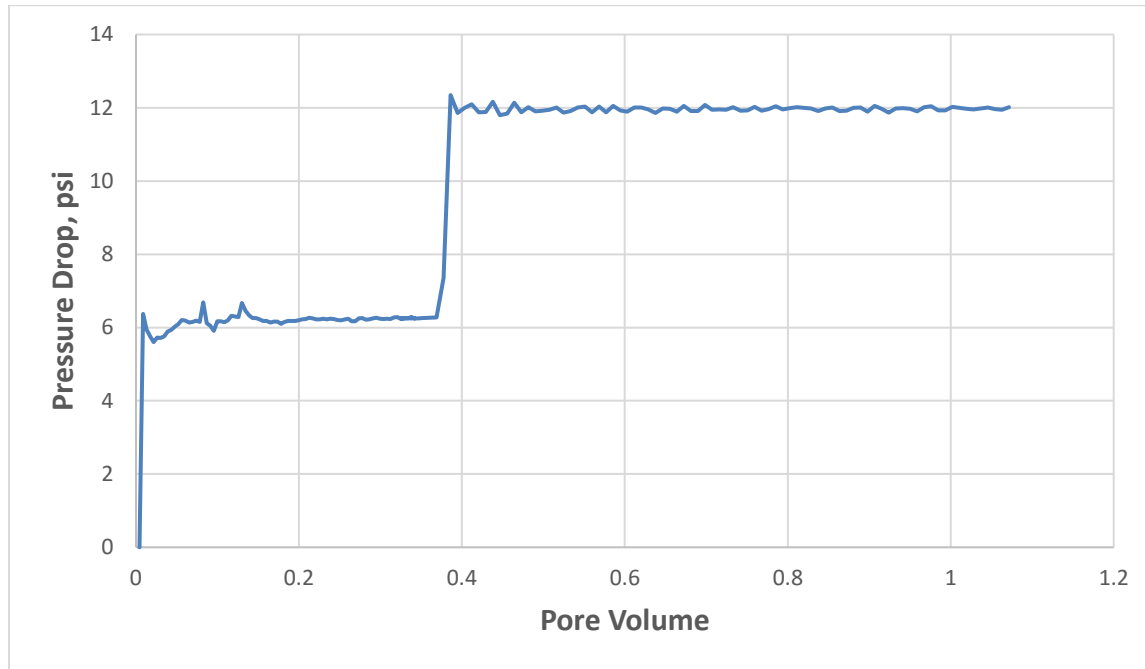


**Figure 21 Brine Permeability Pressure Drop vs Pore Volume Injected (Experiment 3)**

Then, oil injection was performed to saturate the core and to establish initial water saturation, which was about 37.5 %. This  $S_{wi}$  increased by about 4 % from the previous experiments as the permeability is lower compared to the others. Three flow rates were used which were 0.5, 1 and 2 cc/min. Fig. 22 shows the pressure drop across the core sample during crude oil injection.



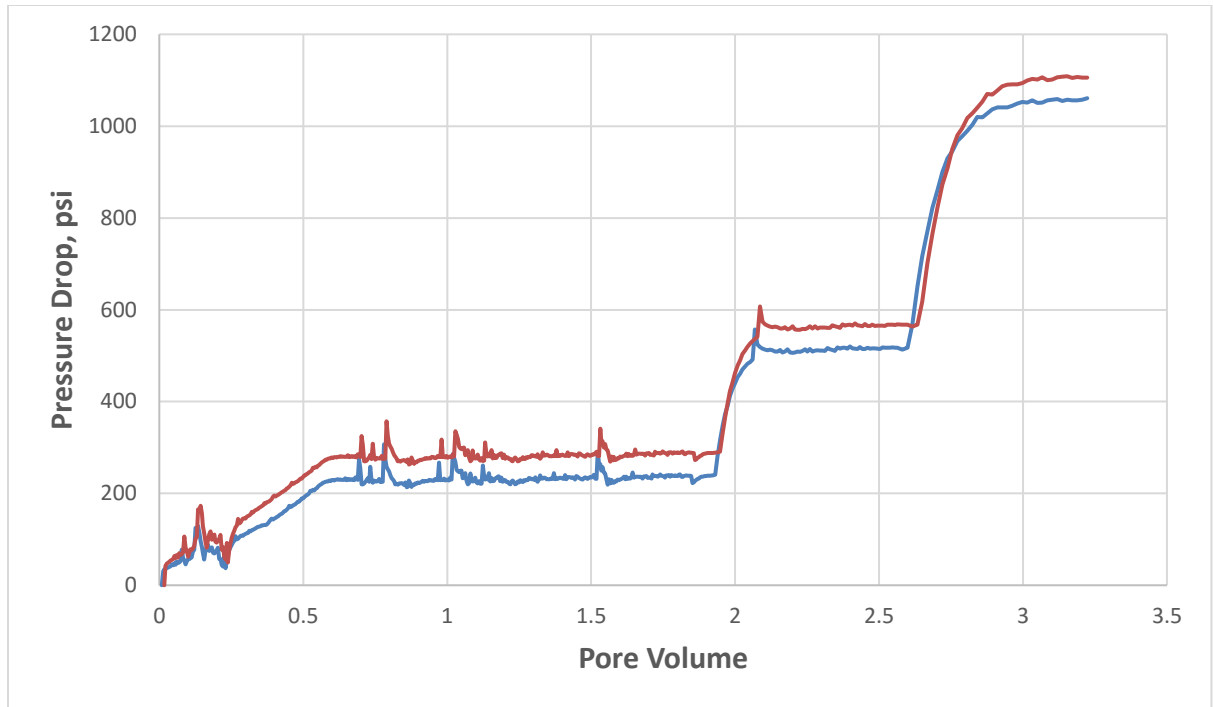


**Figure 22 Oil Injection Pressure Drop vs Pore Volume Injected (Experiment 3)**

The core sample was aged for three months. Afterwards, oil flushing with the same crude oil used for saturation was performed by injecting around two pore volumes. Seawater flooding was performed until no more oil came out of the core. The breakthrough took place after injecting 0.24 pore volume. The recovery factor and the pressure drop during water flooding stage are shown in Fig. 23 and Fig. 24.

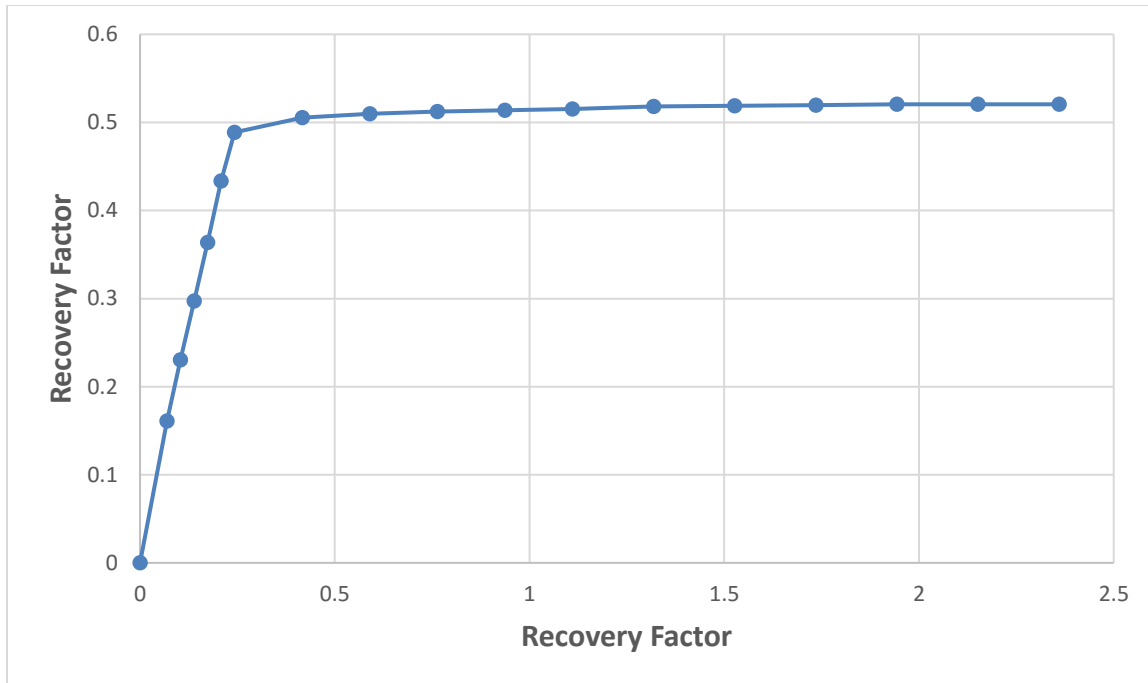


**Figure 23 SW Recovery Factor vs Pore Volume Injected (Experiment 3)**

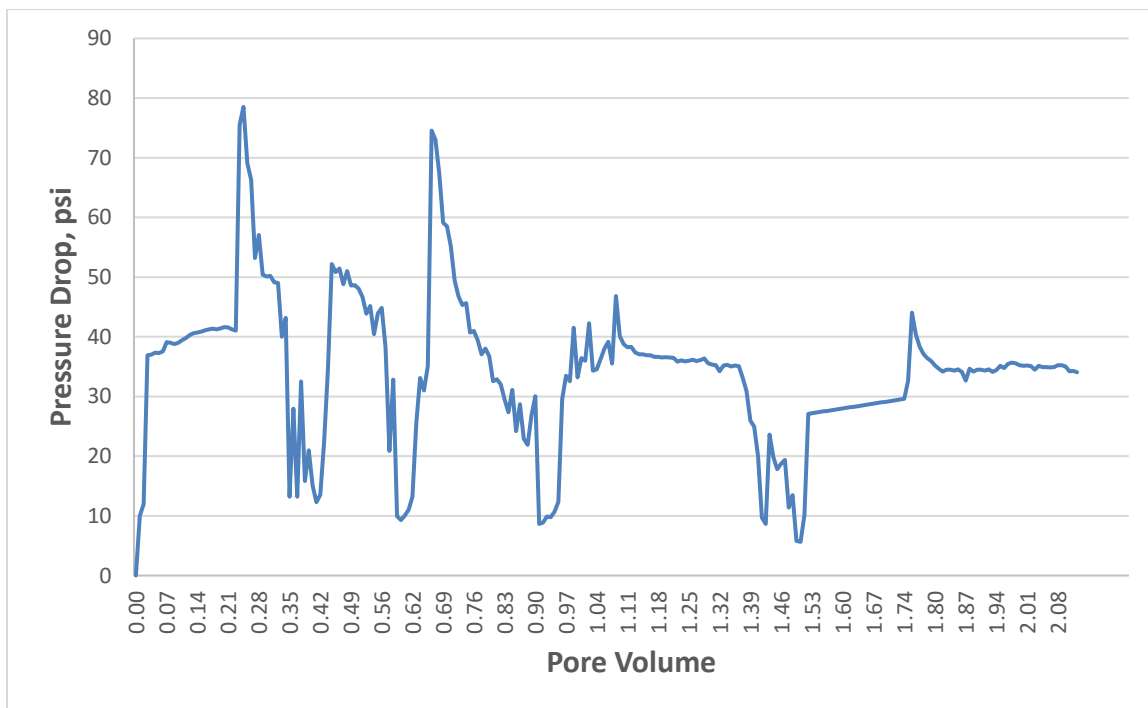


**Figure 24 SW Pressure Drop vs Pore Volume Injected (Experiment 3)**

In this experiment, N<sub>2</sub> was injected with supercritical CO<sub>2</sub> with a percentage of 20% by volume. The foam quality used was 80%. Like experiment 1 where the foam mixture composed of CO<sub>2</sub>, N<sub>2</sub> and AOS, the ratio of CO<sub>2</sub> and N<sub>2</sub> used in this test was 80:20 by volume. The injection rates for CO<sub>2</sub>, N<sub>2</sub>, and AOS were 0.64, 0.16 and 0.2 cc/min respectively, making the 1 cc/min total foam injection rate. Total flow rate was the only parameter changed from 0.75, 0.5 cc/min in the first two experiment to 1 cc/min in this one. Table 9 summarizes the parameters used in this experiment.

**Table 9 Summary of Experiment 3 Parameters**

Experiment No	q total	N <sub>2</sub> Ratio	Foam Quality	CO <sub>2</sub>	q surfactant	q Gas	q N <sub>2</sub>	q CO <sub>2</sub>
	cc/min	Fraction	Fraction	Fraction	cc/min	cc/min	cc/min	cc/min
3	1	0.2	0.8	0.8	0.2	0.8	0.16	0.64

The mixed foam 1 cc/min total flow rate achieved oil recovery of 18.3 %. This is higher than the recovery achieved by 0.75 cc/min foam flooding in the first experiment, which was only 11.5 %. But, experiment 2 with flow rate 0.5 cc/min showed the highest recovery factor of 38.42 %. The ultimate recovery for water flooding followed by foam injection reached 70.4 % while it was 73 % in the first experiment and 90.7 in the second experiment. The gas breakthrough took place after injecting around 0.3 PV calculated from the appearance time of the first droplet of oil. This is relatively in the same range with breakthrough time for the first two experiments, which happened after injection of 0.35 PV and 0.3 PV respectively. Fig. 25 and Fig. 26 show the recovery performance in experiment 3.

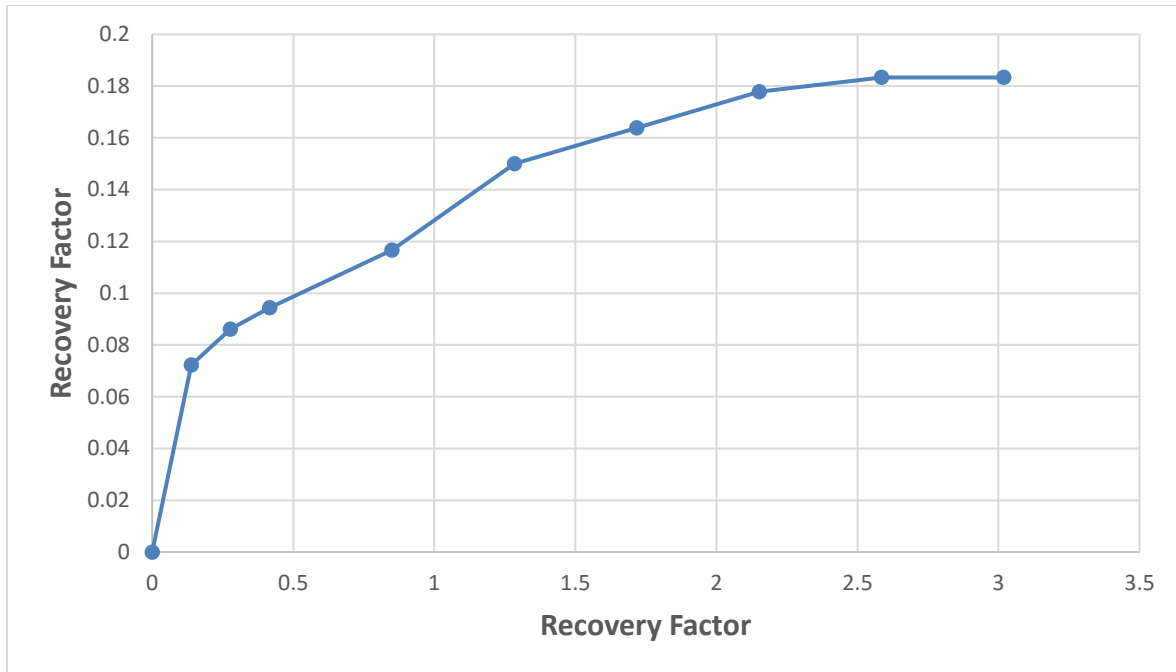


**Figure 25 Foam Flooding Recovery Factor vs Pore Volume Injected (Experiment 3)**

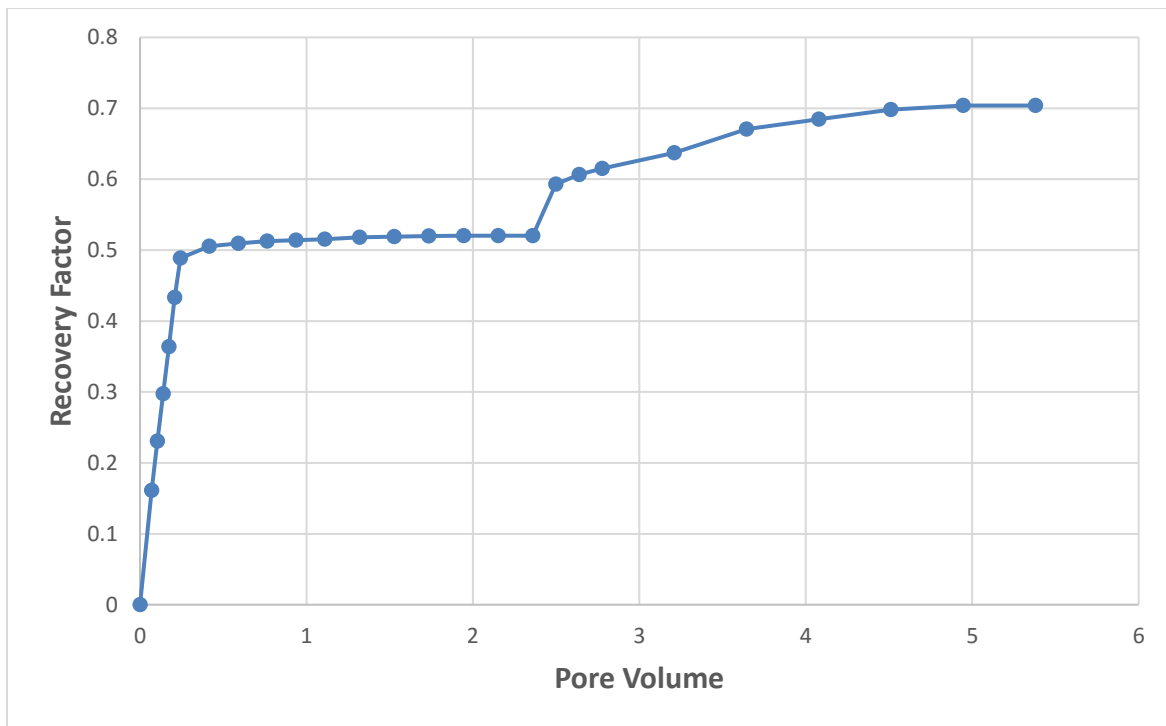


**Figure 26 Recovery Factor vs Pore Volume Injected (Experiment 3)**

Regarding the stability of the foam, the pressure drop chart shows a more stability of differential pressure compared to the first experiment, which showed many remarkable fluctuations up and down. However, this experiment was less stable than experiment 2 with 0.5 injection rate. Fig. 27 shows the pressure drop performance in experiment 2.

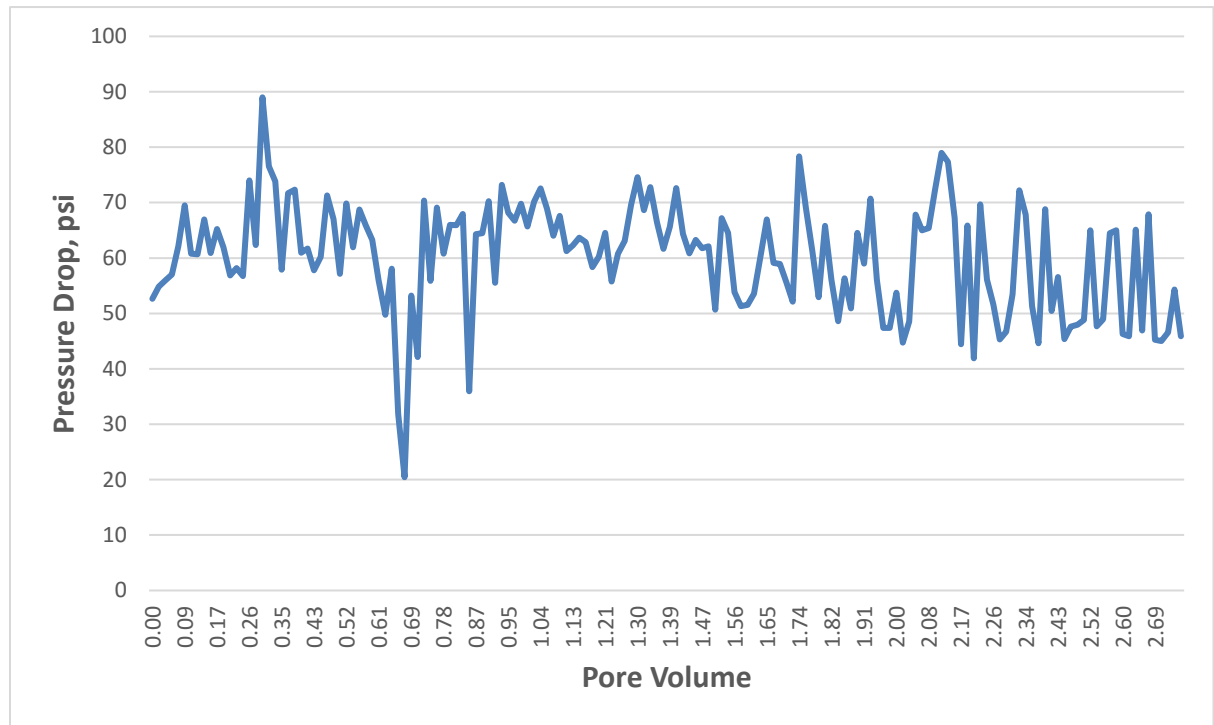


**Figure 27 Foam Recovery Pressure Drop vs Pore Volume Injected (Experiment 3)**

## 5.5 Effect of N<sub>2</sub> Percentage

The second parameter to be investigated was the N<sub>2</sub> percentage to get the optimized range for both foam stability and oil recovery. Three percentages were used during the foam flooding stage.

### 5.5.1 Experiment 4

Three injection rates were used to estimate the absolute permeability for the core, which were 0.5, 1 and 1.25 cc/min. The core permeability is about 79.6 md. The pressure drop across the core sample is shown in Fig. 28.

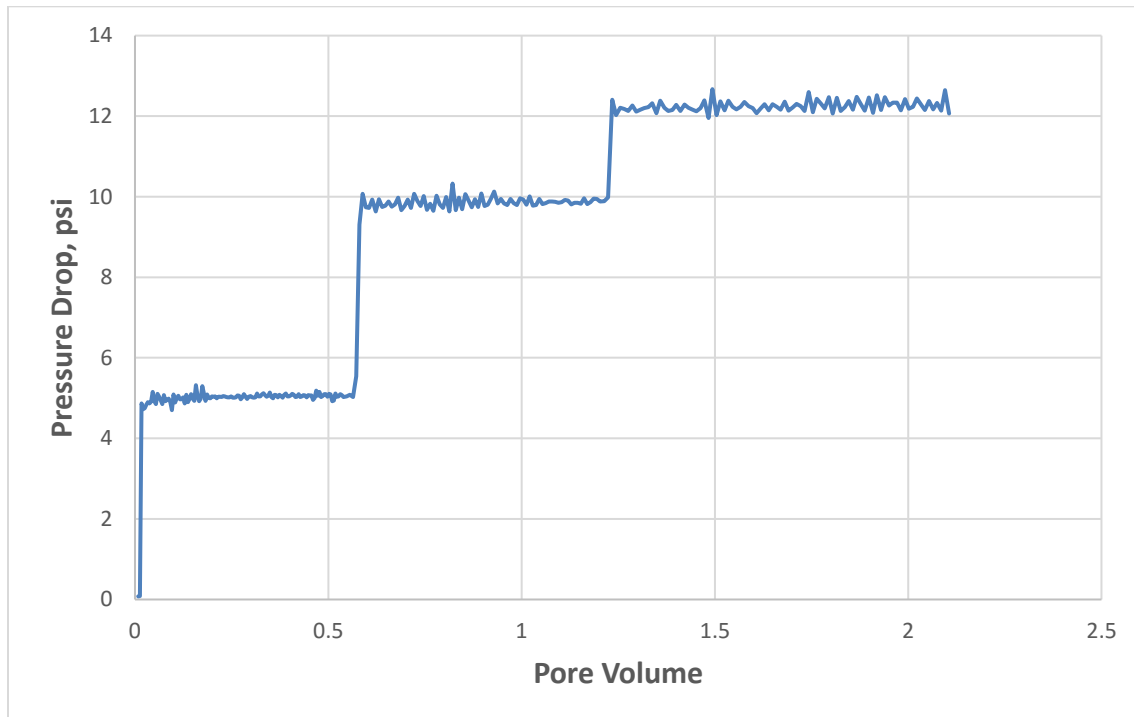
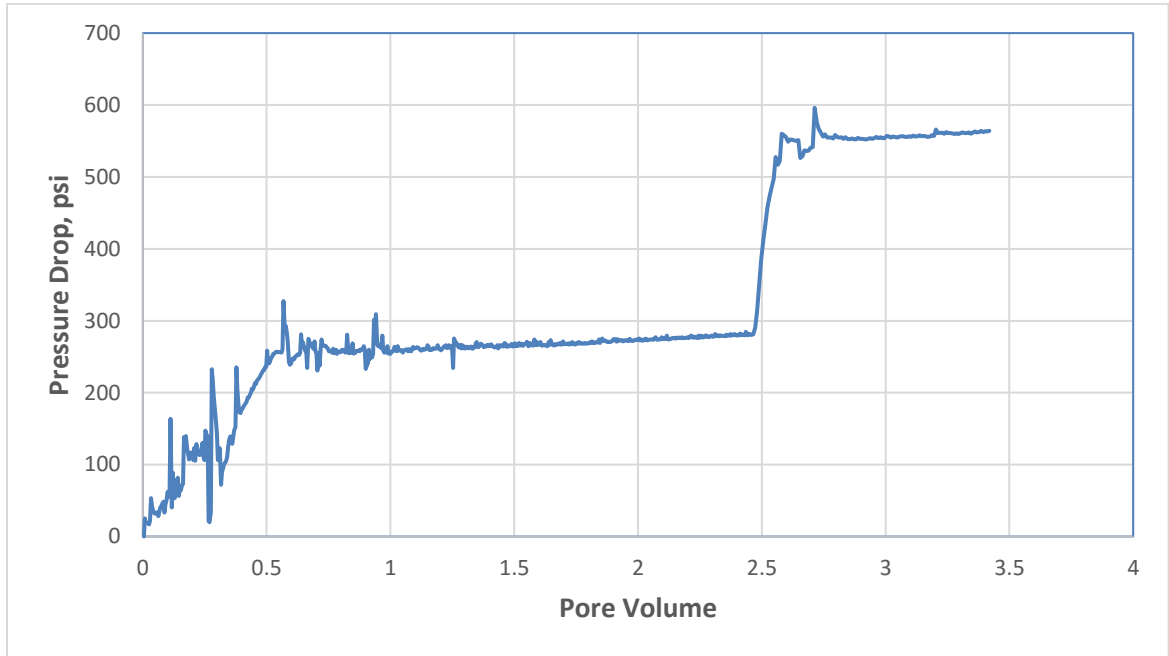


Figure 28 Brine Permeability Pressure Drop vs Pore Volume Injected (Experiment 4)

Then, oil injection was performed to saturate the core and to establish initial water saturation, which was about 33.6 %. Different flow rates were used which were 0.5 and 1 cc/min. Fig. 29 shows the pressure drop across the core sample during crude oil injection.



**Figure 29 Oil Injection Pressure Drop vs Pore Volume Injected (Experiment 4)**

The core sample was aged for three months. Afterwards, oil flushing with the same crude oil used for saturation was performed by injecting around two pore volumes. Seawater flooding was performed until no more oil was coming out of the core. The breakthrough took place after injecting 0.28 pore volume. The recovery factor and the pressure drop during water flooding stage are shown in Fig. 30 and Fig. 31.

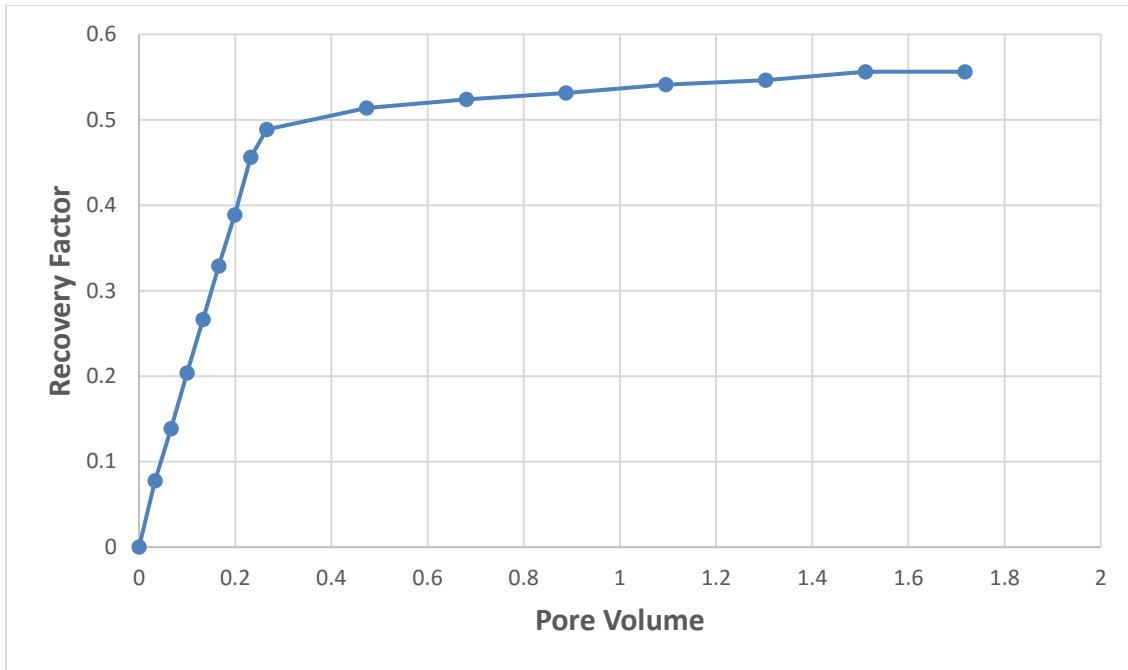


**Figure 30 SW Recovery Factor vs Pore Volume Injected (Experiment 4)**

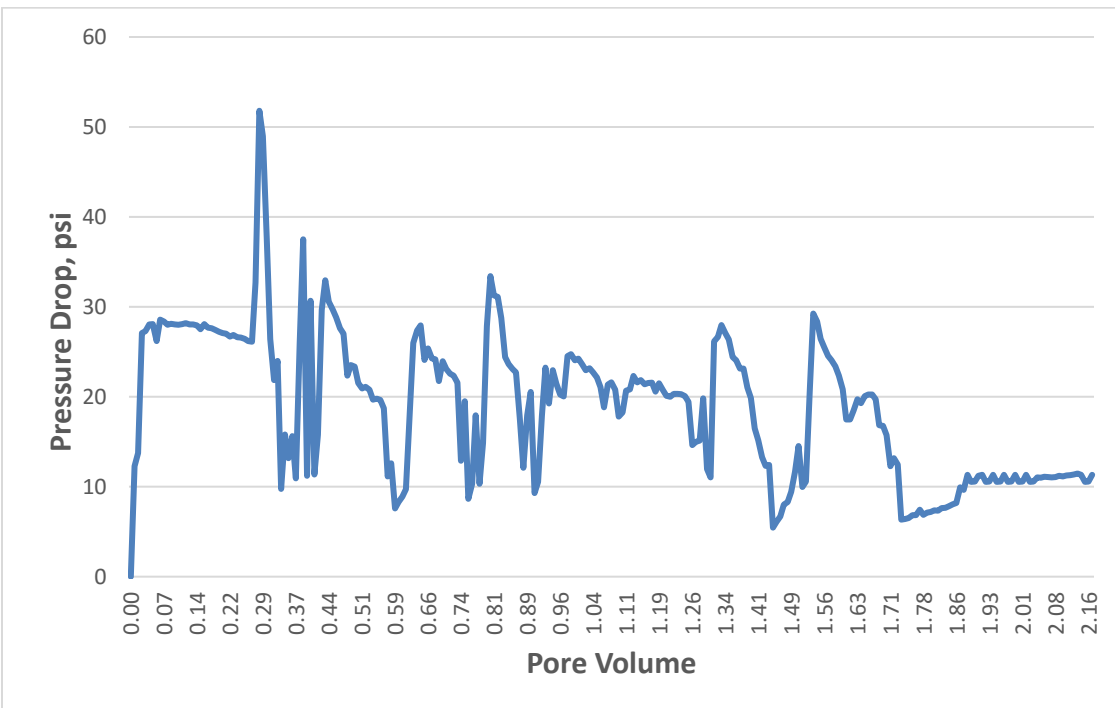


**Figure 31 SW Pressure Drop vs Pore Volume Injected (Experiment 4)**



In this experiment, N<sub>2</sub> was injected with supercritical CO<sub>2</sub> with a percentage of 35 % by volume. The foam quality used was 80%. Like experiment 2 where the foam mixture composed of CO<sub>2</sub>, N<sub>2</sub> and AOS, the ratio of CO<sub>2</sub> and N<sub>2</sub> used in this test was 65:35 by volume. The injection rates for CO<sub>2</sub>, N<sub>2</sub>, and AOS were 0.26, 0.14 and 0.1 cc/min respectively, making the 0.5 cc/min total foam injection rate. CO<sub>2</sub>: N<sub>2</sub> ratio was the only parameter changed from 80:20 in experiment 2 (Base case) to 65:35 in this one. Table 10 summarizes the parameters used in this experiment.

**Table 10 Summary of Experiment 4 Parameters**

<b>Experiment No</b>	<b>q total</b>	<b>N<sub>2</sub> Ratio</b>	<b>Foam Quality</b>	<b>CO<sub>2</sub></b>	<b>q surfactant</b>	<b>q Gas</b>	<b>q N<sub>2</sub></b>	<b>q CO<sub>2</sub></b>
	<b>cc/min</b>	<b>Fraction</b>	<b>Fraction</b>	<b>Fraction</b>	<b>cc/min</b>	<b>cc/min</b>	<b>cc/min</b>	<b>cc/min</b>
4	0.5	0.35	0.8	0.65	0.1	0.4	0.14	0.26

The mixed foam achieved oil recovery of 11.75 %. This is lower than the recovery achieved by foam flooding in the experiment 2 (Base case) which was 38.42 %. The ultimate recovery for water flooding followed by foam injection reached 68.13 % while it was 90.7 % in experiment 2. The gas breakthrough took place after injecting around 0.2 PV calculated from the appearance of the first droplet of oil. This is relatively earlier than the breakthrough time for experiment 2, which took place after injection of 0.31 PV. Fig. 32 and Fig. 33 show the recovery performance in experiment 4.

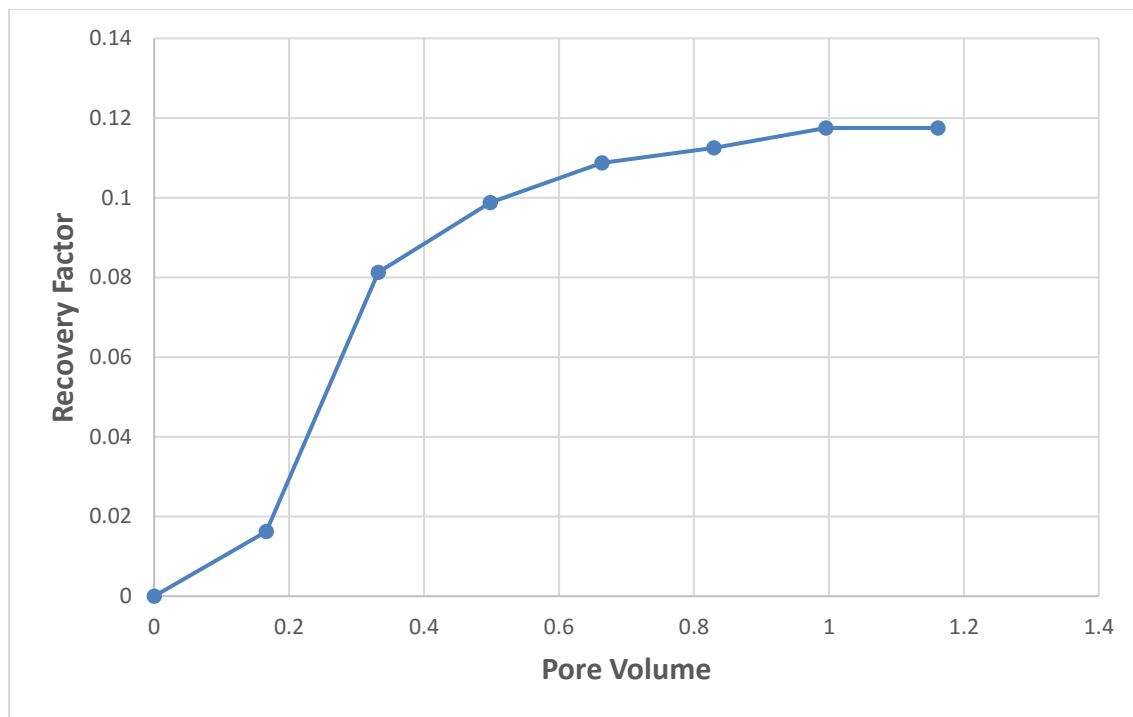


**Figure 32 Foam Flooding Recovery Factor vs Pore Volume Injected (Experiment 4)**

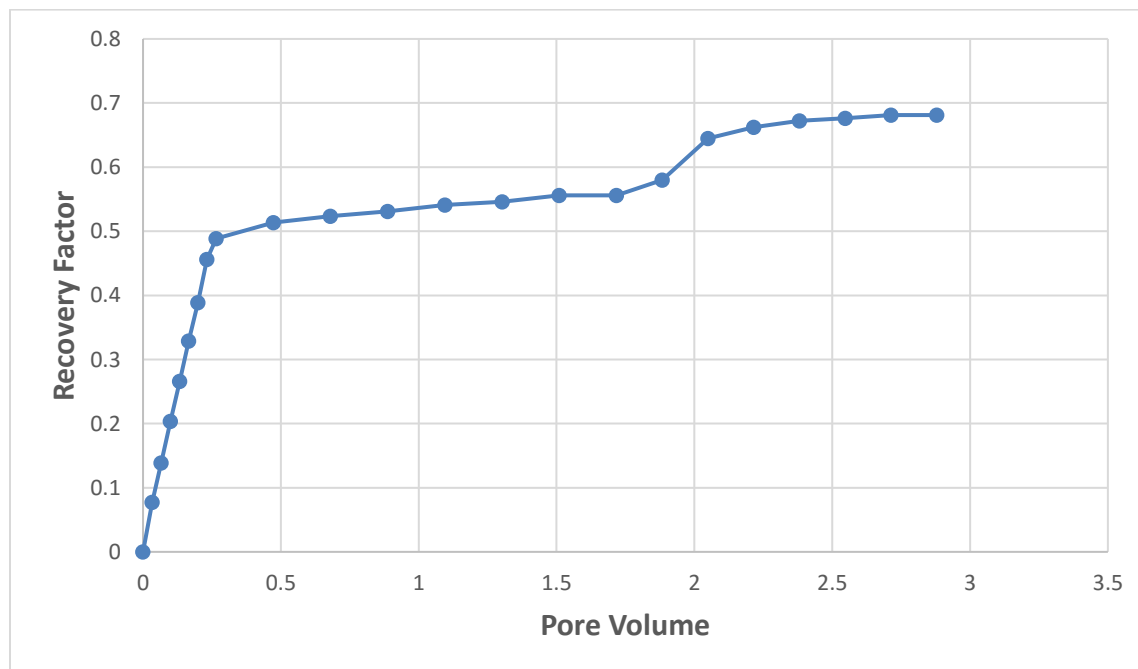


**Figure 33 Recovery Factor vs Pore Volume Injected (Experiment 4)**

Regarding the stability of the foam, the pressure drop chart shows a very good stability of differential pressure like experiment 2. Fig. 34 shows the pressure drop performance during foam flooding in experiment 4.

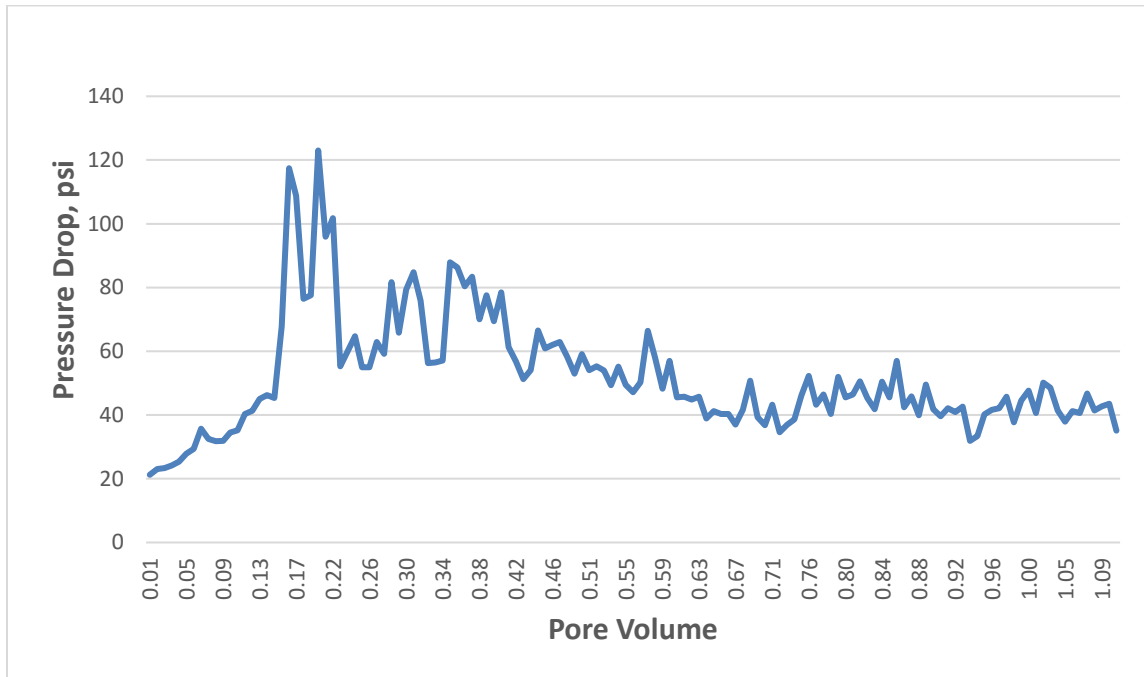


**Figure 34 Foam Recovery Pressure Drop vs Pore Volume Injected (Experiment 4)**

### 5.5.2 Experiment 5

Three injection rates were used to estimate the absolute permeability for the core, which were 0.5, 1 and 1.25 cc/min. The core permeability is about 88.2 md. The pressure drop across the core sample is shown in Fig. 35.

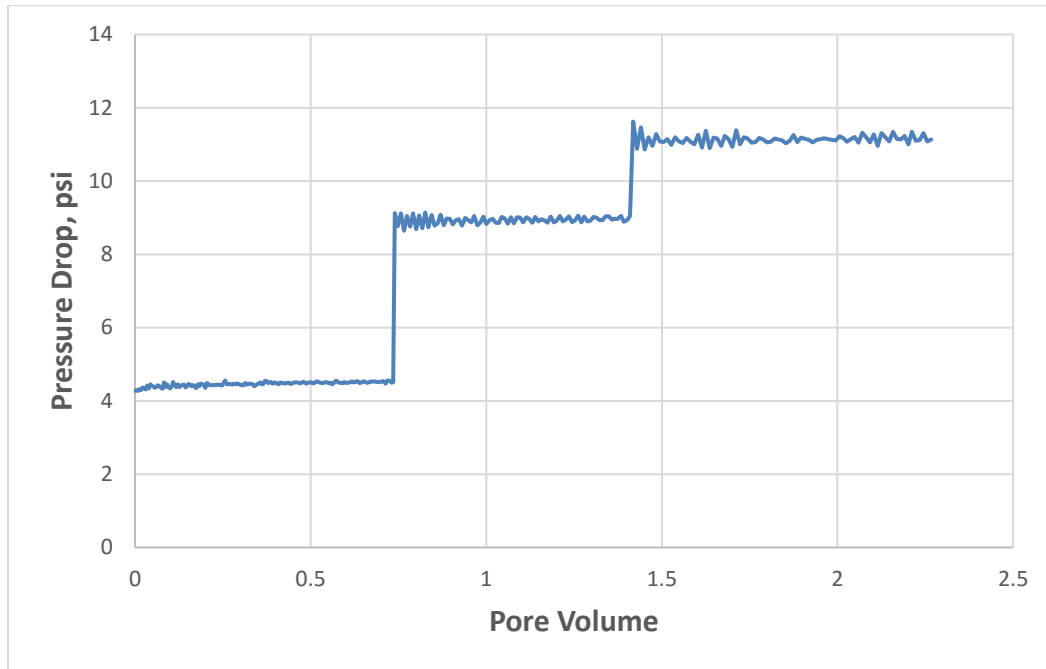


**Figure 35 Brine Permeability Pressure Drop vs Pore Volume injected (Experiment 5)**

Then, oil injection was performed to saturate the core and to establish initial water saturation, which was about 36.3 %. Two flow rates were used which were 0.5 and 1 cc/min. Fig. 36 shows the pressure drop across the core sample during crude oil injection.

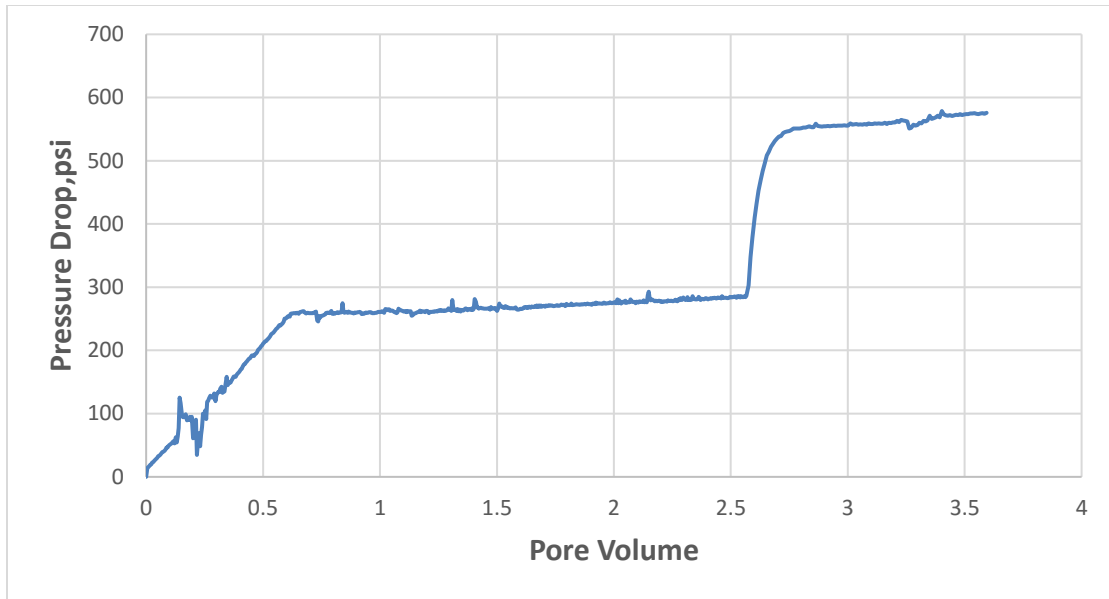


**Figure 36 Oil Injection Pressure Drop vs Pore Volume injected (Experiment 5)**

The core sample was aged for three months. Afterwards, oil flushing with the same crude oil used for saturation was done by injecting around two pore volumes. Seawater flooding was performed until no more oil came out of the core. The breakthrough took place after injecting 0.27 pore volume. The recovery factor and the pressure drop during water flooding stage are shown Fig. 37 and Fig. 38.

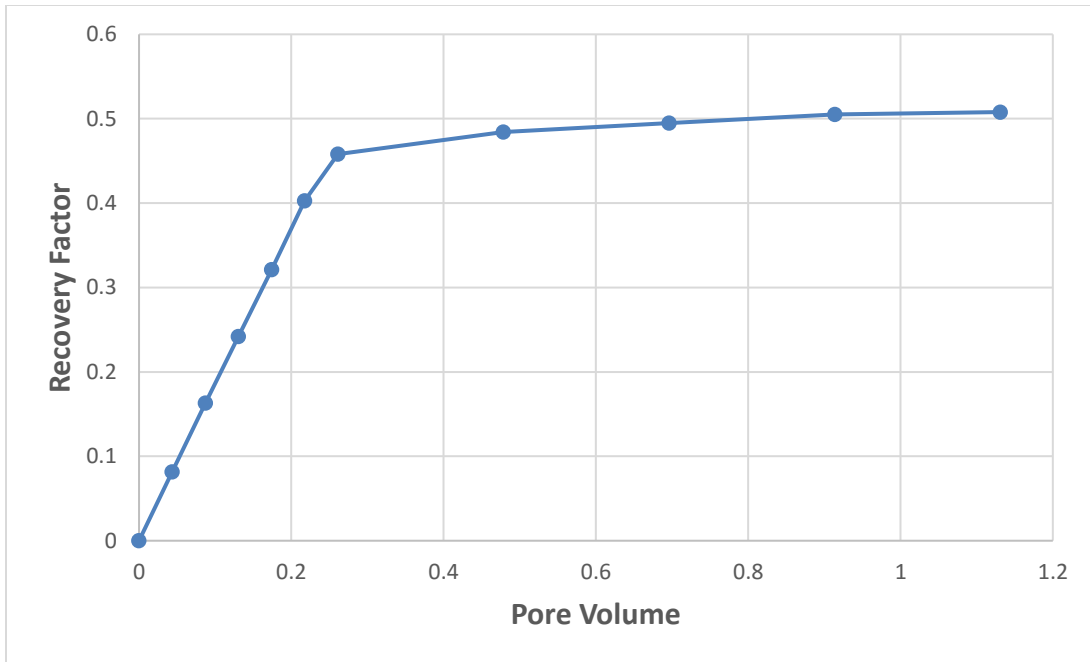


**Figure 37 SW Recovery Factor vs Pore Volume Injected (Experiment 5)**

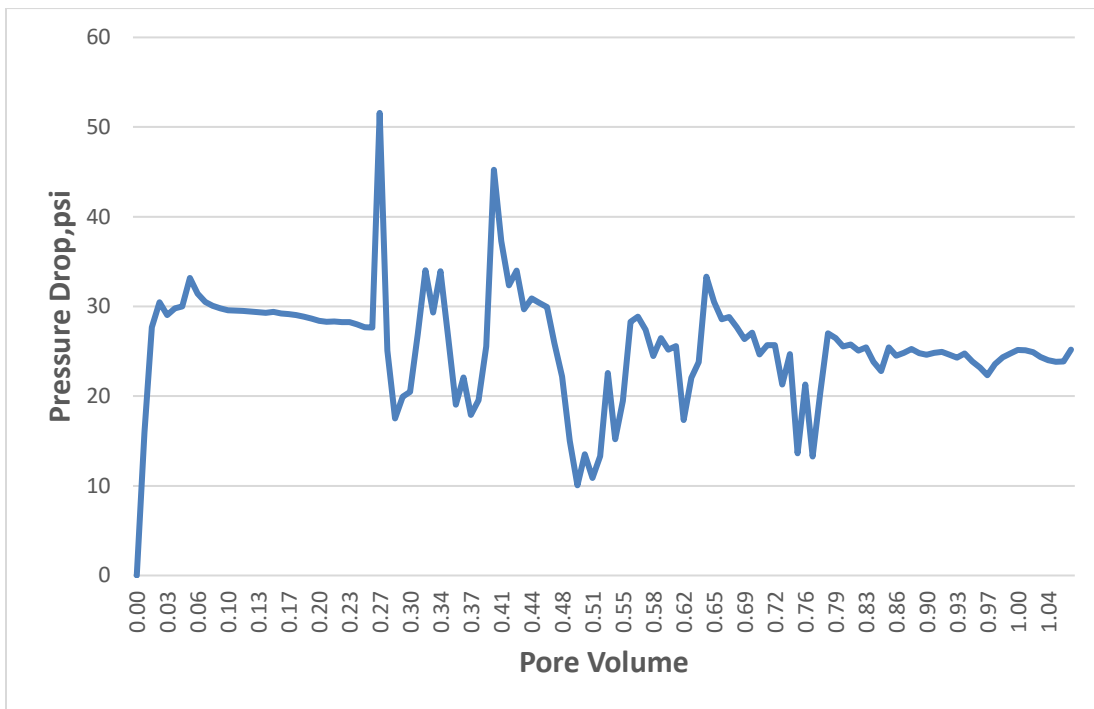


**Figure 38 SW Pressure Drop vs Pore Volume Injected (Experiment 5)**

In this experiment, N<sub>2</sub> was injected with supercritical CO<sub>2</sub> with a percentage of 10 % by volume. The foam quality used was 80%. Like experiment 2, where the foam mixture composed of CO<sub>2</sub>, N<sub>2</sub> and AOS, the ratio of CO<sub>2</sub> and N<sub>2</sub> used in this test was 90:10 by volume. The injection rates for CO<sub>2</sub>, N<sub>2</sub>, and AOS were 0.36, 0.04 and 0.1 cc/min respectively, making the 0.5 cc/min total foam injection rate. CO<sub>2</sub>: N<sub>2</sub> ratio was the only parameter changed from 80:20 in experiment 2 (Base case) to 90:10 in this one. Table 11 summarizes the parameters used in this experiment.

**Table 11 Summary of Experiment 5 Parameters**

<b>Experiment No</b>	<b>q total</b>	<b>N<sub>2</sub> Ratio</b>	<b>Foam Quality</b>	<b>CO<sub>2</sub></b>	<b>q surfactant</b>	<b>q Gas</b>	<b>q N<sub>2</sub></b>	<b>q CO<sub>2</sub></b>
	<b>cc/min</b>	<b>Fraction</b>	<b>Fraction</b>	<b>Fraction</b>	<b>cc/min</b>	<b>cc/min</b>	<b>cc/min</b>	<b>cc/min</b>
5	0.5	.10	0.8	0.9	0.1	0.4	0.04	0.36

The mixed foam achieved oil recovery of 12.89 %. This is lower than the recovery achieved by foam flooding in the experiment 2 (Base case) which was 38.42 %. The ultimate recovery for water flooding followed by foam injection reached 63.7 % while it was 90.7 % in experiment 2. The gas breakthrough took place after injecting around 0.16 PV calculated from the appearance of the first droplet of oil. This is relatively earlier than the breakthrough time for experiment 2, which took place after injection of 0.31 PV. Fig. 39 and Fig. 40 show the recovery performance in experiment 5.

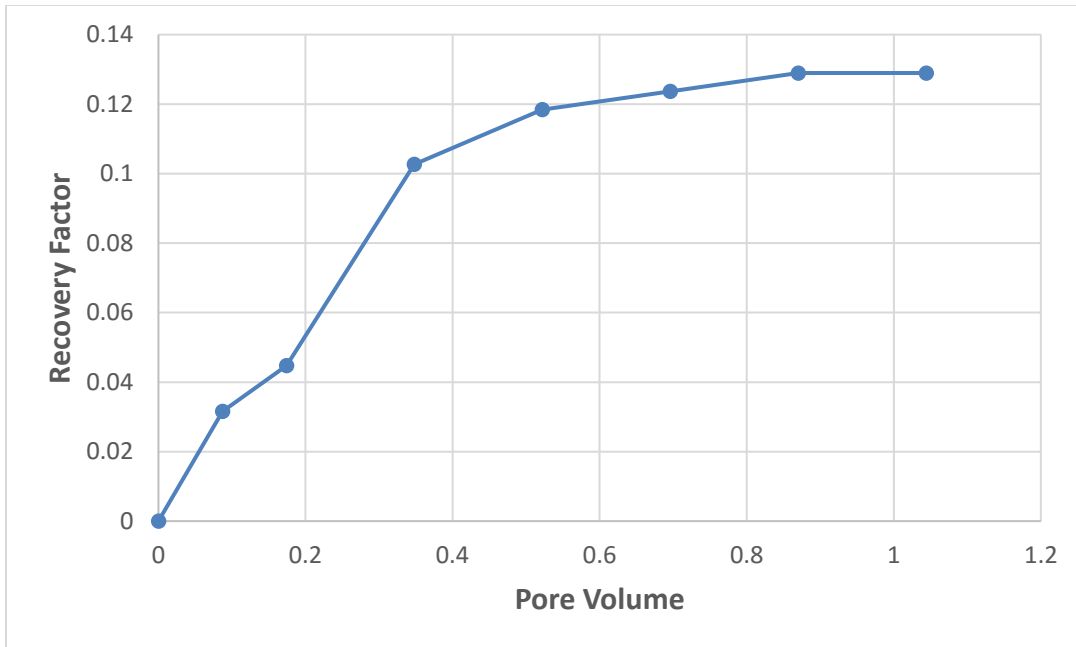


**Figure 39 Foam Flooding Recovery Factor vs Pore Volume Injected (Experiment 5)**

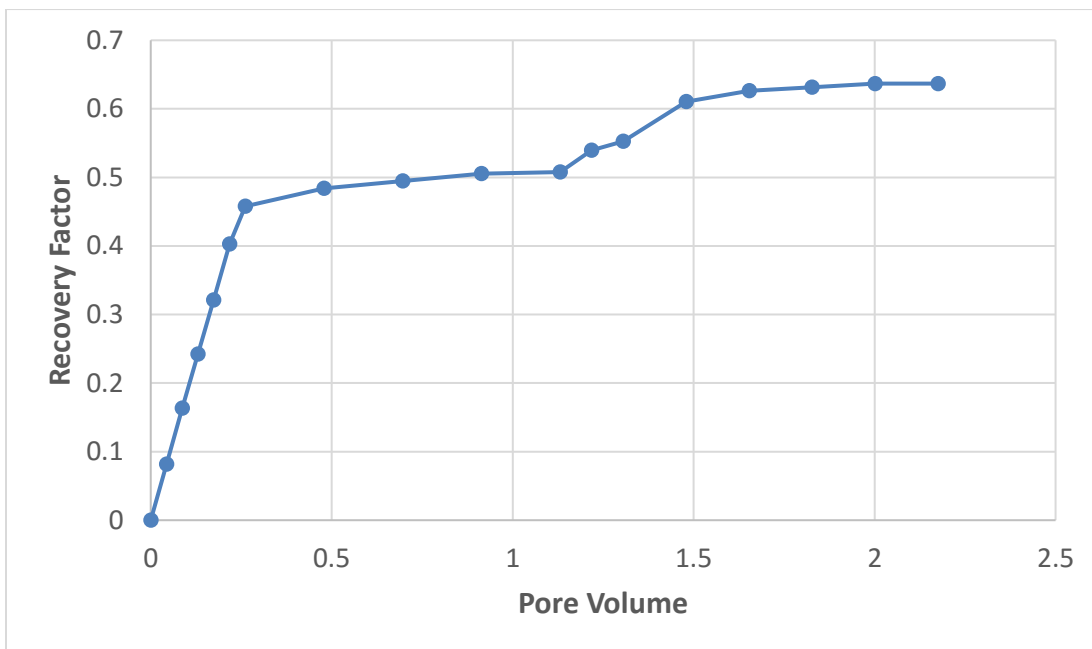


**Figure 40 Recovery Factor vs Pore Volume Injected (Experiment 5)**



Regarding the stability of the foam, the pressure drop chart shows a stability of differential pressure with some fluctuations up and down unlike experiment 2. In addition, experiment 2 shows stability around 50 psi, which is larger than 40 psi in this experiment. This can give an indication about more foam stability in experiment 2. Fig. 41 shows the pressure drop performance during foam flooding in experiment 5.

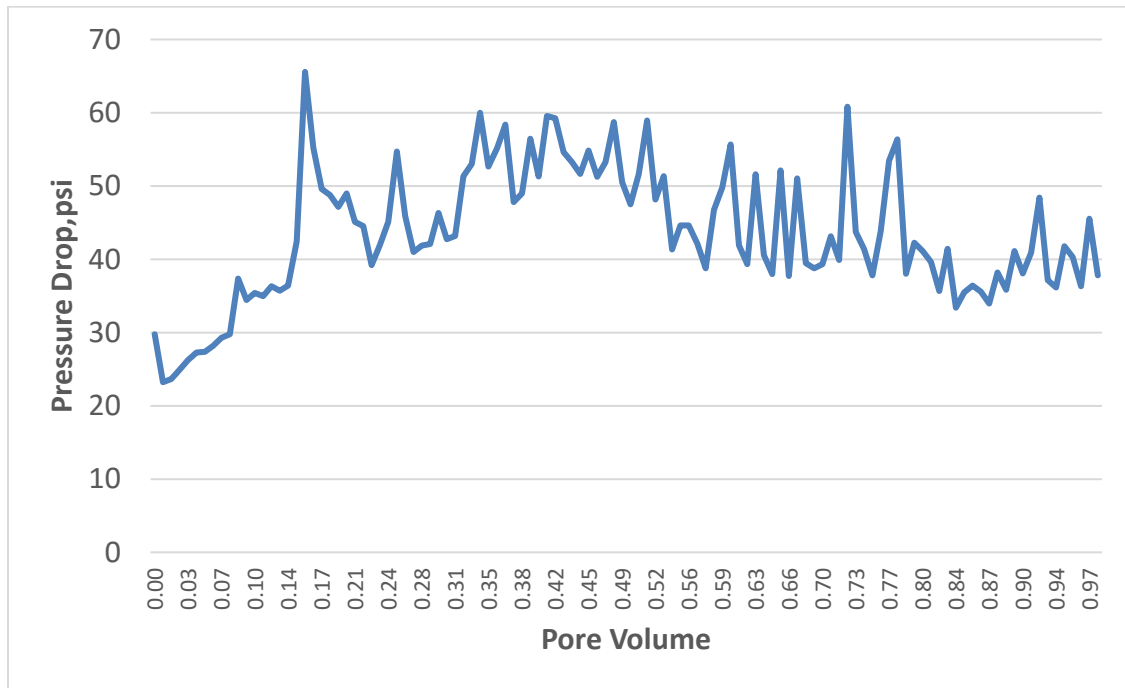


**Figure 41 Foam Recovery Pressure Drop vs Pore Volume Injected (Experiment 5)**

## 5.6 Effect of flow rate

The third parameter to be investigated was the foam quality to get the optimized range for both foam stability and oil recovery. Three values were used during the foam flooding stage.

### 5.6.1 Experiment 6

Three injection rates were used to estimate the absolute permeability for the core, which were 0.5, 1 and 1.25 cc/min. The core permeability is about 77.7 md. The pressure drop across the core sample is shown in Fig. 42.

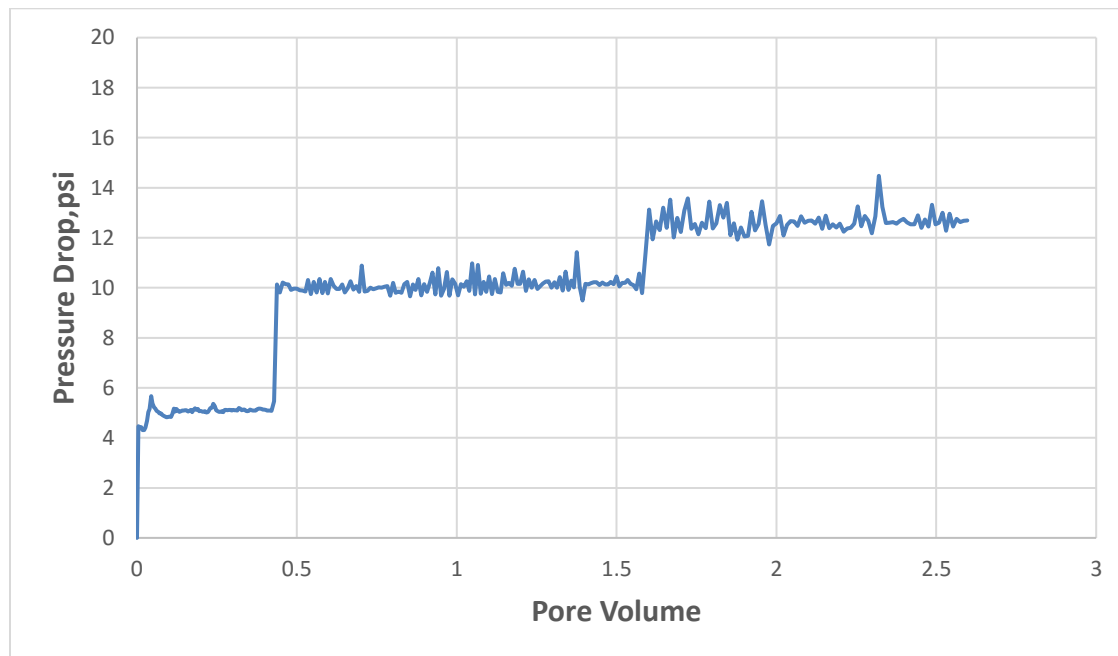
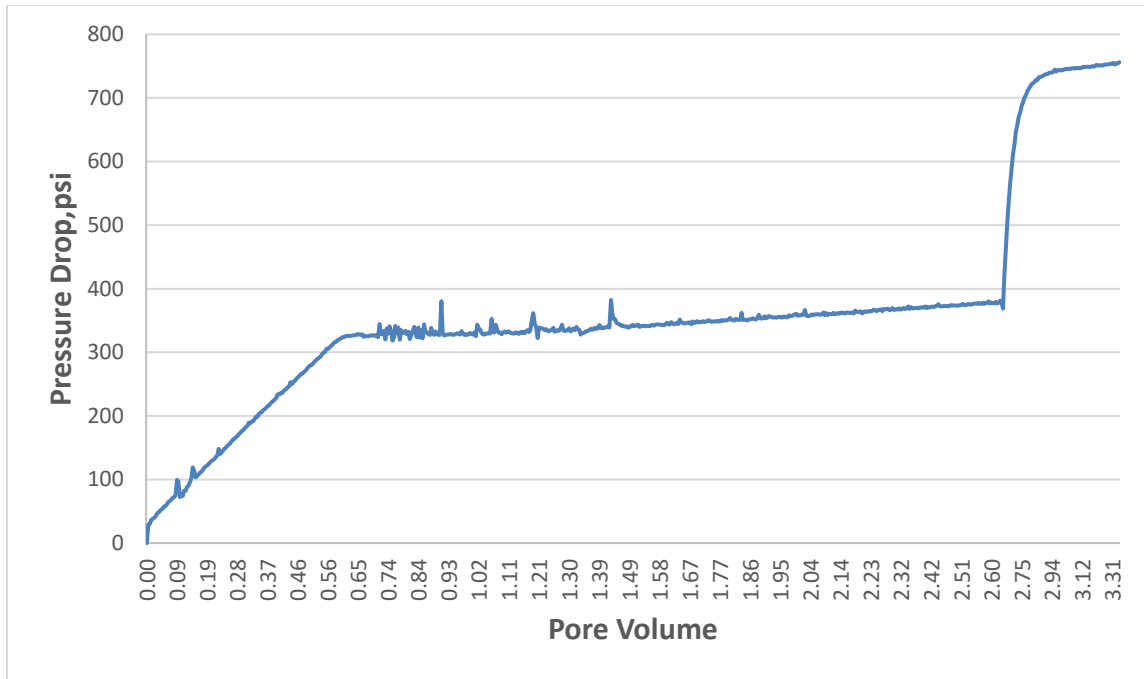


Figure 42 Brine Permeability Pressure Drop vs Pore Volume Injected (Experiment 6 )

Then, oil injection was performed to saturate the core and to establish initial water saturation, which was about 36.3 %. Two flow rates were injected which were 0.5 and 1 cc/min. Fig. 43 shows the pressure drop across the core sample during crude oil injection.



**Figure 43 Oil Injection Pressure Drop vs Pore Volume injected (Experiment 6)**

The core sample was aged for three months. Then, oil flushing with the same crude oil used for saturation was performed by injecting around two pore volumes. After that, water flooding was performed until no more oil was coming out of the core. The breakthrough happened after injecting 0.26 pore volume. The recovery factor and the pressure drop during water flooding stage are shown in Fig. 44 and Fig. 45.

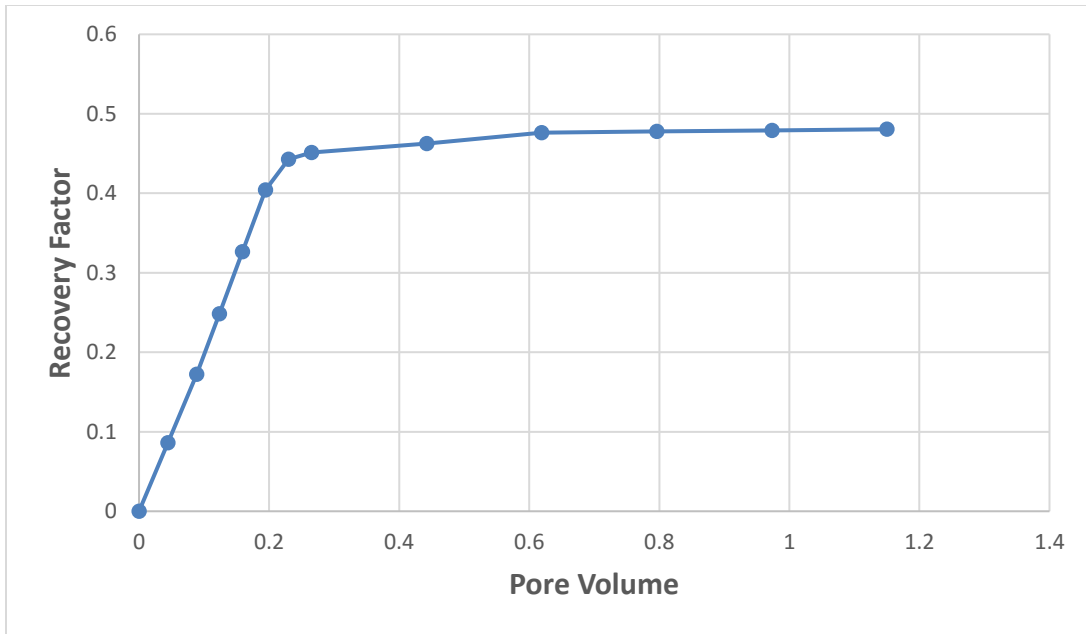


**Figure 44 SW Recovery Factor vs Pore Volume Injected (Experiment 6)**

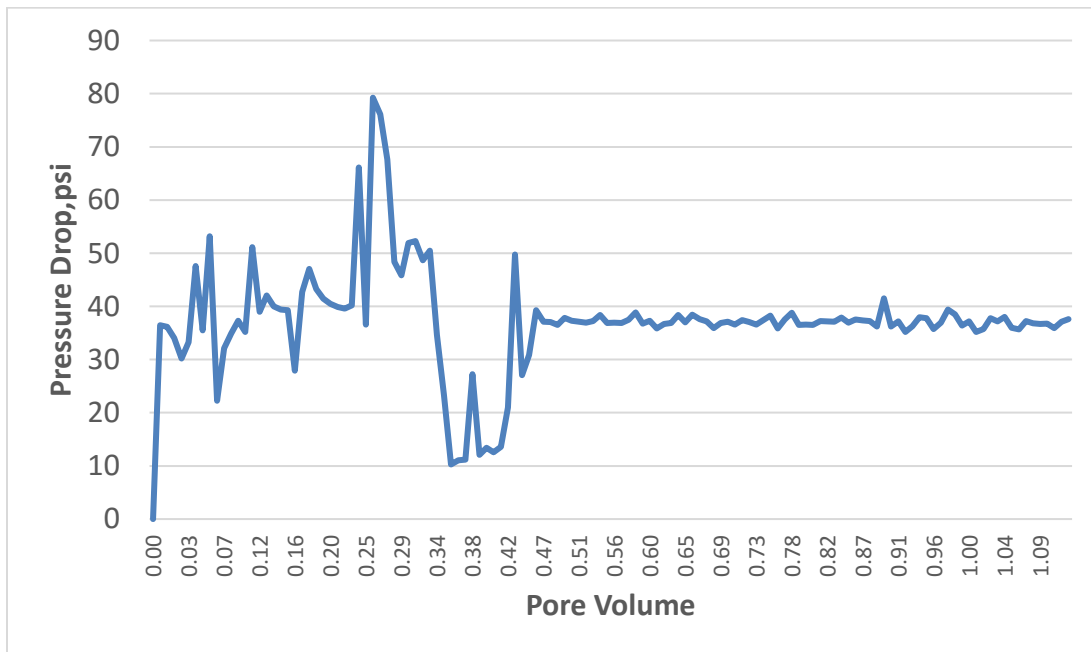


**Figure 45 SW Pressure Drop vs Pore Volume Injected (Experiment 6)**

In this experiment, N<sub>2</sub> was injected with supercritical CO<sub>2</sub> with a percentage of 20 % by volume. The foam quality changed to be 70 %. Like experiment 2 where the foam mixture composed of CO<sub>2</sub>, N<sub>2</sub> and AOS, the ratio of CO<sub>2</sub> and N<sub>2</sub> used in this test was 80:20 by volume. The injection rates for CO<sub>2</sub>, N<sub>2</sub>, and AOS were 0.28, 0.07 and 0.15 cc/min respectively, making the 0.5 cc/min total foam injection rate. Foam quality was the only parameter changed from 80% in experiment 2 (Base case) to 70 % in this one. Table 12 summarizes the parameters used in this experiment.

**Table 12 Summary of Experiment 6 Parameters**

<b>Experiment No</b>	<b>q total</b>	<b>N<sub>2</sub> Ratio</b>	<b>Foam Quality</b>	<b>CO<sub>2</sub></b>	<b>q surfactant</b>	<b>q Gas</b>	<b>q N<sub>2</sub></b>	<b>q CO<sub>2</sub></b>
	<b>cc/min</b>	<b>Fraction</b>	<b>Fraction</b>	<b>Fraction</b>	<b>cc/min</b>	<b>cc/min</b>	<b>cc/min</b>	<b>cc/min</b>
6	0.5	0.2	0.7	0.8	0.15	0.35	0.07	0.28

The mixed foam achieved oil recovery of 18 %. This is lower than the recovery achieved by foam flooding in the experiment 2 (Base case) which was 38.42 %. The ultimate recovery for water flooding followed by foam injection reached 66.1 % while it was 90.7 % in experiment 2. The gas breakthrough took place after injecting around 0.04 PV calculated from the appearance of the first droplet of oil. This took place very fast directly after few minutes from first oil droplet production. Moreover, it was very early compared to breakthrough time for experiment 2, which took place after injection of 0.31 PV. Fig. 46 and Fig. 47 show the recovery performance in experiment 6.

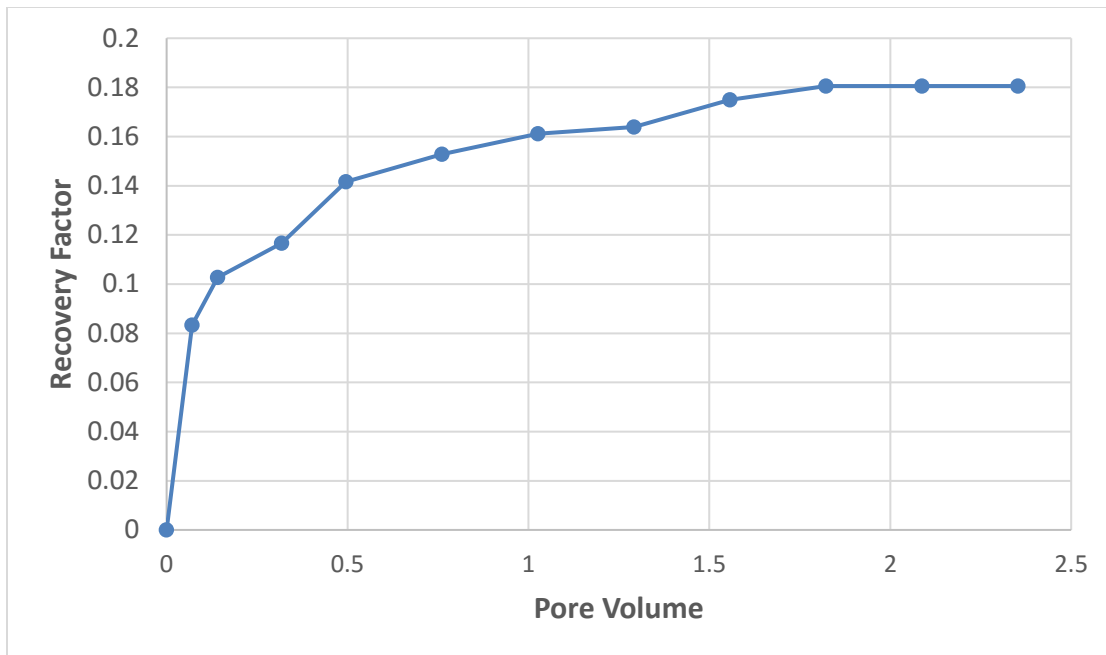


**Figure 46 Foam Flooding Recovery Factor vs Pore Volume Injected (Experiment 6)**

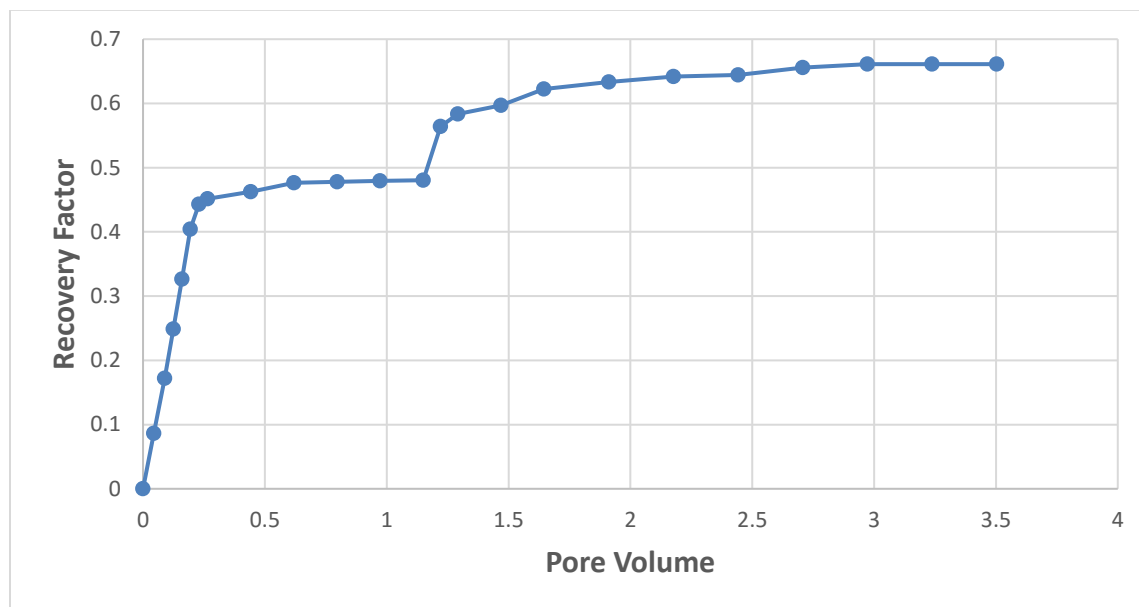


**Figure 47 Recovery Factor vs Pore Volume Injected (Experiment 6)**

Regarding the stability of the foam, the pressure drop chart shows a stability of differential pressure very soon after breakthrough with some fluctuations up and down. This can be attributed to increasing liquid phase in form of AOS solution that may help to stabilize the pressure drop earlier. In addition, experiment 6 shows stability around 50 psi which is within the same range as experiment 2. Fig. 48 shows the pressure drop performance during foam flooding in experiment 6.

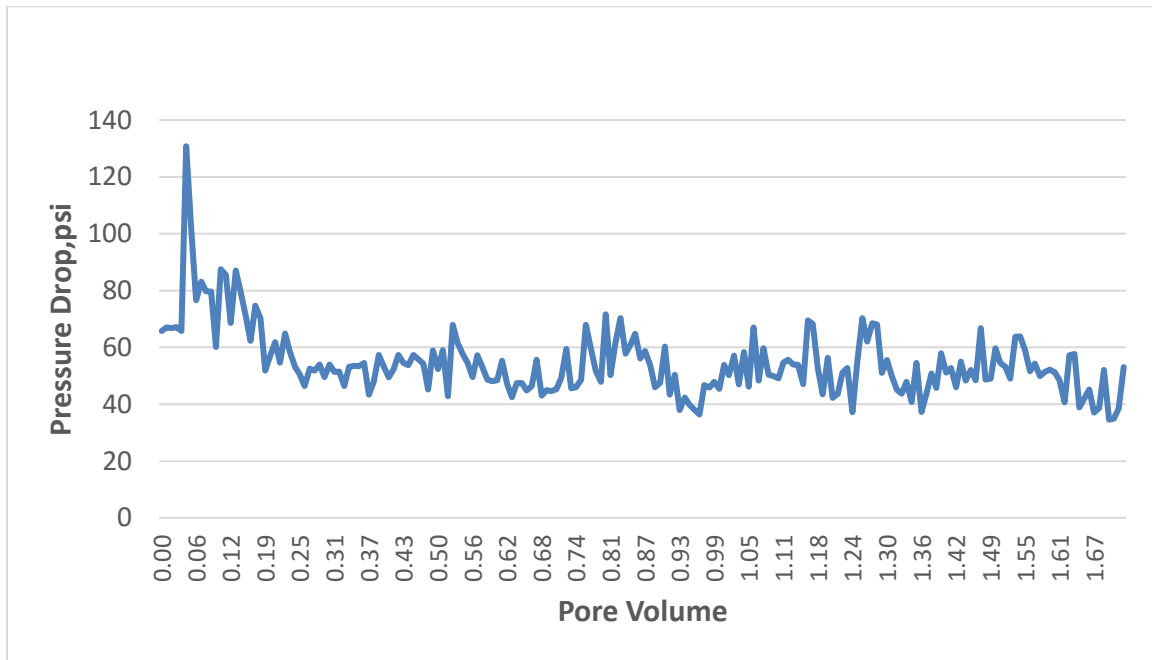


**Figure 48 Foam Recovery Pressure Drop vs Pore Volume Injected (Experiment 6)**

### 5.6.2 Experiment 7

Three injection rates were used to estimate the absolute permeability for the core which were 0.5, 1 and 1.5 cc/min. The core permeability is about 96.8 md. The pressure drop across the core sample is shown in Fig. 49.

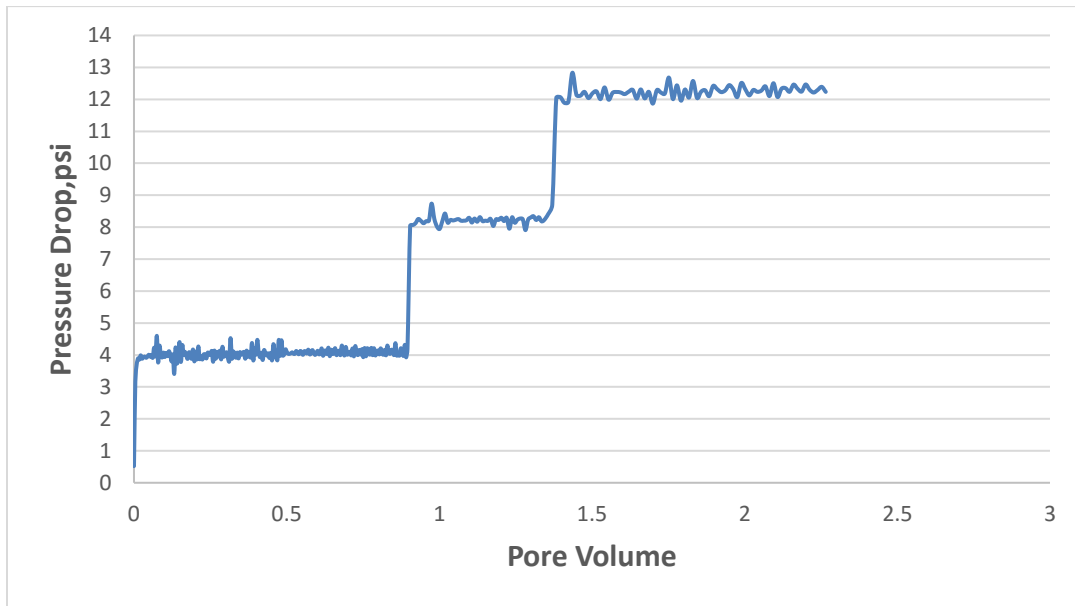


**Figure 49 Brine Permeability Pressure Drop vs Pore Volume Injected (Experiment 7)**

Then, oil injection was performed to saturate the core and to establish initial water saturation, which was about 36.8 %. Three flow rates were injected which were 0.5, 1 and 2 cc/min. Fig. 50 shows the pressure drop across the core sample during crude oil injection.



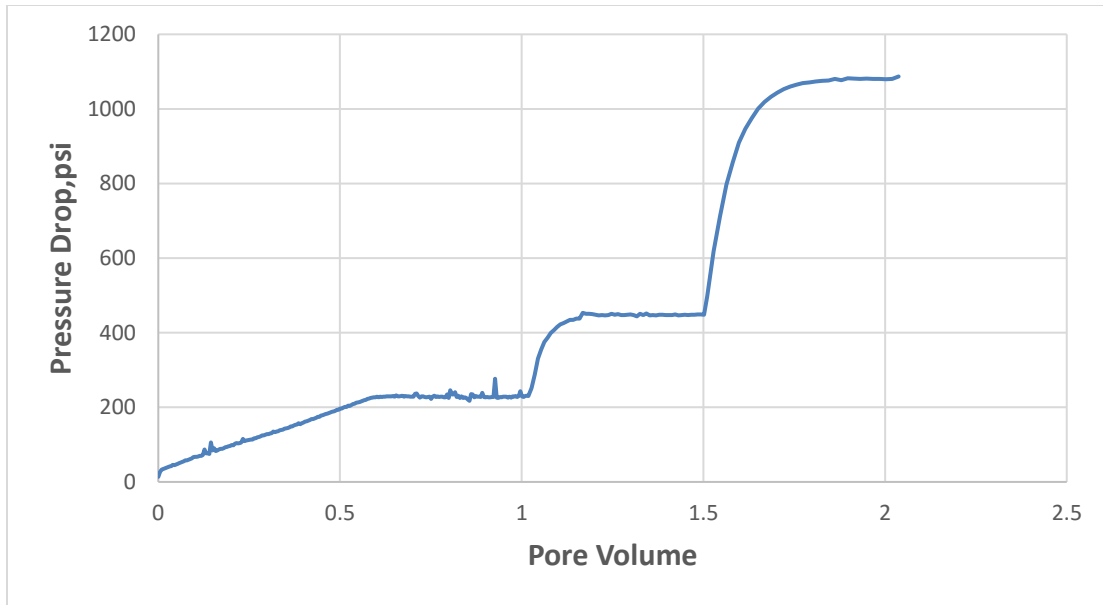


**Figure 50 Oil Injection Pressure Drop vs Pore Volume Injected (Experiment 7)**

The core sample was aged for three months. Then, oil flushing with the same crude oil used for saturation was performed by injecting around two pore volumes. After that, water flooding was performed until no more oil was coming out of the core. The breakthrough happened after injecting 0.31 pore volume. The recovery factor and the pressure drop during water flooding stage are shown in Fig. 51 and Fig. 52.

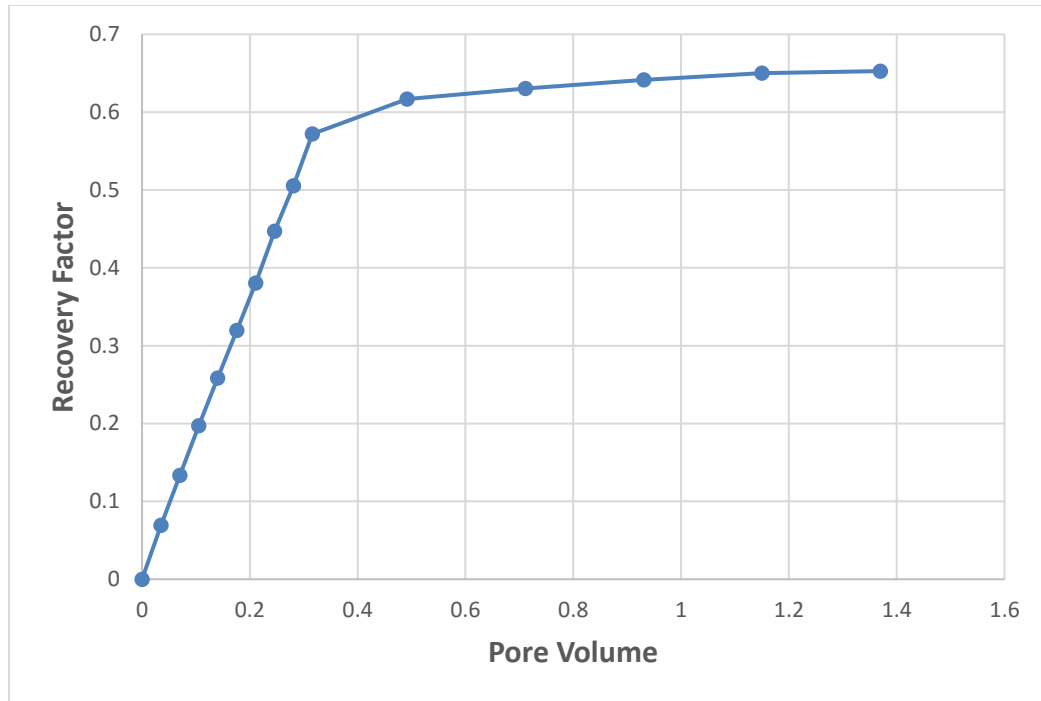


**Figure 51 SW Recovery Factor vs Pore Volume Injected (Experiment 7)**

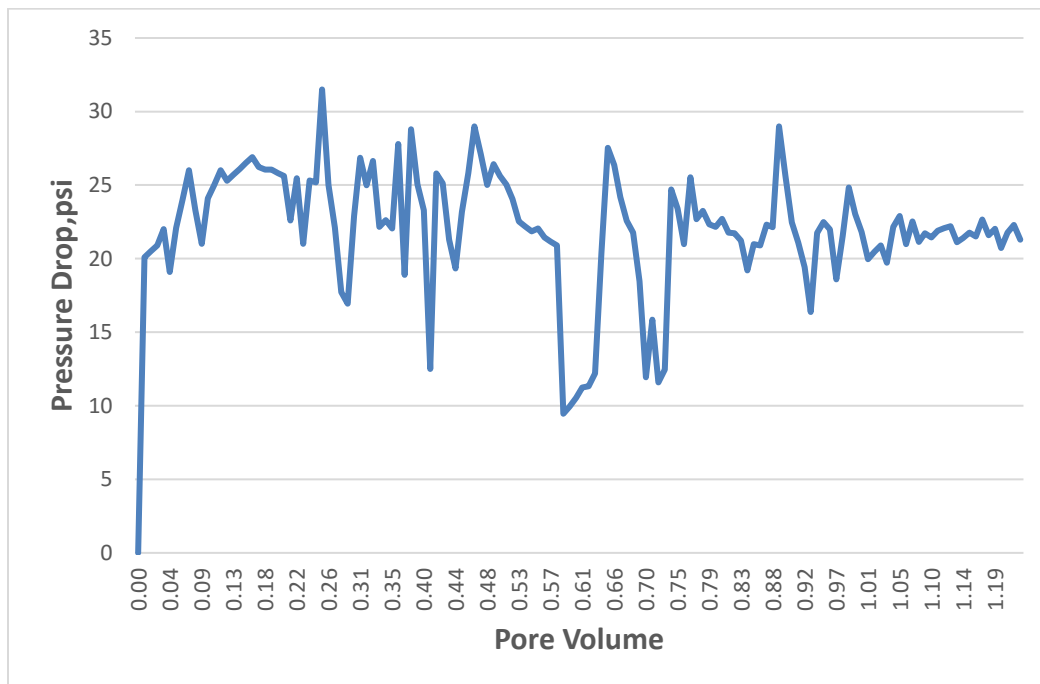


**Figure 52 SW Pressure Drop vs Pore Volume Injected (Experiment 7)**

In this experiment, N<sub>2</sub> was injected with supercritical CO<sub>2</sub> with a percentage of 20 % by volume. The foam quality changed to be 10 %. Like experiment 2, the ratio of CO<sub>2</sub> and N<sub>2</sub> used in this test was 80:20 by volume. The injection rates for CO<sub>2</sub>, N<sub>2</sub>, and AOS were 0.36, 0.09 and 0.05 cc/min respectively, making the 0.5 cc/min total foam injection rate. Foam quality was the only parameter changed from 80% in experiment 2 (Base case) to 90 % in this one. Table 13 summarizes the parameters used in this experiment.

**Table 13 Summary of Experiment 7 Parameters**

<b>Experiment No</b>	<b>q total</b>	<b>N<sub>2</sub> Ratio</b>	<b>Foam Quality</b>	<b>CO<sub>2</sub></b>	<b>q surfactant</b>	<b>q Gas</b>	<b>q N<sub>2</sub></b>	<b>q CO<sub>2</sub></b>
	<b>cc/min</b>	<b>Fraction</b>	<b>Fraction</b>	<b>Fraction</b>	<b>cc/min</b>	<b>cc/min</b>	<b>cc/min</b>	<b>cc/min</b>
7	0.5	0.2	0.9	0.8	0.05	0.45	0.09	0.36

The mixed foam achieved oil recovery of 11.6 %. This is lower than the recovery achieved by foam flooding in the experiment 2 (Base case) which was 38.42 %. The ultimate recovery for water flooding followed by foam injection reached 76.9 % while it was 90.7 % in experiment 2. The gas breakthrough took place after injecting around 0.03 PV calculated from the appearance of the first droplet of oil. It did not take much time to take place as it occurred after few minutes from first oil droplet production. Moreover, it was very early compared to breakthrough time for experiment 2, which took place after injection of 0.31 PV. Fig. 53 and Fig. 54 show the recovery performance in experiment 7.

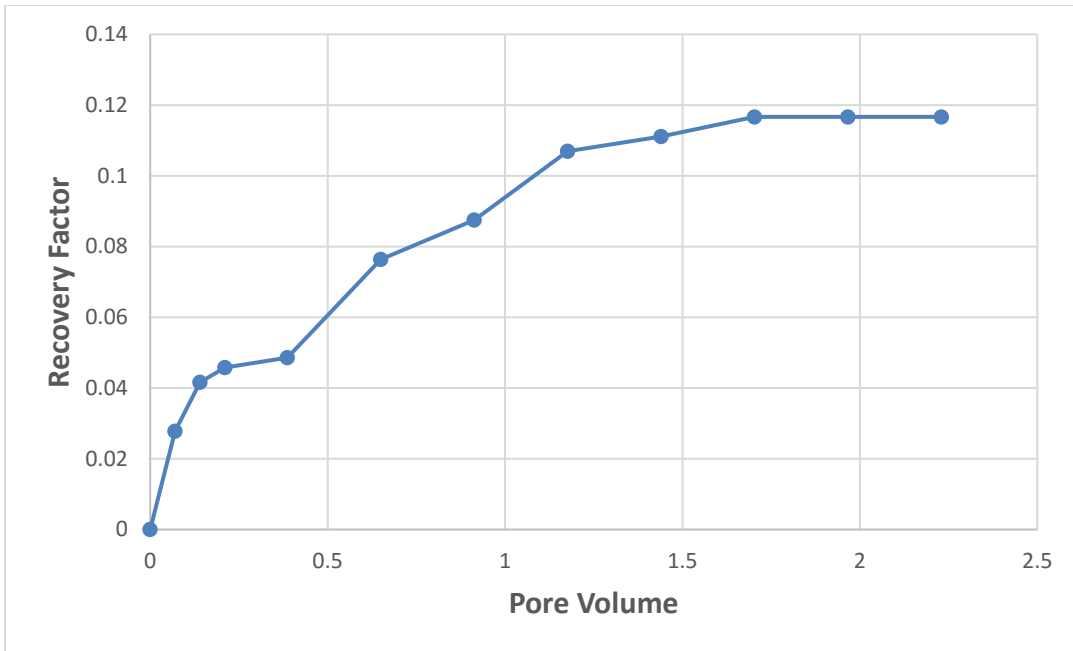


**Figure 53 Foam Flooding Recovery Factor vs Pore Volume Injected (Experiment 7)**

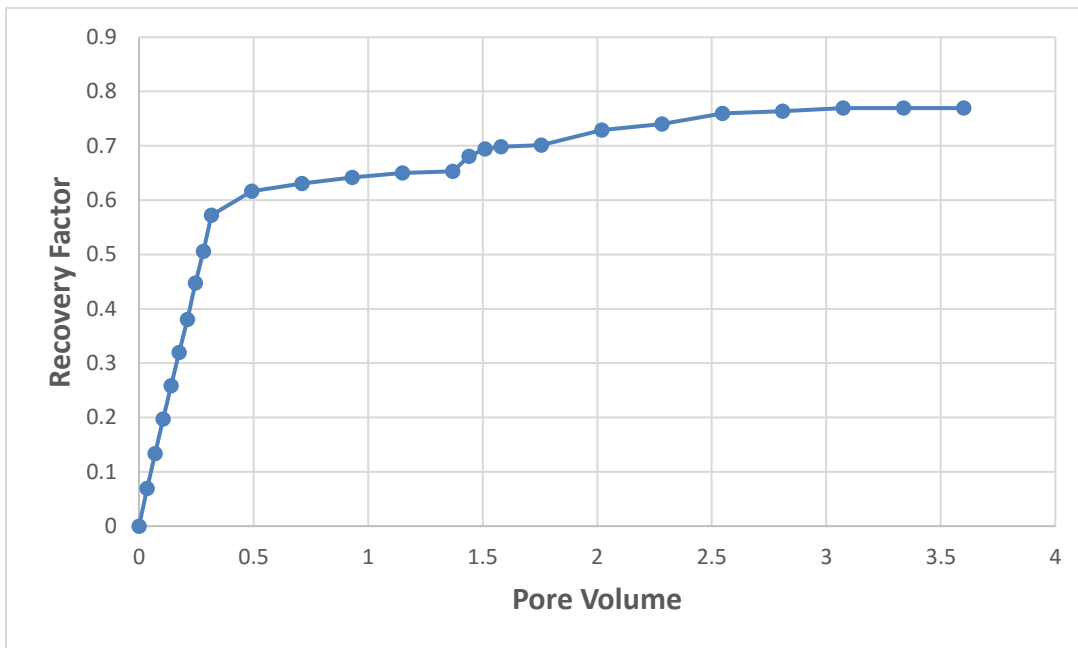


**Figure 54 Recovery Factor vs Pore Volume Injected (Experiment 7)**

Regarding the stability of the foam, the pressure drop chart shows a lot of fluctuations up and down continued to the end of experiment. This can be due to decreasing liquid phase in form of AOS solution that may cause dry foam. Compared to the base case, experiment 7 shows instability regarding pressure drop graph. Fig. 55 shows the pressure drop performance during foam flooding in experiment 7. As foam quality increased initially from 0.7 to 0.8, the foam becomes finer and shows good stability. Then when foam quality increases from 0.8 to 0.9, the foam texture becomes coarser and shows less stability. In addition, when the foam quality reaches 0.9, dry foam starts to be produced due to small amount of AOS. This dry foam has a negative effect also on oil recovery and foam stability.

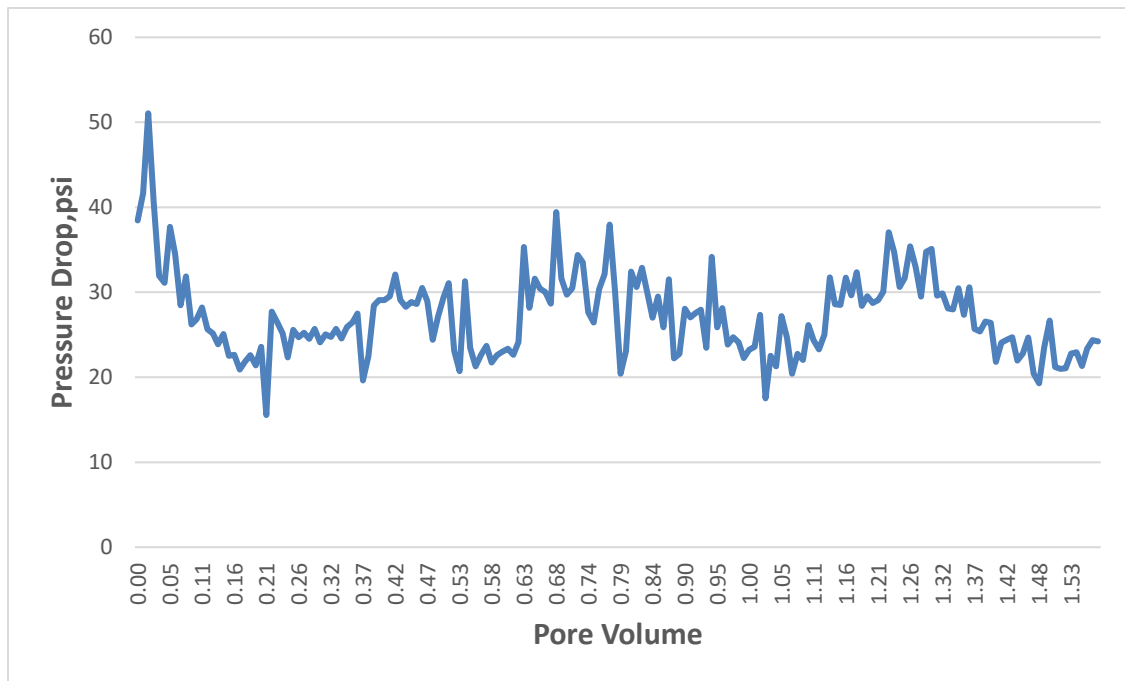


**Figure 55 Foam Recovery Pressure Drop vs Pore Volume Injected (Experiment 7)**

## 5.7 Summary of Discussion and Comparison

### 5.7.1 Injection Rate

As foam injection rate decreases, it gives more stability for the mixed foam. Shear rate increases as injection rate goes up resulting in weaker and less stable foam. Additionally, oil recovery shows enhancement with lower flow rate as more opportunities are given to the foam to contact more regions in the reservoir as shown in Fig. 57. In addition, using different rates did not affect the breakthrough time that much. Normalized pressure drop vs normalized pore volume injected is shown in Fig. 56. It is obvious from the chart that 0.5 cc/min gives the stabilized pressure drop at the end compared to the others.

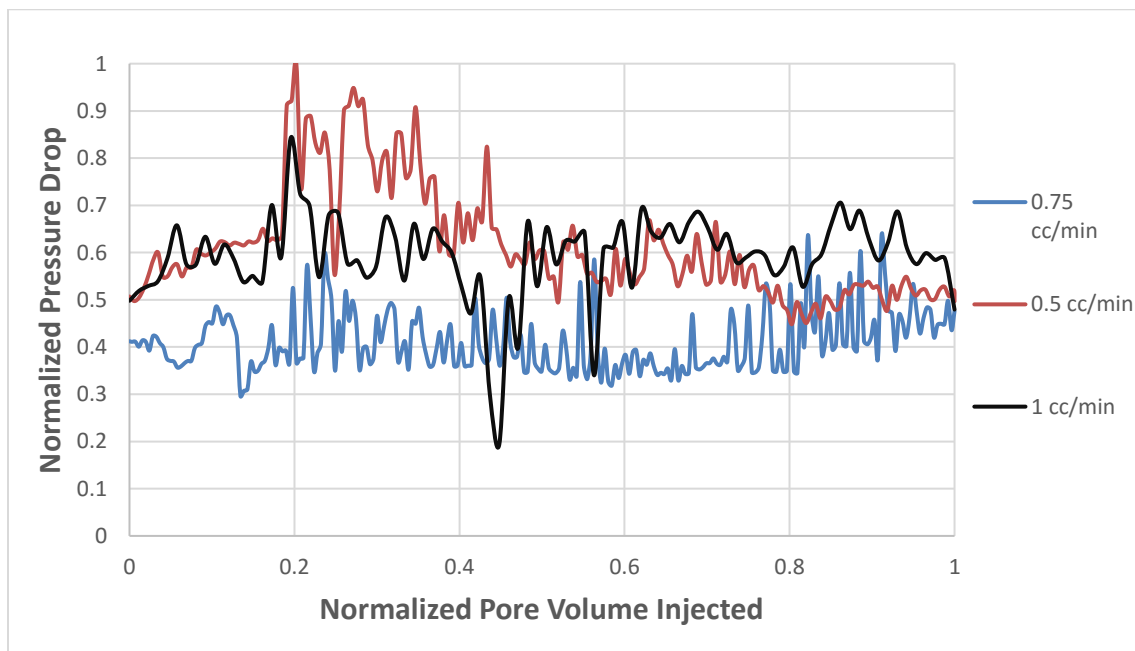


Figure 56 Normalized Pressure Drop vs Normalized Pore Volume Injected

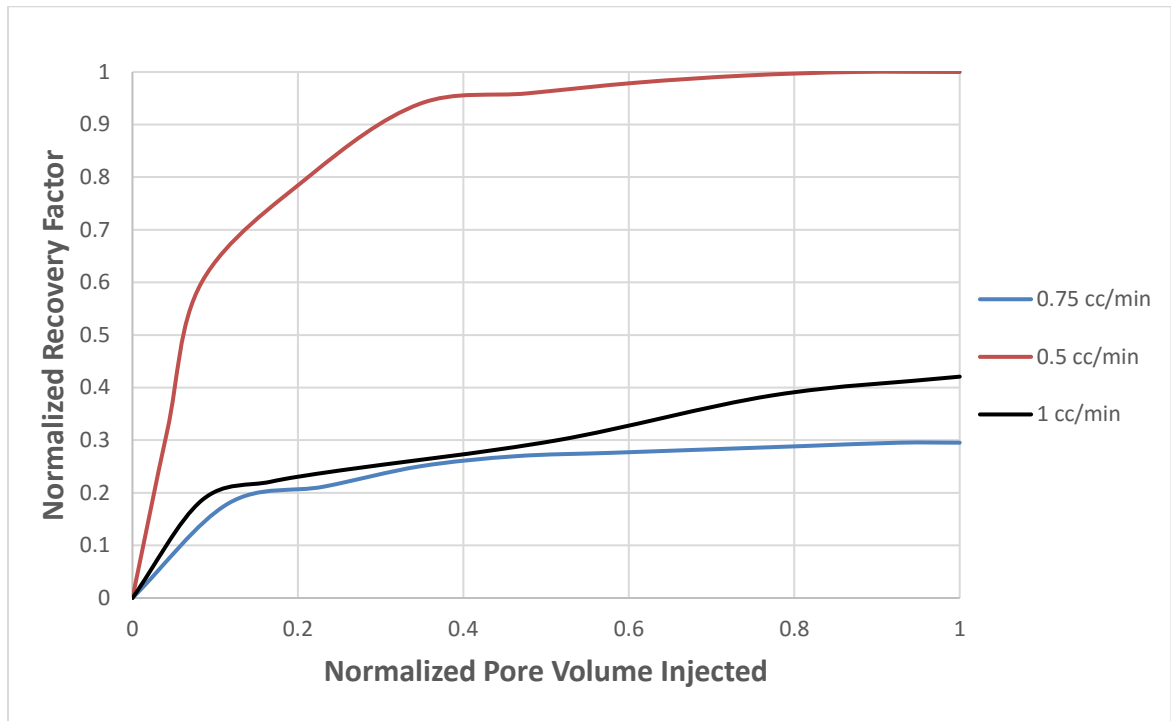


Figure 57 Normalized Recovery Factor vs Normalized Pore Volume Injected

### 5.7.2 N<sub>2</sub> Percentage

As N<sub>2</sub> amount increases from 10 % to 20 %, the foam becomes finer and becomes much more stable. This shows enhancement for both oil recovery and foam stability. Then when N<sub>2</sub> percentage increases from 20 % to 35 %, it shows a very good stability as we increase N<sub>2</sub>, which is the dominant stability factor. On other hand, it gives lower oil recovery as CO<sub>2</sub> was decreased which is the main recovery element. Based on the study, the optimum N<sub>2</sub> amount was in the range of 20 %, which has a satisfied performance for both oil recovery and foam stability. N<sub>2</sub> percentage comparison charts for normalized pressure drop and normalized recovery are shown in Fig. 58 and Fig. 59.

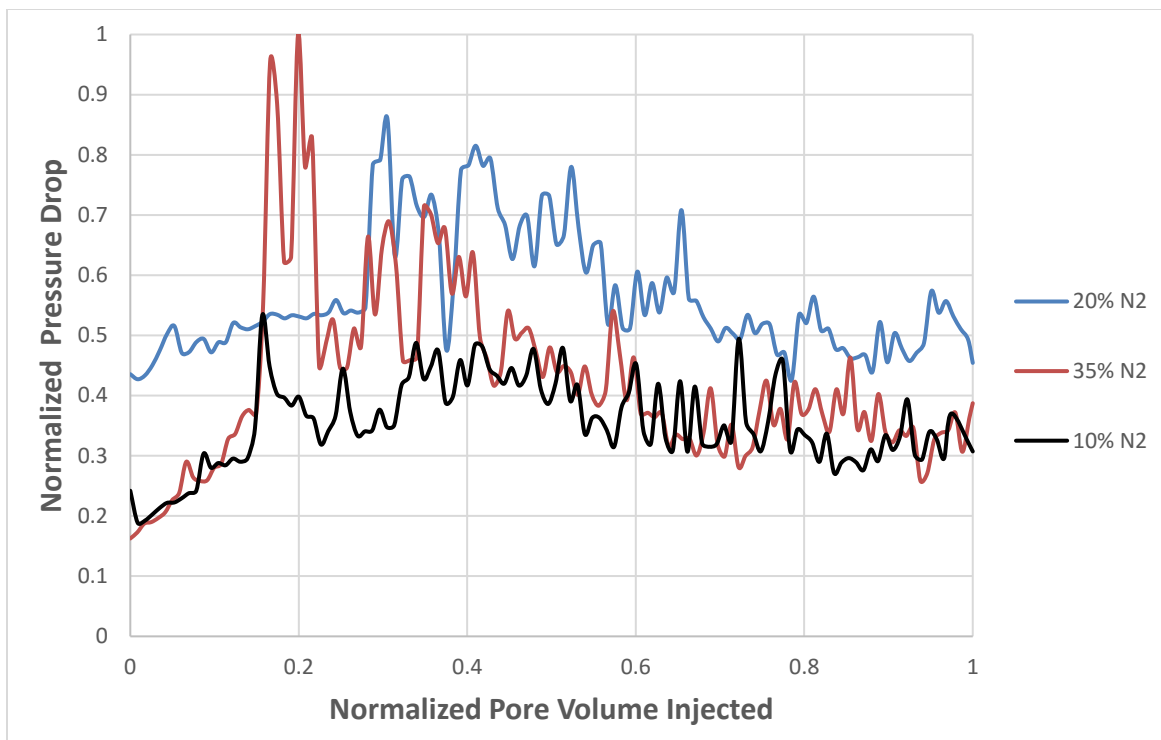


Figure 58 Normalized Pressure Drop vs Normalized Pore Volume Injected

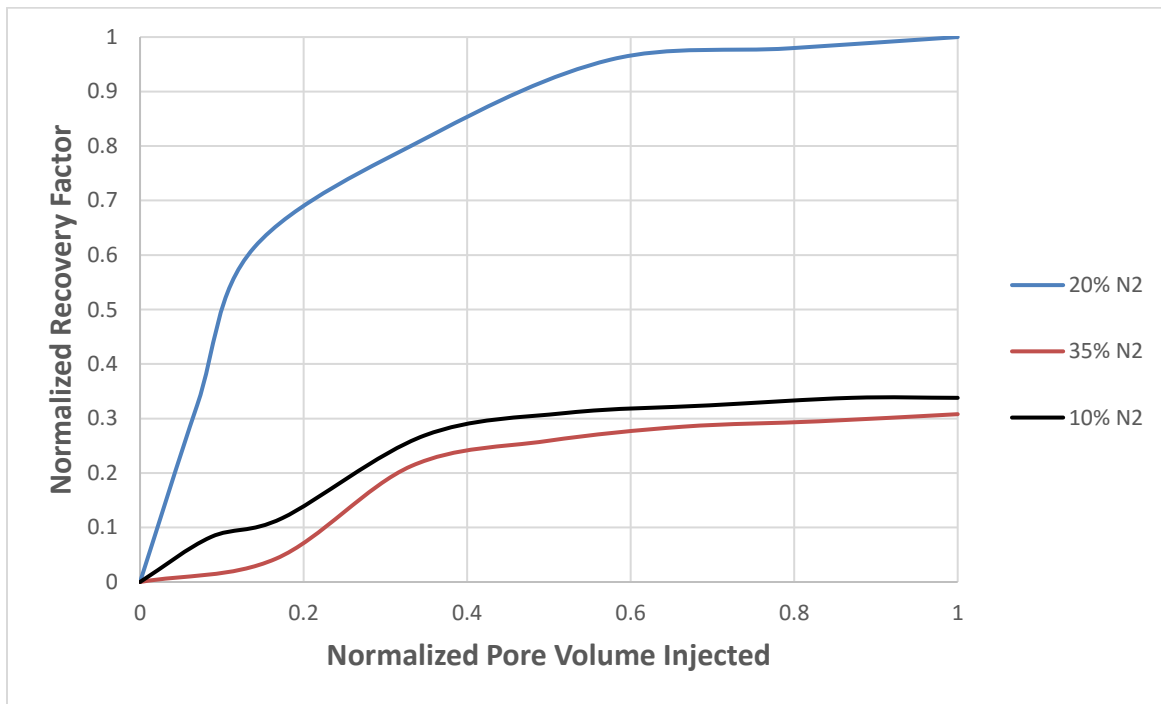


Figure 59 Normalized Recovery Factor vs Normalized Pore Volume Injected



### 5.7.3 Foam Quality

As foam quality increases initially from 0.7 to 0.8, the foam becomes finer and shows good stability. Then when foam quality increases from 0.8 to 0.9, the foam texture becomes coarser and shows less stability. In addition, when the foam quality reaches 0.9, dry foam starts to be produced due to small amount of AOS. This dry foam has a negative effect also on oil recovery and foam stability. There is remarkable improvement in oil recovery as foam stability increases and lower recovery was achieved as foam stability decreases. The optimum value was in the range of 0.8. Decreasing or increasing this value gives very early breakthrough, which results in less recovery. Foam quality comparison charts for normalized pressure drop and normalized recovery are shown in Fig. 60 and Fig. 61.

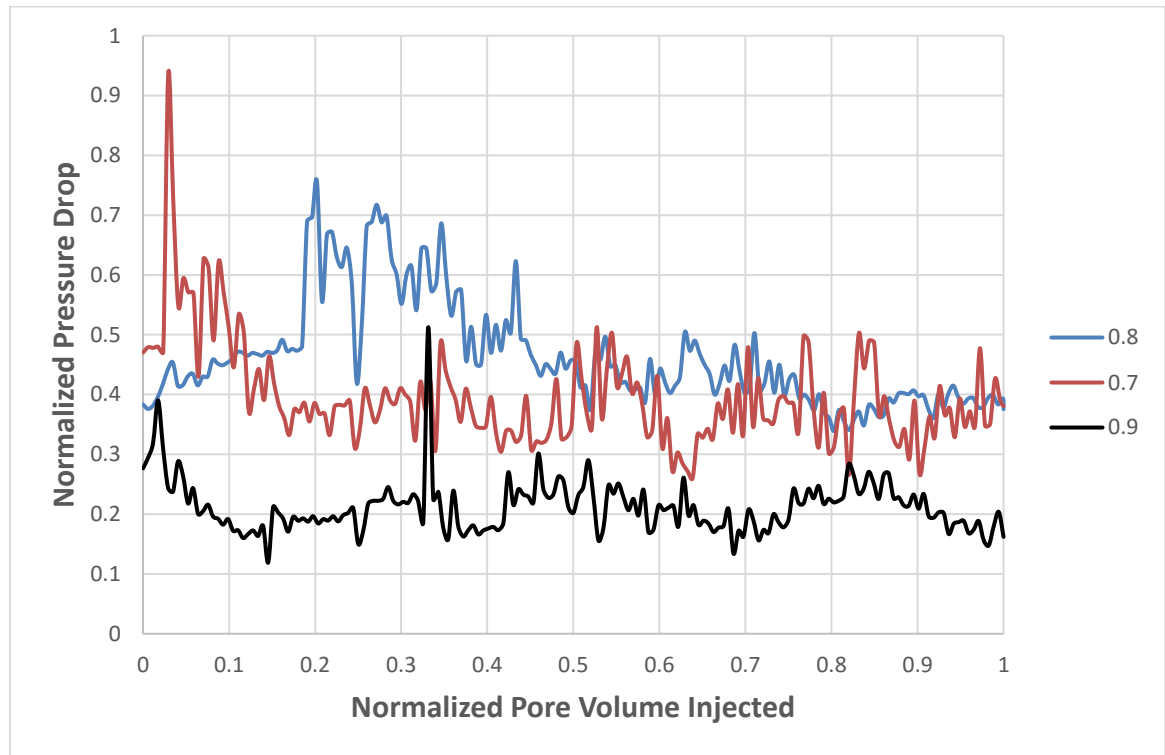
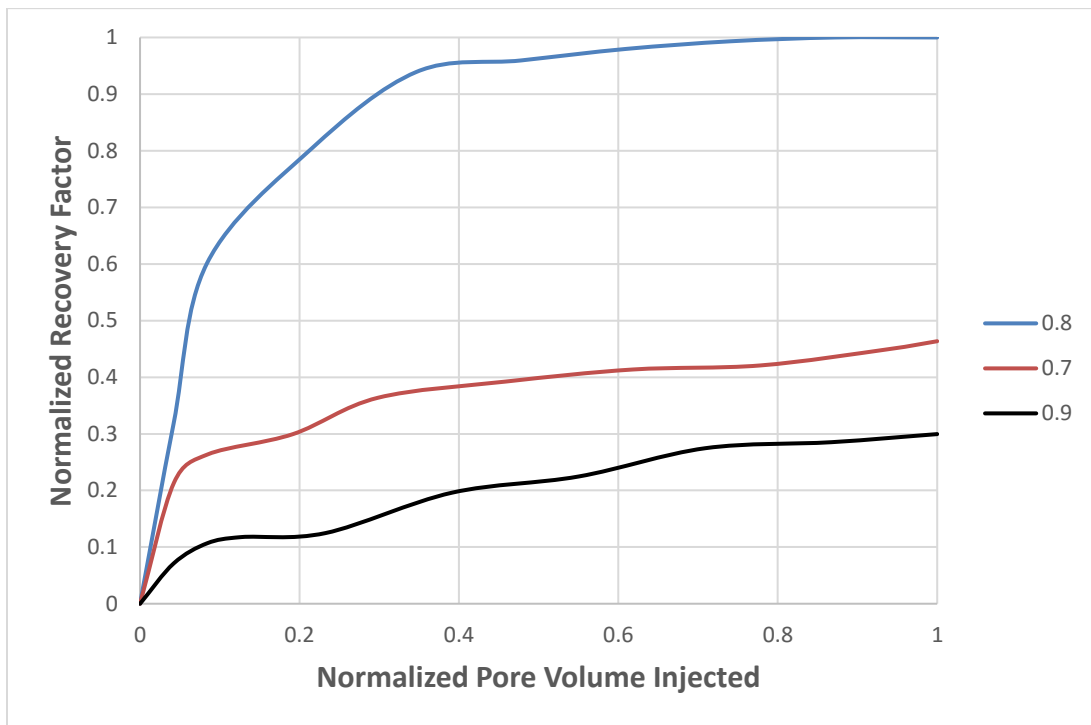


Figure 60 Normalized Pressure Drop vs Normalized Pore Volume Injected



**Figure 61 Normalized Recovery Factor vs Normalized Pore Volume Injected**

## CHAPTER 6 CONCLUSION

For EOR application, carbon dioxide is the most widely used gas for foam flooding in sandstone reservoirs. A foaming agent like a surfactant is mixed with gas to generate foam. Foam stability is the most fundamental key element to ensure the success of any EOR foam flooding. CO<sub>2</sub> exists at supercritical conditions at typical reservoir conditions. Its ability to create a stable foam is reduced at these conditions. CO<sub>2</sub>-foam has a common problem to become weaker above its supercritical conditions of 1100 psi and 31° C. N<sub>2</sub> is found to form stronger foam at the same conditions when compared to CO<sub>2</sub>. As a result, the advantages of using CO<sub>2</sub> foam collapsed due to the weakness of CO<sub>2</sub> at supercritical conditions. The mobility of gas is not effectively decreased resulting in low sweep efficiency. To overcome this issue, a small N<sub>2</sub> fraction was mixed with CO<sub>2</sub> to study its effect on oil free foam stability (M. Siddiqui et.al, 2016). Previously, the novel foam mixture consisting of CO<sub>2</sub> and N<sub>2</sub> has not been investigated for crude oil recovery in sandstone reservoirs.

In this research, co-injection technique is used to inject different schemes of supercritical CO<sub>2</sub> mixed with N<sub>2</sub> and AOS. Total flow rate, gases ratio and foam quality were the independent parameters in this study. On the other hand, oil recovery factor, pressure drop and breakthrough time were the dependent parameters. The core flooding tests were conducted at CO<sub>2</sub> supercritical conditions.

The analysis of the results obtained from the core flooding experiments can be concluded in the following:

1. The addition of  $N_2$  to  $CO_2$  in foam mixtures showed enhancement in terms of foam stability (shown by pressure drop graphs) and oil recovery.
2. Increasing the foam quality to around 90 % produced dry foam which in turn adversely affected the oil recovery and foam stability.
3. The optimum value for foam quality was in range of 80 % that produced the highest recovery, showed more stability and delayed the breakthrough.
4. Decreasing the foam quality below 80 % showed good stability after the breakthrough, but it was not good for oil recovery.
5. Decreasing the injection rate to 0.5 cc/min enhanced the oil recovery and foam stability as increasing the shear rate may lead to foam collapse.
6. The optimum value used for  $N_2$  was around 20 % that gave the best recovery and foam stability.
7. Increasing  $N_2$  percentage may lead to more stability as it shows higher stability at high pressure and temperature, but it will negatively affect the oil recovery.
8. All experiments had some foam bubbles coming out from the production side proving that foam with this mixture did not collapse inside the core.
9. AOS as a foaming agent proved its capability to generate stable foam in high-salinity environment.

This research has proposed many useful outcomes. These outcomes may help to provide a solution for supercritical  $CO_2$  foam instability issues in sandstone reservoirs.

It may help to understand more about foam behavior, as it is a developing research area. Finally, many recommendations can be suggested for future work as following:

1. To change the flooding strategy from the co-injection mode to surfactant alternating gas (SAG).
2. To introduce the technique of visualized testing during the core flooding is thought to be helpful in tracing the flood fronts and the contacted region inside the core by the foam.
3. To investigate phase behavior of the injected gases and surfactant when come in contact with the oil in place. The study of phase behavior is useful to give better understanding of the interactions that takes place on a molecular level.
4. Foam generators with a camera can be used to see foam droplets texture and foam quality before flooding.

## References

- Aarra, M.G., Ormehaug, P.A., Skauge, A., and Masalmeh, S.K., (2011) Experimental Study of CO<sub>2</sub>- and Methane-Foam Using Carbonate Core Material at Reservoir Conditions, in: Proc. of SPE Middle East Oil Gas Show Conf., 25–28 September, Manama, Bahrain, SPE-141614-MS, Society of Petroleum Engineers.
- Aarra, M.G., Skauge, A., Solbakken, J., and Ormehaug, P.A., (2014) Properties of N<sub>2</sub>- and CO<sub>2</sub>-Foams as a Function of Pressure, *J. Pet. Sci. Eng.*, 116, pp. 72–80.
- Adkins, S.S., Chen, X., Nguyen, Q.P., Sanders, A.W., and Johnston, K., (2010) Effect of Branching on the Interfacial Properties of Nonionic Hydrocarbon Surfactants at the Air–Water and Carbon Dioxide–Water Interfaces, *J. Colloid Int. Sci.*, 346(2), pp. 455–463.
- Ahmed, S., Elraies, K.A., Tan, I.M., and Hashmet, M.R., (2017) Experimental Investigation of Associative Polymer Performance for CO<sub>2</sub> Foam Enhanced Oil Recovery, *J. Pet. Sci. Eng.*, 157, pp. 971–979.
- Almajid, M.M. and Kovscek, A.R., (2016) Pore-Level Mechanics of Foam Generation and Coalescence in the Presence of Oil, *Adv. Colloid Interface Sci.*, 233, pp. 65–82.
- Amin Daryasafar, Khalil Shahbazi, (2018) CO<sub>2</sub>-Foam Injection for Enhanced Oil Recovery: A Brief Review, *International Journal of Energy for a Clean Environment*, pp. 237–256.
- Azdarpour, A., Rahmani, O., and Rafati, R., (2013) Laboratory Investigation of the Effects of Parameters Controlling Polymer Enhanced Foam (PEF) Stability, *Asian J. Appl. Sci.*, 1(1), pp. 38–48.
- Bian, Y., Penny, G.S., and Sheppard, N.C., (2012) Surfactant Formulation Evaluation for Carbon Dioxide Foam Flooding in Heterogeneous Sandstone Reservoir, in: Proc. of SPE Improved Oil Recovery Symp., 14–18 April, Tulsa, Oklahoma, USA, SPE-154018-MS, Society of Petroleum Engineers.
- Bond, D.C. and Holbrook, C.C., (1958) Gas Drive Oil Recovery Process, U.S. Patent No. 2,866,507.
- Buchgraber, M., Castanier, L.M., and Kovscek, A.R., (2012) Microvisual Investigation of Foam Flow in Ideal Fractures: Role of Fracture Aperture and Surface Roughness, in: Proc. of SPE Annual Technical Conf. Exhibition, 8–10 October, San Antonio, Texas, USA, SPE-159819-MS, Society of Petroleum Engineers.
- Castanier, L.M. and Hanssen, J.E., (1995) Foam Field Tests: State-of-the-Art and Critical Review, in: Proc. of 8th European Improved Oil Recovery Symp., 15–17 May, Vienna, Austria.
- Chang, S.-H. and Grigg, R.B., (1999) Effects of Foam Quality and Flow Rate on CO<sub>2</sub>-foam Behavior at Reservoir Temperature and Pressure, *SPE Res. Eval. Eng.*, 2(3), pp. 248–254. DOI: 10.2118/56856-PA.
- Chen, Y., Elhag, A.S., Poon, B.M., et al., (2014) Switchable Nonionic to Cationic Ethoxylatedamine Surfactants for CO<sub>2</sub> Enhanced Oil Recovery in High-Temperature, High-Salinity Carbonate Reservoirs, *SPE J.*, 19(2), pp. 249–259.
- Cui, L., Ma, K., Abdala, A.A., Lu, J., Tanakov, I.M., Biswal, S.L., and Hirasaki, G.J., (2014) Adsorption of a Switchable Cationic Surfactant on Natural Carbonate Minerals, *SPE J.*, 20(01), pp. 9. DOI:10.2118/169040-MS
- D. Espinosa, F. Caldelas, K. Johnston, S.L. Bryant, C. Huh, (2010) Nanoparticle-Stabilized Supercritical CO<sub>2</sub> Foams for Potential Mobility Control Applications.

- Dong, X., Liu, H., Hou, J., Liu, G., and Chen, Z., (2016) Polymer-Enhanced Foam PEF Injection Technique to Enhance the Oil Recovery for the Post Polymer-Flooding Reservoir, in: Proc. of SPE Western Regional Meeting, 23–26 May, Anchorage, Alaska, USA, SPE-180426-MS, Society of Petroleum Engineers.
- Du, D.-X., Beni, A.N., Farajzadeh, R., and Zitha, P.L.J., (2008) Effect of Water Solubility on Carbon Dioxide Foam Flow in Porous Media: An X-Ray Computed Tomography Study, *Ind. Eng. Chem. Res.*, 47(16), pp. 6298–6306.
- Elhag, A.S., Chen, Y., Chen, H., Reddy, P.P., et al., (2014) Switchable Amine Surfactants for Stable CO<sub>2</sub>/Brine Foams in High Temperature, High Salinity Reservoirs, in: Proc. of 19th SPE Improved Oil Recovery Symp., 12–16 April, Tulsa, Oklahoma, USA, SPE-169041-MS, Society of Petroleum Engineers.
- Enick, R.M., Olsen, D.K., Ammer, J.R., and Schuller, W., (2012) Mobility and Conformance Control for Carbon Dioxide Enhanced Oil Recovery (CO<sub>2</sub>-EOR) via Thickeners, Foams, and Gels — A Literature Review of 40 Years of Research, in: Proc. of 18th SPE Improved Oil Recovery Symposium, 14–18 April, Tulsa, Oklahoma, USA, Society of Petroleum Engineers.
- Farajzadeh, R., Andrianov, A., and Zitha, P.L.J., (2010), Effect of Water Solubility and Carbon Dioxide Foam Flow in Porous Media: An X-Ray Computed Tomography Study, *Ind. Eng. Chem. Res.*, 49(4), pp. 1910–1919.
- Farajzadeh, R., Andrianov, A., Brunning, H., and Zitha, P.L.J., (2009) Comparative Study of CO<sub>2</sub> and N<sub>2</sub> Foams in Porous Media at Low and High Pressure–Temperatures, *Ind. Eng. Chem. Res.*, 48(9), pp. 4542–4552.
- Farajzadeh, R., Wassing, B.M., and Boerrigter, P.M., (2012) Foam Assisted Gas–Oil Gravity Drainage in Naturally-Fractured Reservoirs, *J. Pet. Sci. Eng.*, 94–95, pp. 112–122.
- Farzaneh, S.A. and Sohrabi, M., (2015) Experimental Investigation of CO<sub>2</sub>-Foam Stability Improvement by Alkaline in the Presence of Crude Oil, *Chem. Eng. Res. Des.*, 94, pp. 375–389.
- Fernø, M.A., Eide, Steinsbø, Langlo, S.A.W., Christophersen, A., Skibenes, A., Ydstebø, T., and Graue, A., (2015) Mobility Control during CO<sub>2</sub> EOR in Fractured Carbonates Using Foam: Laboratory Evaluation and Numerical Simulations, *J. Pet. Sci. Eng.*, 135, pp. 442–451.
- Fernø, M.A., Gauteplass, J., Pancharoen, M., Haugen, A., Graue, A., Kovscek, A.R., and Hirasaki, G.J., (2014) Experimental Study of Foam Generation, Sweep Efficiency and Flow in a Fracture Network.
- G. Yin, R.B. Grigg, Y. Svec, (2009) Oil Recovery and Surfactant Adsorption During CO<sub>2</sub>-Foam Flooding.
- Gauglitz, P.A., Friedmann, F., Kam, S.I., and Rossen, W.R., (2002) Foam Generation in Porous Media, in: Proc. of SPE/DOE Improved Oil Recovery Symp., 13–17 April, Tulsa, Oklahoma, USA, SPE-75177-MS, Society of Petroleum Engineers.
- Hanssen, J.E., Holt, T., and Surguchev, L.M., (1994) Foam Processes: An Assessment of Their Potential in North Sea Reservoirs Based on a Critical Evaluation of Current Field Experience, in: Proc. Of SPE/DOE Improved Oil Recovery Symposium, 17–20 April, Tulsa, Oklahoma, USA, SPE-27768-MS, Society of Petroleum Engineers.
- Harris, P.C., (1987) Dynamic Fluid-Loss Characteristics of CO<sub>2</sub>-Foam Fracturing Fluids, *SPE Prod. Eng.*, 2, pp. 89–94.

Holm, L.W., (1982) CO<sub>2</sub> Flooding: Its Time Has Come, *J. Pet. Technol.*, 34(12), pp. 2739–2745.  
Howard, G. and Fast, C., (1970) Hydraulic Fracturing. Monograph, Vol. 2 of the Henry L. Doherty Series, New York: Society of Petroleum Engineers of AIME.

Huh, C. and Rossen, W.R., (2008) Approximate Pore-Level Model for Apparent Viscosity of Polymer-Enhanced Foam in Porous Media, *SPE J.*, 13(01), pp. 17–25.

J. Yu, N. Liu, L. Li, R. Lee, (2012) Generation of Nanoparticle-Stabilized Supercritical CO<sub>2</sub> Foams.

J.S. Solbakken, A. Skauge, M.G. Aarra, (2013) Supercritical CO<sub>2</sub>-Foam - The Importance of CO<sub>2</sub> Density on Foams Performance.

Khalil, F. and Asghari, K., (2006) Application of CO<sub>2</sub>-Foam as a Means of Reducing Carbon Dioxide Mobility, *J. Can. Pet. Technol.*, 45(1), pp. 37–41.

Kovscek, A.R. and Radke, C., (1994) Fundamentals of Foam Transport in Porous Media, *ACS Adv. Chem. Ser.*, 242, pp. 115–163.

Kovscek, A.R., Tretheway, D.C., Persoff, P., and Radke, C.J., (1995) Foam Flow through a Transparent Rough-Walled Fracture, *J. Pet. Sci. Eng.*, 17, pp. 75–86.

L. Kapetas, S.V. Bonnicu, S. Danells, W.R. Rossen, R. Farajzadeh, A.A. Eftekhari, et al., (2015) Effect of Temperature on Foam Flow in Porous Media.

Lande, S., (2016) Polymer Enhanced Foam in Unconsolidated Sand, MSc, The University of Bergen.

Li, C., Huang, Y., Sun, X., Gao, R., Zeng, F., Tontiwachwuthikul, P., and Liang, Z., (2017a) Rheological Properties Study of Foam Fracturing Fluid Using CO<sub>2</sub> and Surfactant, *Chem. Eng. Sci.*, 170, pp. 720–730.

Li, C., Zu, Y., and Ma, B., (1993) A Study on Foam Rheological Properties, *J. Chem. Ind. Eng. (China)*, 44, pp. 480–485.

Li, D., Ren, S., Zhang, P., Zhang, L., Feng, Y., and Jing, Y., (2017b) CO<sub>2</sub>-Sensitive and Self-Enhanced Foams for Mobility Control during CO<sub>2</sub> Injection for Improved Oil Recovery and Geo-Storage, *Chem. Eng. Res. Des.*, 120, pp. 113–120.

Li, Q., Chen, Z., Zhang, J., Liu, L., Li, X., and Jia, L., (2016) Positioning and Revision of CCUS Technology Development in China, *Int. J. Greenh. Gas Con.*, 46, pp. 282–93.

Li, Z., Song, X., Wang, Q., Zhan, L., Guo, P., and Li, X., (2009) Enhanced Foam Flooding Pilot Test in Chengdong of Shengli Oilfield: Laboratory Experiment and Field Performance, in: *Proc. of Int. Petroleum Technology Conf.*, 7–9 December, Doha, Qatar, pp. 1536–1549.

Llave, F., Chung, F.H., Louvier, R., and Hudgins, D., (1990) Foams as Mobility Control Agents for Oil Recovery by Gas Displacement, in: *Proc. of SPE/DOE Enhanced Oil Recovery Symp.*, 20–25 April, Tulsa, Oklahoma, USA, SPE-20245-MS, Society of Petroleum Engineers.

M. Amro, M. Finck, P. Jaeger, (2015) Foams at Elevated Pressure in EOR.

M. Hassan, (2017), Performance of Mixed CO<sub>2</sub>/N<sub>2</sub> Foam in Enhanced Oil Recovery for Sandstone Reservoirs, King Fahd University of Petroleum & Minerals.

M. Siddiqui, (2016), Stability and Texture of CO<sub>2</sub>/N<sub>2</sub> Foam in Sandstone, King Fahd University of Petroleum & Minerals.



- Malik, Q.M. and Islan, M.R., (2000) Potential of Greenhouse Gas Storage and Utilization through Enhanced Oil Recovery in Canada, in: Proc. of 16th World Petroleum Congress, 11–15 June, Calgary, Canada.
- Mannhardt, K., Novosad, J., and Schramm, L., (1998) Foam/Oil Interactions at Reservoir Conditions, in: Proc. of SPE/DOE Improved Oil Recovery Symp., Society of Petroleum Engineers.
- Mast, R.F., (1972) Microscopic Behavior of Foam in Porous Media, 8–11 October, San Antonio, Dallas, TX, USA, SPE-3997-MS, Society of Petroleum Engineers.
- Mukherjee, J., Norris, S.O., Nguyen, Q.P., Scherlin, J.M., Vanderwal, P.G., and Abbas, S., (2014) CO<sub>2</sub> Foam Pilot in Salt Creek Field, Natrona County, WY: Phase I: Laboratory Work, Reservoir Simulation, and Initial Design, in: Proc. of SPE Improved Oil Recovery Symp., 12–16 April, Tulsa, Oklahoma, USA, SPE-169166-MS, Society of Petroleum Engineers.
- Nguyen, P., Fadaei, H., and Sinton, D., (2014) Pore-Scale Assessment of Nanoparticle-Stabilized CO<sub>2</sub> Foam for Enhanced Oil Recovery, *Energy Fuels*, 28(10), pp. 6221–6227.
- Osei-Bonsu, K., Shokri, N., and Grassia, P., (2016) Fundamental Investigation of Foam Flow in a Liquid-Filled Hele–Shaw Cell, *J. Colloid Interface Sci.*, 462, pp. 288–296.
- Pang, Z., (2010) The Blocking Ability and Flowing Characteristics of Steady Foams in Porous Media, *Transp. Porous Med.*, 85(1), pp. 299–316.
- Patton, J.T., Holbrook, S.T., and Hsu, W., (1983) Rheology of Mobility Control Foams, *Soc. Pet. Eng. J.*, 23(03), pp. 456–460.
- Perttamo, E.K., (2013) Characterization of Associating Polymer (AP) Solutions. Influences on Flow Behavior by the Degree of Hydrophobicity and Salinity, MSc, The University of Bergen. Proc. of SPE Annual Technical Conf. Exhibition, 29 October, Amsterdam, Netherlands, Society of Petroleum Engineers.
- Pu, W., Wei, P., Sun, L., and Wang, S., (2017) Stability, CO<sub>2</sub> Sensitivity, Oil Tolerance and Displacement Efficiency of Polymer Enhanced Foam, *RSC Adv.*, 7(11), pp. 6251–6258.
- P.Y. Zhang, S. Huang, S. Sayegh, X.L. Zhou, Effect of CO<sub>2</sub> Impurities on Gas-Injection EOR Processes, (2004).
- R. Farajzadeh, A. Andrianov, H. Bruining, P.L.J. Zitha, (2009) Comparative Study of CO<sub>2</sub> and N<sub>2</sub> Foams in Porous Media at Low and High Pressure-Temperatures, *Ind. Eng. Chem. Res.* 48 4542–4552. doi:10.1021/ie801760u.
- Ranjit, K. and Baquee, A.A., (2013) Nanoparticle: An Overview of Preparation, Characterization and Application, *Int. Res. J. Pharm.*, 4(4), pp. 47–57.
- S. Shaddel, M. Hemmati, E. Zamanian, N.N. Moharrami, Core Flood Studies to Evaluate Efficiency of Oil Recovery by Low Salinity Water Flooding as a Secondary Recovery Process, *J. Pet. Sci. Technol.* 4 (2014) 47–56.
- Sanders, A.W., Jones, R.M., Linroth, M.A., and Nguyen, Q.P., (2012) Implementation of a CO<sub>2</sub> Foam Pilot Study in the SACROC Field: Performance Evaluation, in: Proc. of SPE Annual Technical Conf. Exhibition, 8–10 October, San Antonio, Texas, USA, SPE-160016-MS, Society of Petroleum Engineers.

Schramm, L.L. and Wassmuth, F., (2009) Foams: Basic Principles. Foams: Fundamentals and Applications in the Petroleum Industry, in L.L. Schramm (Ed.), Advances in Chemistry Series, Vol. 242, Washington, DC: American Chemical Society (ACS), pp. 3–45.

Shen, C., Nguyen, Q.P., Huh, C., and Rossen, W.R., (2006) Does Polymer Stabilize Foam in Porous Media? in: Proc. of SPE/DOE Symp. on Improved Oil Recovery, 22–26 April, Tulsa, Oklahoma, USA, SPE-99796-MS, Society of Petroleum Engineers.

Siddiqui, M.A.Q. and Gajbhiye, R.N., (2017) Stability and Texture of CO<sub>2</sub>/N<sub>2</sub> Foam in Sandstone, Colloids Surf. A: Physicochem. Eng. Asp. , 534, pp. 26–37.

Skoreyko, F.A., Villavicencio, A.P., Rodriguez Prada, H., and Nguyen, Q.P., (2012) Understanding Foam Flow with a New Foam EOR Model Developed from Laboratory and Field Data of the Naturally Fractured Cantarell Field, in: Proc. of SPE Improved Oil Recovery Symp., 14–18 April, Tulsa, Oklahoma, USA, SPE-153942-MS, Society of Petroleum Engineers.

Smith, D.H., (1988) Injectivity and Surfactant-Based Mobility Control, in: Surfactant Based Mobility Control, ACS Symp. Ser., American Chemical Society, Ch. 22, pp. 429–438. DOI: 10.1021/bk-1988-0373.ch022

Stalkup, F.I., Jr., (1984), Miscible displacement: Dallas, Tex., Society of Petroleum Engineers of AIME, SPE Monograph Series, ISBN 0-89520-319-7, 204 p.

Sun, Q., Li, Z., Li, S., Jiang, L., Wang, J., and Wang, P., (2014) Utilization of Surfactant-Stabilized Foam for Enhanced Oil Recovery by Adding Nanoparticles, Energy Fuels, 28(4), pp. 2384–2394.

Sydansk, R., (1994a) Polymer-Enhanced Foams. Part 1: Laboratory Development and Evaluation, SPE Adv. Technol. Ser., 2(02), pp. 150–159.

Sydansk, R.D., (1994b) Polymer-Enhanced Foams. Part 2: Propagation through High Permeability Sandpacks, SPE Adv. Technol. Ser., 2(02), pp. 160–166.

Talebian, S.H., Rahim, M.P., Tan, I.M., and Zitha, P.L.J., (2013) Foam Assisted CO<sub>2</sub>-EOR; Concepts, Challenges and Applications, in: Proc. of SPE Enhanced Oil Recovery Conf., 2–4 July, Kuala Lumpur, Malaysia, SPE-165280-MS, Society of Petroleum Engineers.

Tzimas, E., Georgakaki, A., Cortes, C.G., and Peteves, S.D., (2005), Enhanced oil recovery-using carbon dioxide in the European energy system: European Commission, Directorate General Joint Research Centre (DG JRC).

Van Poollen, H.K., and Associates, (1981), Fundamentals of enhanced oil recovery: Tulsa, Okla., Penn Well Books, Division of PennWell Publishing Company, 155 p.

Wang, Y., Zhang, Y., Liu, Y., Zhang, L., Ren, S., Lu, J., Wang, X., and Fan, N., (2017) The Stability Study of CO<sub>2</sub> Foams at High Pressure and High Temperature, J. Pet. Sci. Eng., 154, pp. 234–243.

Whorton L.P., Brownscombe E.R., and Dyes, A.B., (1952), “Method for Producing Oil by Means of Carbon Dioxide”, U.S. Patent 2,623,596

Xu, X., Saeedi, A., and Liu, K., (2016) Laboratory Studies on CO<sub>2</sub> Foam Flooding Enhanced by a Novel Amphiphilic Ter-Polymer, J. Pet. Sci. Eng., 138, pp. 153–159.

Yan, W., Miller, C.A., and Hirasaki, G.J., (2006) Foam Sweep in Fractures for Enhanced Oil Recovery, Colloids Surf. A: Physicochem. Eng. Asp., 282–283, pp. 348–359.

Yu, H., Yang, B., Xu, G., Wang, J., Ren, S., Lin, W., Xiao, L., and Gao, H., (2008) Air Foam Injection for IOR: From Laboratory to Field Implementation in Zhongyuan Oil field China, in: Proc. of SPE Improved Oil Recovery Symp., 20–23 April, Tulsa, Oklahoma, USA, SPE-113913-MS, Society of Petroleum Engineers.

Zhang, L., Ren, S., Ren, B., Zhang, W., Guo, Q., and Zhang, L., (2011) Assessment of CO<sub>2</sub> Storage Capacity in Oil Reservoirs Associated with Large Lateral/Underlying Aquifers: Case Studies from China, *Int. J. Greenh. Gas Con.*, 5, pp. 1016–1021.

Zhang, Y., Song, H., Li, D., et al., (2013) Experiment on High Pressure CO<sub>2</sub> Foam Stability of Nonionic Surfactants, *J. China Univ. Pet. (Nat. Sci. Ed.)*, 37(4), pp. 119–123.

Zhou, Z.X., (2011) *Inorganic Chemistry*, Beijing: Chemistry Press (in Chinese).

Zhu, T., Ogbe, D.O., and Khataniar, S., (2004) Improving the Foam Performance for Mobility Control and Improved Sweep Efficiency in Gas Flooding, *Ind. Eng. Chem. Res.*, 43(15), pp. 4413–4421.

## Vitae

Name : Ahmed Elsayed Ahmed Ibrahim Abdelaal

Nationality : Egyptian

Date of Birth :3/24/1993

Email : pmeahmed1@gmail.com

Address : Mansoura, Egypt

Postal Code : 35511

Academic Background : Petroleum Engineering

Educational Background : MSc in Petroleum Engineering, KFUPM in Dec 2019.

BSc in Petroleum Engineering, Suez University in Egypt  
in May 2014.

Work Experience : Core Flooding in Central Institute of Petroleum Research in  
2019.

Teaching assistant in Petroleum Engineering Department in  
KFUPM from Jan 2018 to December 2019.

Teaching assistant in Petroleum Engineering Department in  
Suez University from Jan 2015 to December 2017.